AD-A194 648 ADVANCES IN AIR-LAUNCHED WEAPON GUIDANCE AND CONTROL PROCEEDINGS OF THE G..(U) ADVISORY GROUP FOR AEROSPACE RESEARCH AND DEVELOPMENT NEUILLY.. DEC 87 AGARD-CP-431 1/2

UNCLASSIFIED F/G 17/7.3 NL

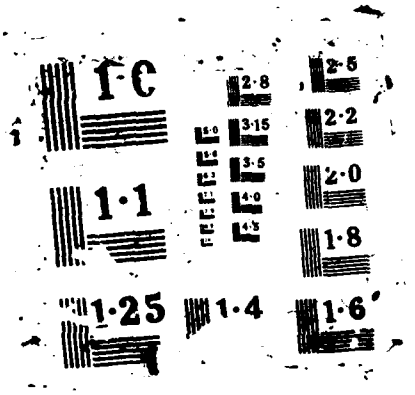
1·C
2·8
2·5
3·15
2·2
3·5
2·0
4·0
1·8
4·5
1·1
1·25
1·4
1·6

DTIC FILE COPY

(2)

AGARD-CP-431

AGARD-CP-431

AD-A194 648

AGARD

ADVISORY GROUP FOR AEROSPACE RESEARCH & DEVELOPMENT

7 RUE ANCELLE 92200 NEUILLY SUR SEINE FRANCE

AGARD CONFERENCE PROCEEDINGS No.431

Advances in Air-Launched Weapon Guidance and Control

DTIC
ELECTE
APR 14 1988
S D
E

NORTH ATLANTIC TREATY ORGANIZATION

DISTRIBUTION AND AVAILABILITY
ON BACK COVER

88 4 13 022

COMPONENT PART NOTICE

THIS PAPER IS A COMPONENT PART OF THE FOLLOWING COMPILATION REPORT:

TITLE: Advances in Air-Launched Weapon Guidance and Control, Proceedings of the Guidance and Control Panel Symposium Held in Athens (Greece) on 5-8 May 1988.

TO ORDER THE COMPLETE COMPILATION REPORT, USE AD-A194 648.

THE COMPONENT PART IS PROVIDED HERE TO ALLOW USERS ACCESS TO INDIVIDUALLY AUTHORED SECTIONS OF PROCEEDING, ANNALS, SYMPOSIA, ETC. HOWEVER, THE COMPONENT SHOULD BE CONSIDERED WITHIN THE CONTEXT OF THE OVERALL COMPILATION REPORT AND NOT AS A STAND-ALONE TECHNICAL REPORT.

THE FOLLOWING COMPONENT PART NUMBERS COMPRISE THE COMPILATION REPORT:

AD#: AD-P005 714 thru AD#: AD-P005 720

AD#: AD#:

AD#: AD#:

Accession For
NTIS GRA&I ☑
DTIC TAB ☐
Unannounced ☐
Justification
Distribution/
Availability Codes
Avail and/or
Dist Special
A-1

DTIC
ELECTE
JUL 07 1988
S D
D

DISTRIBUTION STATEMENT A
Approved for public release;
Distribution Unlimited

DTIC FORM MAR 85 463

OPI: DTIC-TID

NORTH ATLANTIC TREATY ORGANIZATION

ADVISORY GROUP FOR AEROSPACE RESEARCH AND DEVELOPMENT

(ORGANISATION DU TRAITE DE L'ATLANTIQUE NORD)

AGARD Conference Proceedings No.431

ADVANCES IN AIR-LAUNCHED WEAPON GUIDANCE AND CONTROL

By
Distribution/
Availability Codes
Dist | Special
A-1
DTIC COPY INSPECTED

Papers presented at the Guidance and Control Panel 44th Symposium held in Athens, Greece from 5 to 8 May 1987.

This document has been approved for public release and sale; its distribution is unlimited.

THE MISSION OF AGARD

According to its Charter, the mission of AGARD is to bring together the leading personalities of the NATO nations in the fields of science and technology relating to aerospace for the following purposes:

— Recommending effective ways for the member nations to use their research and development capabilities for the common benefit of the NATO community;

— Providing scientific and technical advice and assistance to the Military Committee in the field of aerospace research and development (with particular regard to its military application);

— Continuously stimulating advances in the aerospace sciences relevant to strengthening the common defence posture;

— Improving the co-operation among member nations in aerospace research and development;

— Exchange of scientific and technical information;

— Providing assistance to member nations for the purpose of increasing their scientific and technical potential;

— Rendering scientific and technical assistance, as requested, to other NATO bodies and to member nations in connection with research and development problems in the aerospace field.

The highest authority within AGARD is the National Delegates Board consisting of officially appointed senior representatives from each member nation. The mission of AGARD is carried out through the Panels which are composed of experts appointed by the National Delegates, the Consultant and Exchange Programme and the Aerospace Applications Studies Programme. The results of AGARD work are reported to the member nations and the NATO Authorities through the AGARD series of publications of which this is one.

Participation in AGARD activities is by invitation only and is normally limited to citizens of the NATO nations.

The content of this publication has been reproduced
directly from material supplied by AGARD or the authors.

Published December 1987

Copyright © AGARD 1987
All Rights Reserved

ISBN 92-835-0439-9

Printed by Specialised Printing Services Limited
40 Chigwell Lane, Loughton, Essex IG10 3TZ

PREFACE

A GCP Symposium on the subject of "Tactical Air Launched Missiles" was held in 1980 at Eglin AFB, Florida, USA. Many advances in guidance sensor technology and guidance/control implementation techniques have taken place since that time. In addition, there have been advances in various guided weapon subsystem technologies which have important impacts on guidance and control requirements and design techniques.

The direct cost of guidance and control system design as well as test and evaluation has placed much more emphasis on simulation. In particular, physical simulation using hardware/software-in-the-loop techniques has experienced considerable importance.

However, all advances in sensor-and signal processing technology and guidance/control techniques only lead to improvements in operational effectiveness if a total systems approach to the vehicle/weapon/mission environment is pursued.

It was felt, therefore that a symposium on this subject in 1987 was timely. The symposium treated both air-to-air and air-to-surface weapon systems and emphasised guidance and control technology advances and guidance impacts from advances in other areas.

***

La Commission Guidage et Pilotage avait organisé à EGLIN (Floride), une conférence sur le thème des "Missiles Tactiques Air-Sol et Air-Air". Depuis lors, de nombreux progrès ont été réalisés dans la technologie du capteur de guidage et dans les techniques de mise en oeuvre du guidage et du pilotage. Ces progrès concernent également les technologies des sous-systèmes d'armes guidées et plus précisement les exigences du guidage et du pilotage ainsi que les techniques de conception.

Le coût direct de la conception du guidage et des essais et évaluations correspondants a amplifié l'importance de la simulation. C'est le cas, en particulier, de l'utilisation des techniques de simulation physique avec éléments réels dans la boucle.

Toutefois, les progrès de la technologie des capteurs et du traitement de leurs signaux ne conduisent à des avancées que si se poursuit une approche globale de l'environnement véhicule-arme-mission.

Il est donc apparu qu'un symposium consacré à ce sujet en 1987 serait approprié. Cette conférence a traité des systèmes d'armes air-air et air-sol. Elle a mis l'accent sur les progrès du pilotage et du guidage et sur les répercussions, en ce qui concerne le guidage, des avancées realisées dans d'autres domaines.

GUIDANCE AND CONTROL PANEL OFFICERS

Chairman: Mr Kenneth A.Peebles
Director, Electro-Optics Division
Defence Research Establishment Valcartier
2459 Pie XI Boulevard Nord
Courcelette, P.Q. G0A 1R0, Canada

Deputy Chairman: Ir P.Ph Van den Broek
Department of Aerospace Engineering
Delft University of Technology
Kluyverweg 1
2629 HS Delft, Netherlands

TECHNICAL PROGRAMME COMMITTEE

Chairman:	Mr U.K.Krogmann	GE
	Dr W.P.Albritton	US
Members:	Mr J.B.Senneville	FR
	Dr Th.Spathopoulos	GR
	Ir G.J.Alders	NE
	Mr S.Leek	UK
	Mr R.S.Buffum	US

PANEL EXECUTIVE

From Europe:
Lt Colonel A.Rocher, FAF
AGARD-OTAN
7 Rue Ancelle
92200 Neuilly-sur-Seine, France

From USA and Canada only:
AGARD-NATO
APO New York 09777

Telephone: (1) 4738 5780 — Telex: 610176 F

HOST PANEL COORDINATOR

Dr Th.Spathopoulos
Director of Research and Development
Hellenic Aerospace Industry Ltd
Building 31, 13—0 i
PO Box 23
GR 32009 Schimatari, Greece

ACKNOWLEDGEMENTS/REMERCIEMENTS

The Panel wishes to express its thanks to the Hellenic National Delegates to AGARD for the invitation to hold this meeting in their country and for the facilities and personnel which made the meeting possible.

Le Panel tient à remercier les Délégués Nationaux de la Grèce près l'AGARD de leur invitation à tenir cette réunion dans leur pays et de la mise à disposition de personnel et des installations nécessaires.

CONTENTS

	Page
PREFACE	iii
PANEL OFFICERS AND PROGRAMME COMMITTEE	iv
TECHNICAL EVALUATION REPORT by C.Baron	viii
	Reference
KEYNOTE ADDRESS by P.Kontodios	K†
SESSION I – GUIDANCE DATA SOURCE ADVANCES **Chaiman: Dr Th.Spathopoulos, GR**	
A PROTOTYPE FIBRE OPTIC GYROSCOPE FOR MISSILE GUIDANCE APPLICATIONS by C.J.Kay	1
GYROMETRE LASER TRIAXIAL MONOBLOC DE PETITE DIMENSION par S.Petit, M.Perbet et Y.Touze	2*
LOW COST TACTICAL RING LASER GYRO by J.Hanse, J.Killpatrick and M.Weber	3*
A MINIATURE, LOW COST INERTIAL MEASUREMENT UNIT by R.E.Stewart and S.N.Fersht	4*
VELOCITY UPDATER STUDY AND FLIGHT TEST by J.T.Ritland and J.R.Cloutier	5*
Paper 6 withdrawn	
ACOUSTICAL TERMINAL GUIDANCE FOR DECELERATED SUBMUNITION by J.Lang and D.Kalus	7*
SESSION II – FLIGHT PATH CONTROL ADVANCES **Chairman: S.Leek, UK**	
AUTOPILOT DESIGN FOR HIGHLY MANEUVERABLE WINGLESS MISSILES by G.Grebing, U.Hartmann and J.Schnatz	8*
APPROXIMATE NONLINEAR FILTERING FOR PIECEWISE LINEAR SYSTEMS by A.H.Haddad, E.I.Verriest and P.D.West	9*
DECOUPLAGE DE LA LIGNE DE VISEE D'UN AUTODIRECTEUR GRACE A UNE REFERENCE INERTIELLE A ELEMENTS LIES par M.Lemoine	10*
AN INVESTIGATION OF STEEP DESCENT GUIDANCE FOR TERMINALLY GUIDED SUBMUNITIONS by G.Trottier	11
PASSIVE TERRAIN FOLLOWING FOR STAND-OFF WEAPONS APPLICATIONS USING A DIGITAL TERRAIN ELEVATION DATA BASE by S.R.Morgan	12*
EFFECTS OF CLOSING SPEED UNCERTAINTY ON OPTIMAL GUIDANCE by W.W.Willman	13

*Printed in Classified Publication CP 431 (Supplement)
†Not available at time of printing

Reference

SESSION III: OPERATIONAL REQUIREMENTS, SYSTEMS CONSIDERATIONS
Chairman: G.J.Alders, NE

GUIDAGE ET PILOTAGE DES ARMEMENTS TIRES D'AVION: POINT DE VUE DE L'AVIONNEUR
par P.Pagniez et F.Chivot 14

SYSTEME DE CONTROLE AUTOMATIQUE DU VOL POUR HELICOPTERES MODERNES
par J.C.Derrien et P.Cauvy 15

COMPUTER AIDED TACTICS FOR AIR COMBAT
by N.Mitchell 16

TACTICAL SUPPORT AVIONICS FOR THE TARGETTING OF AIR LAUNCHED WEAPONS
by M.J.E.Peacock and G.Mann 17*

STAND-OFF MISSILE NAVIGATION USING TERRAIN-REFERENCED NAVIGATION AND SCENE-MATCHING CORRELATION
by A.R.Runnals and D.S.Henderson 18*

MODULAR STANDOFF WEAPONS (MSOW) PROGRAM
by R.H.Hoh, J.L.Ruttler and S.E.Adams 19*

SESSION IV: SUBSYSTEM TECHNOLOGY ADVANCES, GUIDANCE AND CONTROL IMPACTS
Chairman: U.K.Krogmann, GE

DEVELOPMENT, TEST AND EVALUATION OF THE TRANSFER ALIGNMENT FOR AN AIR LAUNCHED ANTISHIP MISSILE
by J.Bardal and O.Hallingstad 20*

A FIBER OPTIC GYRO STRAPDOWN REFERENCE SYSTEM FOR GUIDED WEAPONS
by D.Rahlfs, W.Auch, O.Glaser and D.Ruppert 21

Paper 22 withdrawn

INTERACTIONS AERODYNAMIQUES DE JETS TRANSVERSAUX SUR MISSILES
par M.Leplat, P.Champigny et M.Robert 23*

SPEED CONTROL OF A MISSILE WITH THROTTLEABLE DUCTED ROCKET PROPULSION
by D.Thomaier 24

SESSION IV (Cont'd): SUBSYSTEM TECHNOLOGY ADVANCES, GUIDANCE AND CONTROL IMPACTS
Chairman: J.B.Senneville, FR

ANALYSIS, DEVELOPMENT AND TESTING OF STRAPDOWN SIGNAL PROCESSING FOR HIGH VIBRATION AND DYNAMIC ENVIRONMENT
by D.Wick and M.Kopf 25*

SYSTEM PARTITIONING AND VLSI IMPLEMENTATION FOR MULTI-MODE MISSILE GUIDANCE
by A.W.Walker 26*

AN ADA PROGRAMMABLE FLIGHT COMPUTER
by R.Cook and I.M.Kay 27*

Papers 28 and 29 withdrawn

SESSION V: TEST AND EVALUATION TECHNIQUES
Chairman: Dr W.P.Albritton, Jr, US

HIGH RESOLUTION TARGET SIGNATURES AT 94 GHZ
by E.P.Baars and H.Essen 30*

*Published in Classified Publication CP 431 (Supplement)

	Reference
REAL-TIME H.W.I.L. DUAL MODE RADAR TARGET SIMULATION by M.W.Hosking	31*
HARDWARE IN THE LOOP TESTING OF PENGUIN MK3 CONTROL UNIT by K.Loewe	32*
THE USE OF HARDWARE-IN-THE-LOOP TECHNIQUES IN THE DEVELOPMENT OF A MODERN AIR-TO-SURFACE MISSILE SYSTEM by T.Küstner	33
RESULTS OF AN AIR COMBAT SIMULATOR TRIAL EMPLOYING A FAST FLYOUT MISSILE MODEL by N.R.T.Seavers	34**

*Published in Classified Publication CP 431 (Supplement)
**Paper not cleared for publication

TECHNICAL EVALUATION REPORT

by

C.Baron, MSc
18 Vicarage Lane
The Bourne
Farnham, Surrey GU9 8HN
UK

1. INTRODUCTION

The Symposium was held in the National War Museum, Athens, from the 5th to the 8th May, 1987. The programme Co-Chairmen were Dr W P Albritton of Rexham Aerospace, USA and Mr U K Krogmann, Bodenseewerk, FRG. The meeting was attended by 161 people, the largest delegations coming from the FRG, the UK, France and the US, in that order. In addition to the Symposium, a special session was organised at the request of the Hellenic authorities on the subject of "Simulation Aspects of Air Launched Weapons". Since this was solely for the benefit of the Host Nation's engineers, however, it is not reported here.

2. THEME AND OBJECTIVES

Modern defences ensure that aircraft will have extreme difficulty in penetrating heavily defended areas, and the development of improved stand off weapons is therefore of the greatest importance. Current weapons which have sufficient stand off suffer however through being effectively limited to targets of high value and physical prominence, the former because of the high cost of the weapons themselves and the latter because of their limitations in navigation and target discrimination. Since the guidance and control system plays a large part in determining both cost and performance, there should obviously be great value in holding a symposium on the subject, enabling the presentation and comparison of recent progress, and the informal interchange between national experts which so often is even more valuable than the formal programme itself.

3. OPENING ADDRESSES

On behalf of the Host Nation, the Symposium delegates were welcomed to Greece by Major General G Stafilidis who in addition to being Chief of C Branch of the Hellenic Air Force General Staff, is also Greek National Delegate to AGARD. He stressed the importance of achieving more effective and affordable weapons; this would require improved collaboration between experts of different disciplines and different nations, and he welcomed the meeting as a contribution to this end.

The Keynote Address was given by Major General P Kontodios, lately National Delegate to AGARD and now Adviser to the Deputy Minister of Defence. He envisaged the programme doing justice to the subject, covering the range from low cost reliable components through to complex weapon systems. Smaller nations like Greece must adapt to use new technology because it offers the possibility of resistance to superior numbers, but experience has taught them that complex systems are often unreliable. This led him to pose a number of questions. Can improved performance be reliably achieved at lower cost? Cannot simpler solutions be found by the exercise of ingenuity? Can they be developed without imposing increased workload on the humans in the system, whose capability cannot be increased?

For the less developed nations co-operation in research, development and production of new weapon systems has great attraction, and it may be that their very situation will make it possible for them to contribute towards simpler solutions to problems. The Alliance should make serious efforts to facilitate their participation, and a range of modular ASM's may provide a very suitable opportunity for it.

4 TECHNICAL CONTENT

SESSION I: GUIDANCE DATA SOURCE ADVANCES

This session provided an interesting view of progress in missile navigation components and technology. Papers 1 and 3 dealt with gyros in contrasting states of development. Kay (1) described a fibre optic gyro which, while still in the laboratory stage, has shown promising performance combined with ruggedness, quick starting and low cost. Hanse (3) on the other hand presented a miniature version of the well known and highly developed Honeywell range of ring laser gyros; ingenuity was displayed in both papers in design and production techniques towards achieving cost aims of $500 and $1000 respectively, which should be attractive to missile designers.

More radical solutions however may also be available in the future. Petit (2) described the achievement of three axis gyrometry using multiple orthogonal paths with common mirrors, etc, within an octahedron block. Feasibility had been demonstrated in a 250mm diameter (sic) model, and tests were now under way on a unit of maximum dimension 80mm. Though in principle this should yield a low cost system, this may not be achieved easily. In an equally innovative approach, an inertial measurement unit based entirely

on accelerometers was described by Stewart (4); by measuring the induced Coriolis acceleration of a vibrating accelerometer, angular rate and linear acceleration can both be measured in a single accelerometer. The key to the successful demonstration of the concept was a silicon accelerometer, a cantilever beam suspended pendulum, electrostatically nulled, within a silicon wafer. Unfortunately, whereas most other papers aroused discussion,this one followed the lunch break and delegates failed to extract the vital missing information on this system's performance. However, given its small size and power requirement and a quoted system cost of around $2000, interest cannot fail to be sustained. Contrasting with these revolutionary approaches, a perennial topic of the past was now brought to light again by Ritland (5). Improvements in Doppler radar sensors have now made it worthwhile to consider their possible application, in combination with modern inertial sensors, to missile navigation, and this study had been carried through to flight testing. Where high precision and long range is required it appears that Doppler with a low cost IMU could be competitive with a high quality pure inertial system. Given the alternatives, and the limitations of Doppler (e.g. over water) applications of real promise are not obvious however.

Finally, leaving navigation aside, Lang (7) discussed the use of acoustic sensors for terminal guidance of low velocity submunitions. While in many ways it might appear unpromising, such a system offers some attractions: it is passive, self limiting to noisy objects (tanks, helicopters), can operate at night, in fog or dust or any but heavy rain, and is not decoyed by dead targets. The slow measurement rate, however, places limitations on vehicle speed which make it difficult to deal with target motion, at least at normal helicopter speeds. Simulation, however, indicated good results against tanks, though the audience expressed some doubts about discrimination between multiple targets. It may be that acoustic homing could provide a complementary addition to IR without excessively increasing the cost.

SESSION II: FLIGHT PATH CONTROL ADVANCES

In many missile applications the problems of flight control have been effectively solved, but there remain a number of areas where the search for improved performance in more exacting situations calls for fresh advances, and the availability of digital systems of almost unlimited capability offers solutions hitherto unattainable.

Perhaps the most obvious such case is that of the short range air to air missile; all such missiles so far have been seriously limited at the shortest ranges, and the increased manoeuvre capabilities of modern fighters have accentuated the problem. The papers by Hartmann (8) and Willman (13) directly addressed this situation, the former dealing with a practical design for a high performance wingless missile, and the effects of the associated non linear aerodynamics, while Willman offered a means of achieving an optimized guidance law over all ranges by a weighting approach to flight conditions. A theoretical route to non linear system design, based on Markov procedures, was discussed by Haddad (9) providing the possibility, with today's computing capabilities, of practical non linear filtering. For air to air missiles of longer range the strapdown inertial reference system has its attractions, and Lemoine (10) described its use to decouple the homing head from missile body motion, and compensate for radome aberration, so improving homing accuracy.

The terminally guided submunition poses an equally critical but rather different problem, that of achieving accurate guidance in very small size and at very low cost, though in relatively simple flight conditions. Kindly substituting at the last moment for a withdrawn paper, Trottier (11) considered the design problem of attacking a tank from a TGSM initially in level flight; an assumed upper limit to seeker sightline rate determined a low TGSM speed and hence a large wing size, suggesting that the more usual vertical approach from parachute suspension may be preferable.

Finally Moyan (12) described the design of a passive terrain following system integrated with terrain reference navigation, showing how the required system performance characteristics led to the autopilot design, which was unusual mainly in taking advantage of the opportunity to use pre-knowledge of required manoeuvres. The paper concluded with an interesting analysis of exposure and vulnerability in relation to TF performance.

SESSION III: OPERATION REQUIREMENTS, SYSTEM CONSIDERATIONS

In a session which gave interesting coverage of overall system design issues the first part was taken by the aircraft designers. Reviewing the various types of air launched weapon Pagniez (14) showed how the increasing performance and complexity of modern missiles is making ever more demands on the aircraft system. Close collaboration between aircraft and weapon designers was rightly demanded, and the weapon designer must take particular care not to make excessive demands on the single seat aircraft pilot, or to place requirements on the aircraft which increase its vulnerability.

In a slightly smaller canvas, Derrien (15) discussed the particular manoeuvres and profiles that the armed services call for from their helicopters, and demonstrated how this had led to design methods and ultimately to system designs for helicopter flight control.

The complex tactical situations facing the fighter pilot in the central European theatre were the concern of Mitchell (16) who described an attempt, through battle simulation, to design systems to assist pilots in tactical decision taking.

The next three papers in their different ways represented the avionics and weapons designers' approach to system problems. Peacock (17) described the collaboration of several UK firms in an attempt to relieve workload of the fighter ground attack pilot through the automatic management of his mission systems; one component of this endeavour is a technique to display ridge lines derived from a stored digital terrain data base, augmenting FLIR information to provide a more readily assimilable picture of the terrain ahead.

In a well presented paper Runnalls (18) described two methods of navigation based on stored terrain data, by contour matching and scene matching respectively. He showed that their properties are such as to make them complementary, and presented the results of flight trials in which the improvement in accuracy from using them together was clearly evident.

Finally, and rather from a project office stand point, Hoh (19) presented the seven nation Modular Stand Off Weapon programme. The operational need for stand off weapons has been evident for some years and has been discussed in previous symposia and in many other NATO fora. The problem remains that of finding a way to meet it economically. Multinational sharing of development costs and summation of production numbers offers a possible solution, and modularity may enable the differing requirements of the nations to be met at much less cost than that of providing a different weapon for each of them While we must all hope for the success of the programme, many delegates felt the time scale presented to be optimistic.

SESSION IV: SUBSYSTEM TECHNOLOGY ASPECTS, GUIDANCE AND CONTROL IMPACTS

This session brought together a number of somewhat diverse topics, which had however the common thread that software, and its interaction with hardware, is playing an ever-increasing role. A succession of AGARD symposia have heard descriptions of aspects of the superb engineering of the Norwegian Penguin missile system, and on this occasion it was the transfer alignment between aircraft and missile navigation systems that was presented by Bardal (20). The problems encountered were candidly reviewed, from which emerged the importance of achieving integration of subsystems in simulation at as early a stage as possible, and the cost savings achievable through first, simulation, and second, captive flight testing, before missile flight trials.

In a paper closely related to paper (1), and which might well have found its place in Session I, Rahlfs (21) described the development of fibre optic gyros and their incorporation in strapdown IN systems. The wide bandwidth and simple error structure of this type of gyro are shown to have advantages which, combined with their small size, make them attractive for missile systems.

The high manoeuvrability and rapid response demanded of short range air to air missiles make the use of transverse reaction jets attractive for manoeuvre control. Leplat (23) had carried out a series of wind tunnel investigations to determine the aerodynamic effects for a variety of nozzle-wing-tail configurations. It was evident that a full understanding of these effects would be necessary to take full advantage of the technique in control system design.

Control of axial acceleration has rarely been considered for tactical missiles, but developments of long range air to surface missiles are now calling for high speed and flexibility of trajectory and launch conditions, making control of motor thrust essential. Thomaier (24) dealt with thrust-control for a ducted rocket motor; the control system design was severely constrained by the practicalities of the situation, but the test results presented showed that an effective system had been achieved.

In the first of these papers devoted specifically to software, Wick (25) described the design of a signal processing system for laser gyro based strapdown IN systems, in which the processing was designed to minimise the errors induced by vibration and other motions.

In the next paper (26) an integration of the functions of scene matching navigation, target detection and correlation terminal homing was proposed by Walker. These functions have much in common in principle, and the idea is that some re-arrangement of their processing architecture would make their integration in a single system economic, with large savings in volume and power.

The need for standardisation raised at various times in this symposium would be advanced by the general adoption of the ADA language, and Cook (27) described one firm's attempt to build up facilities and experience for its use. While some drawbacks were acknowledged, he concluded that ADA has very worthwhile advantages, its deficiencies are steadily being whittled away, and it offers facilities which are otherwise unobtainable. In the discussion period a show of hands indicated that few participants had so far made any use of ADA, but an increasing number are likely to use it in the future.

SESSION V: TEST AND EVALUATION TECHNIQUES

The first paper of this session (Baars, 30) described some very thorough and accurate measurements of tank target signatures at 94GHz, demonstrating the effects of mud and camouflage.

The rest of the papers dealt with simulation, with hardware in the loop, and those interested in the topic would be advised to read first paper 33 by Kuestner, which provides a very clear general introduction to the subject.

Hoskins (31) dealt rather more specifically with the methods used to simulate the response of a missile with a radar seeker to a complex electromagnetic environment, including the wide variety of ECM, clutter, reflection and diffraction effects which can occur.

In paper 32, Loewe described a simulator facility used to carry out hardware in the loop testing of the Penguin Mk3 missile control system. It was in fact the software in the hardware in the loop (!) which was under test, and valuable results in terms of detection of software errors and avoidance of wasted flight tests ensued.

ROUND TABLE DISCUSSION

The formal programme was completed by a Round Table Discussion in which Dr Albritton chaired a panel of experts in the discussion of three vitally important and contrasting topics.

It is clear that co-operative development of modular weapons will only be achievable with any degree of economy if effective standards exist. One panel member, Mr Trottier traced the history of NATO's effort in this area stemming from a Defence Research Group Working Group of 1982, and in its continuation offering hope that suitable standards may become available. Mr Leek, also from the panel, drew attention to the standardisation potential to the ADA language system. From the floor however, there was a good deal of scepticism; many examples of the disadvantages of the 1553 bus standard, if used in missiles, were quoted, though its value in some more complex aircraft applications was acknowledged, and its ability to be evolved into the more advanced standard 3910 was welcomed. There were also those who feared that standards would limit technological progress, and there is no doubt that the length of time it takes to develop standards does tend to produce this effect. As Dr Albritton pointed out, early action to anticipate the need for standards, and rapid decisions on their adoption could do much to improve the situation.

The next question tackled was that of optimal control; why has it been so little used, in contrast to the popularity of optimal estimation? Here the responses both from the panel and the audience tended to be pessimistic. There were those who felt that the theoreticians had failed to provide practically usable techniques, to which Prof Haddad responded that optimality is difficult to define for a problem as full of uncertainty as missile guidance; he felt that designers would be better advised to place emphasis on robustness to the wide range of target and environmental conditions encountered. Agreeing from the panel, Mr Hartmann pointed out that to achieve this the second best solution is often the most practical. Clearly in the minority, perhaps through looking further ahead, the Chairman argued that, for example, proportional navigation is only optimal for a constant speed missile and a non-manoeuvring target - in this respect a fully optimal system must be more robust; moreover, while he conceded that the computing requirements would be greatly increased, a fully integrated optimal system could reduce the requirements in other areas, such as sensors.

Finally attention was focussed on the high cost of missiles, now clearly leading to the reduction of military stocks to dangerous levels. The rapid reduction in the cost of electronic components has had little apparent impact on system costs. For the panel, M Lemoine suggested that this was because too much emphasis is continually laid on increased performance, too little on reducing costs; there is much scope, given the will, for reducing the number of components in missiles. Mr Krogmann considered that closer collaboration between Service staffs and technologists in the writing of military requirements could not only reduce areas where excessive performance demands lead to very high costs, but in some instances eliminate over cautious requirements where extra performance might be obtained a little extra cost. A good deal of attention was focussed on the high costs imposed by excessive bureaucracy, particularly as regards quality control. It is sad that in spite of this, or possibly even because of it, military equipment reliability often leaves much to be desired, greatly increasing system lifetime costs; the increase in complexity stemming from demands for high performance contribute to this. Both panel and audience laid much of the blame for high costs on politicians and military staffs; changes in requirements while development is in progress frequently give rise to design compromises, unreliability and high cost. Failure of governments to order large enough batches, even though their total requirements are large, prevent the use of the most economic manufacturing systems, and government policies discourage industry from bearing the risk themselves. However, it was pointed out that both technologists and industry have a vested interest in complexity - the former as an interesting challenge and the latter as a source of profit. It was surprising that no reference was made to the Proceedings of the 39th Symposium of the Panel, held in October 1984, which contain a great deal of value on this subject.

So ended a very stimulating discussion, from which most of those present must have taken home something to think about -- a fitting end to a very worthwhile symposium.

5. AUDIENCE REACTION

Only eight members of the audience completed the questionnaires issued, a sample unworthy of statistical examination. Their remarks however did confirm my own impressions and those gleaned in conversation. The poor standard of many visual aids was a disappointment, given the great improvements achieved in this area previously. The lack of any presentation of the users' point of view was a frequent source of complaint; while such presentations have often proved disappointing in the past, one wonders whether their absence in recent symposia indicates a widening gulf between technologists and the military. The most fundamental complaint however concerned the lack of depth in the papers; there can be little doubt that this was due to the excessive concern for security which is stifling of scientific interchange across the Alliance, but perhaps one can detect a slightly improving trend.

6. TECHNICAL APPRECIATION

In relation to its declared aims the symposium had serious limitations, for the critical aspects of target sensing and terminal guidance were almost completely unrepresented in the programme. However, progress was visible across the remainder of the spectrum, with interesting and original developments in navigation components and systems, and, in spite of the pessimism of the Round Table Discussion some early signs of a movement towards optimal control.

On the whole, air-to-air missiles received better treatment than air-to-surface, partly perhaps because most of the outstanding papers fell in the air-to-air field, and partly because of the paucity of papers on terminal guidance. In view of the importance of achieving advances in air-to-surface weapons this is to be regretted; given the impending competition for contracts in this area it seems likely that commercial secrecy is to blame - if so, firms should reflect that they may be losing more than they gain by this policy. Nevertheless, the meeting provided excellent coverage of navigation components and systems, flight control, and simulation, and touched upon a wide variety of other aspects of missile design, many of which rarely get a hearing.

7. MILITARY POTENTIAL

The symposium provided evidence of continuing progress in air-launched missile capability, though most of the papers would be of direct interest to systems designers rather than to the military, who will receive the benefits in the future. Many of the technical advances described could lead to lower cost weapon systems in due course, and in this connection the final Round Table Discussion aired many points which merit serious consideration by military staffs.

8. PRESENTATION AND ADMINISTRATION

The host country is to be congratulated on the high standard of conference facilities they provided. The Programme Committee had clearly had a difficult task in mounting a coherent programme from a very diverse set of offered papers; it was unfortunate, however, that one afternoon had been overloaded with a programme of six papers, and when two papers were withdrawn from other sessions, a re-arrangement to reduce the load on that afternoon would have been welcomed by participants. Apart from the poor visual aids already mentioned, the standard of presentation was generally good.

9. RECOMMENDATIONS

There can be no doubt of the long term importance of the subject and that it will be necessary to return to it in due course; the timing must depend on the readiness of those in the field to reveal progress made. Much interest in modular stand-off weapons was expressed by the delegates, and it is clear that this subject offers a wide range of significant technical problems which could form the basis of a valuable symposium in due course.

AD-P005 714

A PROTOTYPE FIBRE OPTIC GYROSCOPE FOR MISSILE GUIDANCE APPLICATIONS

C. J. KAY

British Aerospace plc
Army Weapons Division
Precision Products Group
Site A PB 181
Six Hills Way
Stevenage
Herts SG1 2DA
ENGLAND

ABSTRACT

The paper describes the design of a prototype fibre optic gyro, made by the Fibre Gyro Research team at British Aerospace, which is intended for missile guidance applications. Important design constraints for the next generation of missiles are wide dynamic range, rapid switch-on, extreme ruggedness, low cost, and digital operation.

These features are all embodied in the design described, which employs optical phase modulation in an integrated optical waveguide device. This also incorporates a Y-branch beam-splitter. Serrodyne phase ramps are impressed on the light propagating round the fibre optic sensor coil connected to the integrated optics chip, and rotation rate is measured by the serrodyne frequency needed to null the rotation-induced Sagnac phase shift. The gyro performance (drift and random walk), and errors up to 1000°/Sec., ~~will be~~ presented.

1. INTRODUCTION

In the future there will be an increasing demand for more agile missiles for both air and ground launched applications. Guidance systems will be included in gun-launched missiles where high accelerations at launch are common. The inclusion of strap-down guidance systems in missiles facing high roll and high acceleration has highlighted the need for more rugged navigation instruments having a dynamic range greater than that available from conventional gyros.

Fibre optic gyroscopes are ideal candidates for such applications since, being all solid-state, they are rugged and do not suffer from the restricted dynamic range of spinning mass gyroscopes. An additional advantage is that with very few component changes the fibre gyro can be designed around several different architectures to suite a wide range of applications. For instance if one wishes to increase the sensitivity it is possible to increase the fibre length used, with little excess loss, using currently available low-loss fibre. It is also possible to increase the sensitivity and scale factor by increasing the fibre coil diameter. Because the fibre gyro is all solid-state it is expected to be a very reliable device with a long shelf life. If the right choice of architecture and components are made, such that simple manufacturing methods can be used, then the cost will be low.

Several configurations of fibre optic gyroscope have been reported over the last few years using different modulation systems chosen to suit particular cost and performance goals. We report here on the performance of a prototype gyroscope made during our development programme. The programme aim was to produce a low cost, wide dynamic range gyroscope with an output suitable for connection to digital guidance systems. Such a gyroscope is intended to be used in three-axis strap-down inertial measurement units in low to medium accuracy missiles and guided mortars.

2. MARKET CONSIDERATIONS

The fibre gyroscope should be capable of satisfying future gyroscope markets which are not at present covered by existing gyroscope technology. The required performance and size requirements should be achieved at a cost equal to or below that of current instruments. Three market sectors can be immediately identified:-

i. At the high accuracy end, such as North seeking gyros used while borehole logging for mineral exploration, where high accuracy is required in a very severe environment, where very high temperatures are encountered, and where very high levels of shock and vibration are reached. The market for such devices is modest though the market could stand a fairly high individual sensor cost.

ii. Medium accuracy agile missiles where fast turn rates, up to 2000°/Sec, may be encountered. Launch conditions are not expected to be severe in this particular application, though instant start and wide bandwidths are important requirements. This is a medium volume market.

iii. Artillery shells are a large volume market where the accuracy requirements are relaxed but the g-hardening requirement is severe and high rates of turn and high acceleration (~ 20,000g) are likely to be encountered at launch.

The gyro whose performance is being described is being developed by British Aerospace for applications in the medium accuracy missile market.

3. TYPICAL DESIGN GOAL SPECIFICATION

Within the fibre gyroscope development programme, the prototype gyro design specification should demonstrate the capabilities of current technology showing that all of the performance parameters necessary for the intended market can be achieved. Using available technology, British Aerospace has been developing a fibre optic gyroscope with the following performance goals.

TABLE 1 - GYRO PERFORMANCE DESIGN GOALS

SCALE FACTOR.....	30,000 to 50,000 pulses/rad
SCALE FACTOR STABILITY.....	100 ppm of FSD
WARM UP TIME.....	<0.1 Sec
RANDOM WALK.....	1°/√Hr
BIAS UNCERTAINTY.....	10°/Hr
TEMPERATURE RANGE.....	-40 to +55°C
ACCELERATION.....	20,000g
RESOLUTION OF OUTPUT.....	16 BITS
OUTPUT DATA RATE.....	up to 1 KHz
ANALOGUE BANDWIDTH.....	400 Hz
SIZE.....	50-75mm x 30mm
COST AIM.....	< $500 per axis

3.1 Performance vs size

Whilst the performance aspects have carried most weight so far, the size consideration has not been ignored. However the sizes of certain 'off the shelf' components (designed mainly for the communications market) do not at this time lend themselves to the size constraints embodied in Table 1. Our development programme so far has therefore sacrificed size in respect of availability of components such as the light source which comes packaged in a 14 pin DIL hermetically sealed case. Using such components we have developed a prototype gyroscope which occupies a volume of 0.42 litres (75mm cube). This package contains all the optical components of the gyroscope together with the associated control and interface electronics boards. The digital electronics package performs counting and interface functions, and a microprocessor is included to perform compensation of temperature and other environmental effects, necessary for this single axis sensor. It also provides scaling to produce an output as required by the user.

Since it is likely that such a gyro would form part of an integrated Inertial Measurement Unit (IMU), the unit has been designed so that most of the digital interface electronics package could be used by all three axes, so reducing total IMU cost.

The fibre optic gyro by its very nature is a modular design, each module being connected to the next by optical fibre. This characteristic enables it to be fitted into any available space. One of the existing limitations is the length of the integrated optics (currently 40mm), together with its associated fibre coupling system, which form part of the optical processing in the device. In the current prototype the integrated optics are placed inside the fibre coil perpendicular to its axis. However this is not the only possible arrangement and the integrated optics could be located remotely if packaging constraints required it.

The optical fibre used in this gyroscope is made to standard telecomms dimensions, though in future both the fibre and jacket dimensions could be reduced substantially to fit a smaller package. The coil in the prototype has been wound on a large (68mm) diameter spool to avoid excess bend loss and to retain as large a scale factor as possible. However if the requirement were to sense movement of say a seeker head, use of different fibres would enable very small coils to be wound. The sensor coil could then be located on its own, for instance in a seeker head or, perhaps, in the arm of say an industrial robot, whilst the integrated optics and other gyro components could be located remotely and joined together only by single mode fibres. The gyro is a sensitive optical component and although it can be made modular, once the optical paths of all modules are joined together during assembly, they cannot subsequently be separated easily.

4. THE FIBRE OPTIC GYRO

The fibre optic gyroscope uses the Sagnac effect to sense rotation rate [1] whereby beams of light propagating in opposite directions around a circular path see different path lengths when subject to a rotation about a common axis orthogonal to the direction of light propagation.

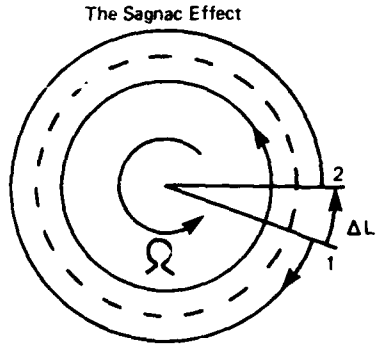

Fig. 1 The Sagnac Effect

The output beam from a light source is divided into two counter-rotating beams by an optical beam-splitter at 1(Fig. 1). These two beams are launched into either end of a fibre coil which is rotating with rate Ω. On recombining at the beam splitter, now at 2, they interfere, now having a relative path difference of 2ΔL due to the rotation. The path difference can be expressed in terms of a phase shift which is directly proportional to rotation rate, and is seen as the change in intensity produced by the interference of the two returning beams. The magnitude of a rate-induced phase shift is proportional to the area enclosed by the coil, and so the relative sensitivity of the fibre optic gyro can be increased by using more fibre, winding larger diameter coils, or both.

Because the size of the rate-induced phase shift is so small (about $1/10^6$ of a wavelength at the limit of performance of the gyro), care must be taken to ensure that all other non-reciprocal phase shifts are eliminated by confining both beams to travel the same optical path. To achieve this, the coil is made from single mode fibre and a single-mode spatial filter and polariser form the common input/output arm to the interferometer (Fig. 2), following the well established guidelines of the minimum gyro configuration [2]; this ensures single mode and single polarisation propagation.

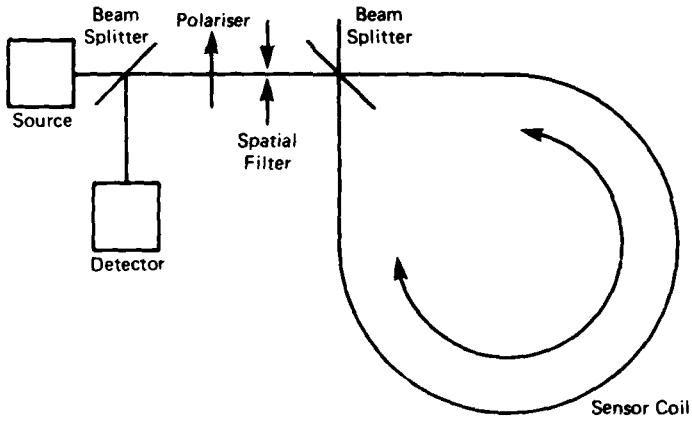

Fig. 2 Spatial Filter and Polariser

It is also necessary to ensure that no other beam except the two desired beams reach the detector coherently; this implies that steps must be taken to avoid reflections at joins by making sure that all reflections do not re-enter the guided path [3] and to remove the effects of Rayleigh backscatter [4] in the fibre by ensuring that such backscattered light is incoherent and does not interfere with the Sagnac beam.

A suitable detection technique must be employed to measure the small induced phase shifts. The actual phase shift is linearly proportional to rotation rate, however the intensity at the detector is a $\cos^2$ function of phase. At rest, the gyro is normally biased at the peak of the zero order fringe where the detected intensity is a maximum but the phase sensitivity is a minimum. It is also a point where intensity changes suffer from directional ambiguity. The application of a $\pi/2$ bias to a modulator at one end of the sensor loop (Fig. 3) removes the ambiguity and moves the detection point to the most sensitive and most linear portion of the fringe pattern. The bias is normally applied as an AC phase modulation, which brings with it the advantage of an AC detection scheme reducing the effect of 1/f noise at low frequency [5].

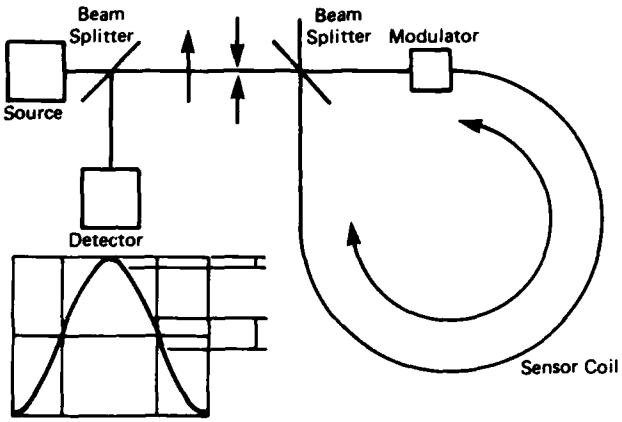

Fig. 3 Modulation and the Fringe Pattern

4.1 Modulation and control system

We apply an AC dither phase modulation to bias the gyro away from the peak of a fringe and use a synchronous detection system. A square wave dither signal drives a modulator at one end of the coil and applies a $\pi/2$ phase shift to the beam (Fig. 4). Though we use the term dither this must not be confused with the mechanical dither applied to ring laser gyroscopes to avoid lock-in. The period of the dither is equal to twice the delay time around the fibre coil. Taking advantage of this delay, dither applies the phase shift first to one beam and then the other, alternately biasing the gyro to the half intensity points of the fringe on either side of the maximum. At rest the same signal is then observed at the detector in each loop-time and the a.c. component is at a null.

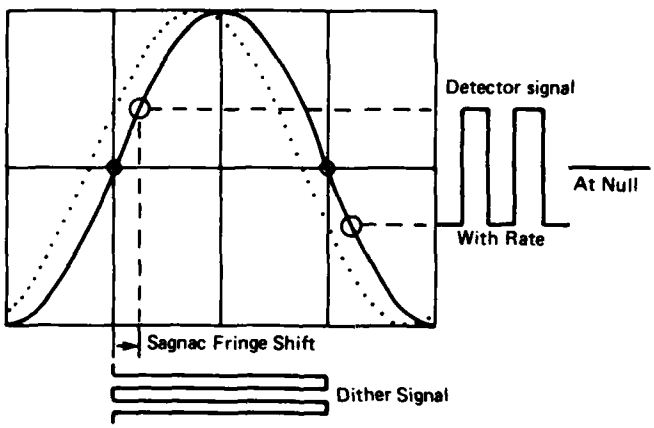

Fig. 4 Dither Modulation

If a rate is applied to the sensing coil then a signal appears at the detector synchronous with the dither signal. This signal is demodulated synchronously with the dither and the resulting output carries direction and phase information. However this signal is not linear with rate and has a dynamic range limited by the width of a fringe.

4.2 The frequency nulling gyro

One way of overcoming this non-linearity and dynamic range restriction is to operate the gyro in a frequency nulling closed loop [6]. In a frequency-nulling gyro, a frequency shifter is placed at one end of the coil (Fig. 5). A frequency shift can then be applied to one beam of light prior to propagating through the coil. The other beam is also shifted by the same frequency, but AFTER it has been round the coil. Because both beams propagate at different optical frequencies around the loop, a differential phase shift is set up between them when they arrive back at the beam-splitter at the same frequency. This differential phase shift can be used to null out the Sagnac phase shift by varying the applied frequency with the filtered output of the demodulated detector signal. The correcting frequency is linearly proportional to the applied phase shift and hence rotation rate.

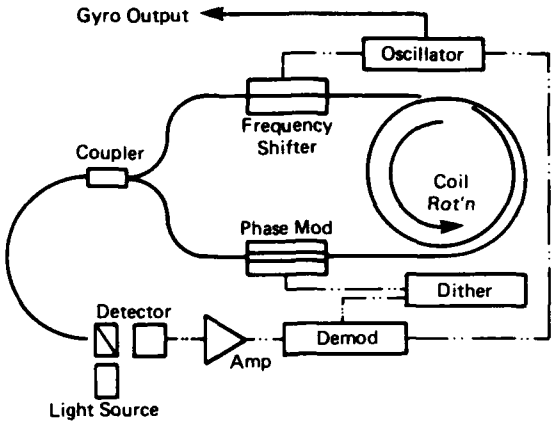

Fig. 5 Frequency Nulling Gyroscope

4.3 Development programme at BAe to date

At British Aerospace we have concentrated on the frequency shift approach since we began a development programme in 1980. In the early stages bulk optic gyroscopes using acousto-optic modulators for frequency shifting were built for source wavelengths of 633 and 1300nm. Closed loop electronics were built around these configurations, and bias uncertainties better than 100°/Hr were achieved. Encouraged by these results, we looked for an integrated solution to the frequency shifting problem. At the time there appeared to be two major options: the use of integrated optics or the miniaturisation of bulk optic devices. Of the two options, integrated optics was chosen because it requires less power, it is easier to mass produce, it is inherently more rugged, it is easier to assemble and align than acousto-optic devices which need expanded beams, and no high frequency standing bias is required. However there is no direct integrated optic equivalent to the acousto-optic modulator. One approach to creating a frequency shifter in integrated optics is the single sideband (SSB) modulator [7]. This however is a complicated waveguide structure requiring highly stable quadrature driving signals to ensure suppression of unwanted sidebands. The conversion efficiency and stability requirements of such a device make it impractical to use in a fibre optic gyro. Another alternative SSB modulator has been devised by Heismann [8], but this appears to be rather complicated and hence costly to construct.

The simplest active device to make in integrated optics is the phase shifter. For this reason we looked for an approach that was in principle the same as the frequency nulling approach but which utilised only simple phase shifters. A modelling programme [9] revealed that serrodyne phase ramps applied to phase shifters should give similar results to those obtained with acousto-optic modulators when employed in a fibre optic gyroscope, and early experiments confirmed the feasibility of such an approach. The serrodyne fibre optic gyroscope has since been chosen for our main line development programme.

4.4 The serrodyne gyro

A serrodyne modulator achieves a phase shift by driving a phase modulator with a linear ramp [10]. This ramp is periodically reset to zero when the applied phase reaches 2π. Under this condition, there is an induced frequency shift in the light passing through the phase shifter which is equivalent to the repetition frequency of the applied ramp. In this respect the serrodyne modulator can be regarded as behaving in the same way as an acousto-optic frequency shifter in a bulk-optic gyro.

However it is easier to consider the serrodyne modulator as a phase shifter. The serrodyne phase modulator is situated at one end of the loop (replacing the frequency shifter in Fig. 5), and so the phase shift is applied to one beam (Fig. 6), at a time equal to the delay time of the fibre, before the other beam. Thus a differential phase shift will appear between the two beams. The magnitude of this phase shift is dependent on the slope of the applied ramp. If the magnitude of the ramp is kept constant then the applied phase shift is linearly proportional to the frequency of the ramp.

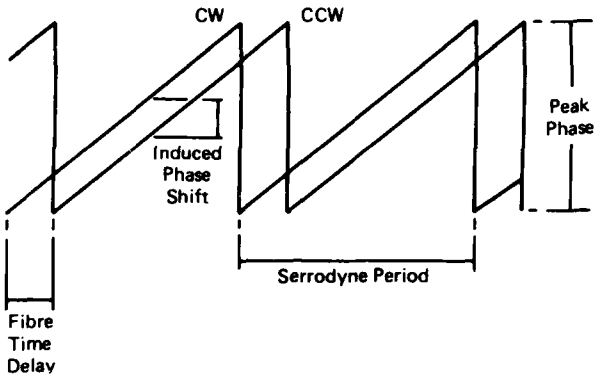

Fig. 6 The Serrodyne Ramp

There are however a few problems associated with serrodyne modulation. In particular the peak phase shift applied by the ramp needs to be maintained at 2π, and the flyback time of the ramp should be kept as short as possible. It is also necessary to maintain linearity of the ramp. These errors and the associated detector signal are depicted in Fig. 7, and have been modelled by the group at British Aerospace [9]. Practical tests on early serrodyne gyroscopes show that these error sources can be overcome [11].

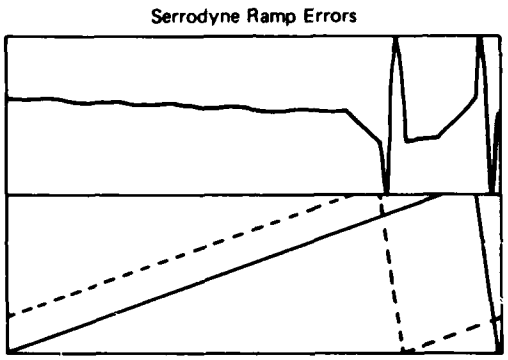

Fig. 7 Serrodyne Error Sources

In particular if the amplitude of the serrodyne ramp changes for any reason (temperature, etc.), a pulse appears at the output at a frequency equal to the serrodyne frequency and with a width equal to the time delay of the fibre. This can be used to control the point at which the ramps are reset and hence maintain the desired 2π amplitude using a loop to correct the ramp amplitude and null the pulse.

Strong effort has been made in designing the electronics to keep the flyback time to less than 15nsecs. This keeps the error associated with this parameter small and its effect is insignificant until the rates to be detected reach 500°/Sec, at which point, for most applications, accuracy becomes less critical.

4.5 <u>The gyro output interface</u>

Each time the serrodyne ramp reaches 2π a threshold detector generates a pulse to reset the ramp. The reset pulse appears on one of two output lines from the serrodyne ramp generator (Fig. 8), depending on whether there are positive or negative ramps, corresponding to a clockwise or anti-clockwise rotation. These pulses are fed to an up/down counter. Since the pulses appear at the same frequency as the serrodyne ramp, we can measure the frequency of these pulses - this will give a rate output. However each individual pulse represents a fixed small incremental angular movement, and thus the total pulse count can be used as a measure of current angular position. Frequency and hence rate can be measured by dividing the counts by the integration time.

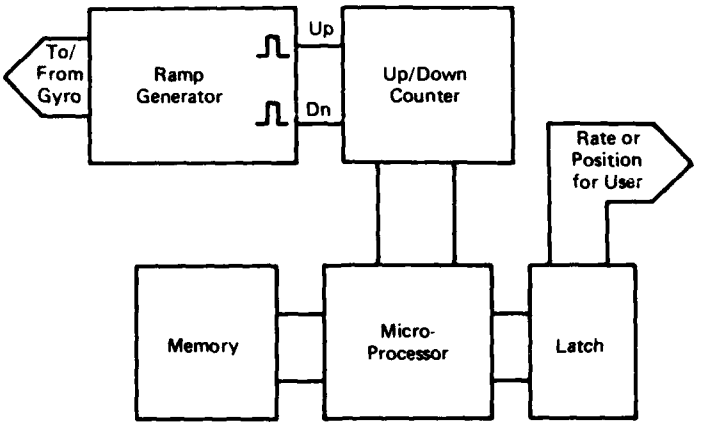

Fig. 8 The Counter and the Output Interface

In order to make measurements from the gyroscope easy for the user we use a microprocessor to control the pulse counting. The microprocessor reads the up/down counters at regular intervals and accumulates the total in its memory; it also keeps track of the number of clock periods over which the total is being taken. When the user demands a measurement the microprocessor is used to calculate the rate or position from the stored data. This value is then multiplied by the gyro scale factor and sent to the user who has the option, by use of a coded request signal, of receiving position or rate information.

5. CONSTRUCTION AND COMPONENTS

In the prototype gyroscope we describe here, we have chosen to use, wherever possible, components which are readily available from suppliers to the telecommunications industry. The exception to this is the integrated optics. We at present have integrated optic phase shifters and modulators made for us to our specification by various UK companies. The performance of all the components that we use in the prototype gyro match as closely as possible that required by a production gyroscope. The components are packaged to the requirements of the communications industry and so their size is larger than we would like.

The cost of the components that we currently use is rather high, since most of them are state of the art devices at 1300nm. With the introduction of volume production the price of such components will fall. We are in some ways dependent for this on the expansion of local area network (LAN) usage of fibre optics at 1300nm, but the gyro market we are aiming at should be sufficiently large by itself to force the fall.

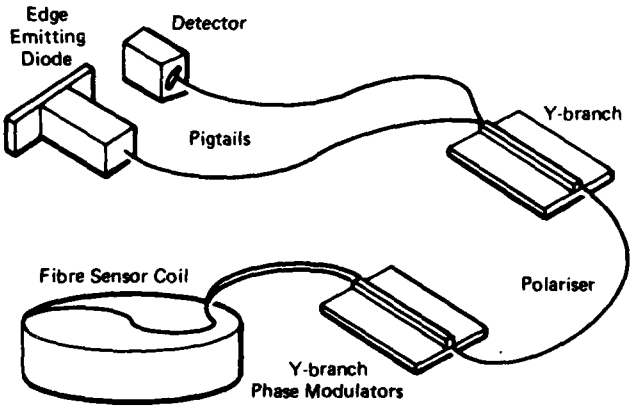

Fig. 9 Gyroscope components

The constituent components of a prototype gyroscope are shown schematically in a typical configuration in Fig. 9. The gyro light source is coupled to one port of an integrated optic Y-branch. The Y-branch output passes through a polariser and then to another integrated optic circuit consisting of a Y-branch and two phase shifters. The High Birefringence polarisation-maintaining (HiBi) fibre coil is coupled to the output waveguides of this chip. The detector is coupled via fibre to the second port of the first coupler to receive light returning from the gyro.

5.1 Source

The source is a single-mode fibre-pigtailed edge emitting diode (ELED) operating at 1300nm wavelength with an output of typically 8μW from the fibre. We use an ELED to minimise the effect of coherent back reflections which occur from interfaces between fibres and integrated optic components in the gyro. It also reduces the effects of Rayleigh backscatter from the fibre and to a limited extent the optical Kerr effect which causes a bias if the counter-propagating beams are of different intensity [12].

Because scale factor in the frequency nulling gyro is directly proportional to wavelength, it is necessary to ensure that the wavelength remains stable to the required level. It is also necessary to ensure that the source wavelength is accurately matched to the fibre's absorption and second mode windows. The temperature dependence of the wavelength of an ELED is typically -1nm/°C and so we use a source with a thermo-electric cooler, to maintain the ELED at a constant temperature and hence wavelength.

The disadvantages associated with the use of a cooler are the increased power consumption since the cooler is continually pumping heat away from the ELED, and the increased gyro start-up time required as the cooler cools the ELED down. However this does not prevent the gyro working as soon as it is turned on, but reduces its initial scale-factor accuracy.

5.2 Detector

The inherent detection limitation in a fibre optic gyroscope is photon shot noise. To approach this limit the noise introduced by the detector and its pre-amplifier must be kept to the absolute minimum. This is especially important with a low intensity source such as the ELED, where the light intensity reaching the detector is very low. Excess noise due to leakage current in the detector, or excessive DC light returning to the detector from back-reflections increases the random walk figure of the gyro. The commercially available InGaAsP detector used in the prototype gyroscope has a 1nA dark current at room temperature which increases by a factor of 10 at 80 Degrees.

A multimode fibre is fixed near the centre of the active area of the detector which is on a ceramic sub-mount. The detector sub-mount is mounted directly onto a low-noise wide-band transimpedance pre-amplifier designed for detection of both the AC dither frequency and error control signals. The complete detector and head-amplifier are mounted in a carefully screened enclosure.

5.3 Fibre and coil design

In order to ensure reciprocal propagation throughout the fibre coil HiBi single-mode fibre is employed in the gyroscope. This also serves to minimise the effect of the earth's magnetic field [13] on the phase shift in the fibre coil. It also prevents total signal fade since the polarisation state is preserved whilst propagating through the fibre [14]. The fibre is currently wound on an aluminium former and techniques have been employed during the winding to ensure a low winding- induced mode-coupling and to minimise the effect of temperature on loss and polarisation cross-coupling between the two modes in the fibre. Measurements have been made to determine the nature of any excess cross-coupling in the coils using a method proposed by Takada [15]: we have found there is only a very small amount of winding-induced cross-coupling ~-30dB.

5.4 Polariser

A high extinction polariser is required [16] in the input/output arm of the gyroscope to prevent light propagating in the unwanted mode and reaching the detector. We have chosen a metallised fibre polariser [17] since very high extinction ratios (>40dB) are achievable in very short lengths and the polarisers are easy to splice into the system.

5.5 Integrated optics

Two Titanium In-diffused Lithium Niobate integrated optic circuits have been used in the gyro for the Y-branch beam-splitters and the phase-shifters. The chip for the first beam-splitter in the gyro contains just a simple Y-junction. The second chip contains a Y-branch, and on each of the two output branches of the Y there is a phase-shifter (Fig. 10).

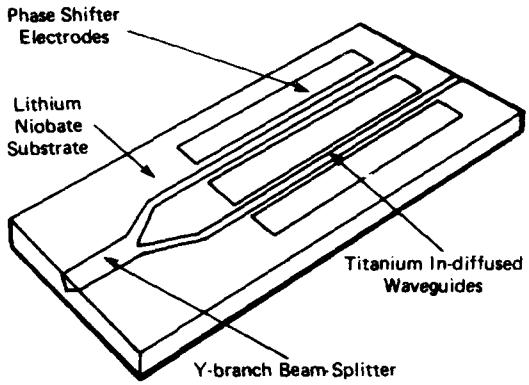

Fig. 10 Integrated Optics

The ends of both chips are polished at an angle to ensure that any reflections generated at the interfaces do not couple back into the waveguides. Such reflections would form spurious Michelson interferometers, which could interfere with the primary beam to produce a secondary signal at the detector. This signal would be synchronous with the required signal and produce a bias. The integrated optics are mounted on ceramic substrates for stability and ease of coupling to fibres.

Special alignment and bonding equipment has been developed to join the HiBi fibres to the integrated optics. The alignment system is used to align the axes of the fibre to the axes of the waveguides sufficiently accurately to ensure that the cross-coupling between the axes at the joins is adequate to obtain the specified bias and bias drift performance. In addition, because the chip is polished at an angle, we must ensure that during alignment the angle between the fibre and the waveguide is correct to ensure maximum coupling between the fibre and the integrated optics, and that no reflected light is coupled into the fibre-core or waveguide. Any excess loss when using an ELED as a source becomes increasingly critical owing to the initial low level of light from the source. The alignment equipment consists of mechanical positioners and a polarisation detection system utilising optical techniques similar to those published by Barlow [18] for fibre characterisation.

Once the fibre and integrated optics are aligned correctly they are bonded with a UV curing adhesive, whose refractive index closely matches that of the fibre, between the cleaved fibre end and the integrated optics end face. An additional adhesive support is also used a few millimetres down the fibre from the integrated optics to strengthen the fibre joint.

5.6 Electronics

The electronics associated with the gyro includes power supplies for the ELED and associated cooler, a pre-amplifier to amplify the detector signal, and analogue signal processing and control system, and a digital counting and interface system.

The digital electronics has been constructed entirely of surface mounted components to minimise the circuit size. All these components including the microprocessor are CMOS devices to ensure low power consumption. Power consumption is an even more critical requirement when the electronics are mounted in close proximity to the fibre coil, since thermal gradients in the coil produce non-reciprocal phase shifts which represent a bias drift in the gyroscope [19]. Compromises have been made between power consumption, size and speed in the analogue electronics but where possible low power and surface mounted devices have been used.

6. ASSEMBLY

The prototype gyroscope has been designed to be assembled complete with its electronics into a single housing. A modular approach to the design has been taken to ensure easy assembly and testing and if necessary easy modification. The gyroscope is assembled into four basic modules:-

1. Electronics.
2. Source, detector and first Y-branch.
3. Polariser, integrated optics Y-branch and modulators.
4. Coil assembly.

The optical paths of the modules are first joined using the alignment and glueing techniques described above. The mechanical assembly of the modules is then straightforward, coiling excess fibre between modules and securing where necessary. The integrated optics modules are positioned inside the fibre coil, whilst the source

and detector and all the electronics are located above the coil. The whole assembly is housed in a metal enclosure with a 25-way micro-miniature connector to convey power to the gyro and data from the gyro. Fig. 11 below shows a photograph of the prototype gyroscope with the outer case removed.

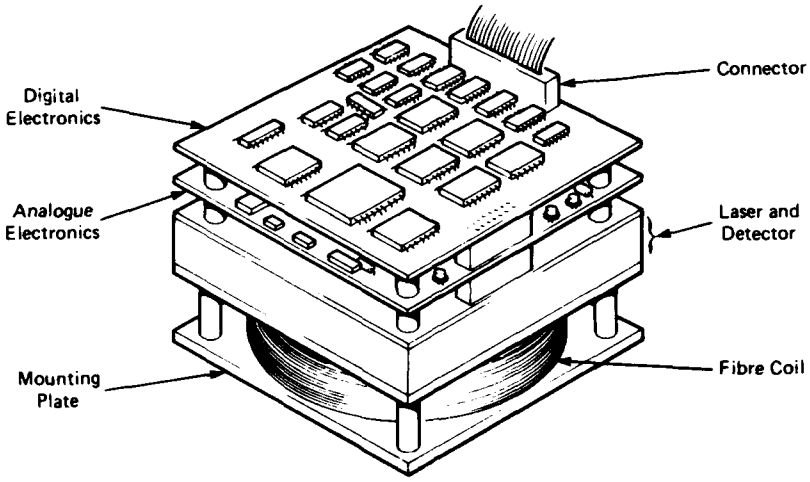

Fig. 11 Drawing of the Assembled Gyro

7. PERFORMANCE

The performance of the gyroscope has so far been measured at room temperature in terms of rate response, random walk, bias and drift.

7.1 Bias

The bias was measured over both short and long periods. In order to assess the statistical behaviour of the noise, a large amount of consecutive data was saved using a computer. Since this data was consecutive it was possible to group several data points together as if different integration times were used for the data collection. Using typically 50,000 data points taken over a half hour period, we were able to produce a plot of the magnitude of the 1 Sigma noise magnitude vs integration time. Systematic drift (noise) can then be isolated from random walk; since random walk is a statistical process which increases as the square-root of sample time.

Figures 12 and 13 below show the raw noise data as received from a gyro, with bias offset removed, together with the RMS noise data plotted for three integration times. The bias offset is caused mainly by residual alignment errors and a small electronic bias.

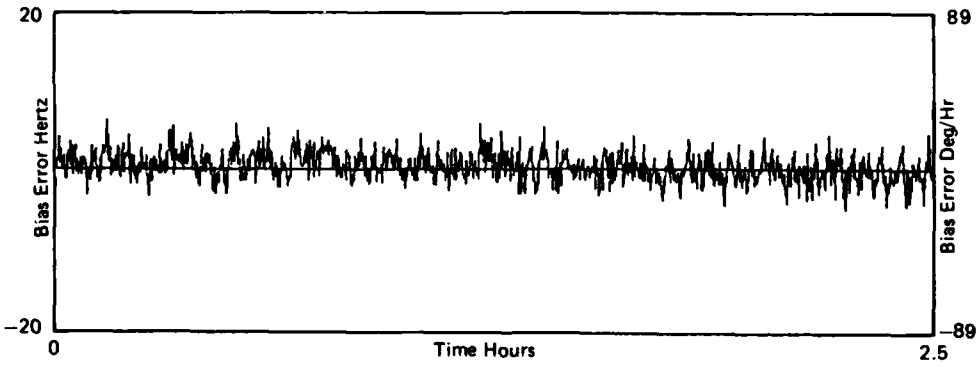

Fig. 12 Drift in the Gyro

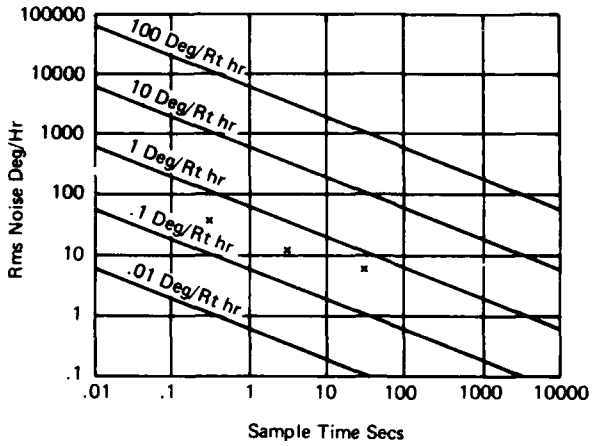

Fig. 13 RMS and Random Walk

7.2 Rate sensitivity

The rate sensitivity was measured by applying rate over a constant time interval and measuring the average output frequency of the gyro over this interval. The readings were used to make scale-factor (Fig. 14), and scale-factor error plots (Fig. 15). The non-linearity of the scale-factor over the range of rates for which the prototype gyroscope was designed to operate is shown clearly in Fig. 15 where the expected frequency calculated from the average slope of the graph in Fig. 14 has been subtracted from the actual reading at each rate to show the output error. The data from which the figures were plotted have NOT been corrected to compensate for the previously mentioned serrodyne error sources.

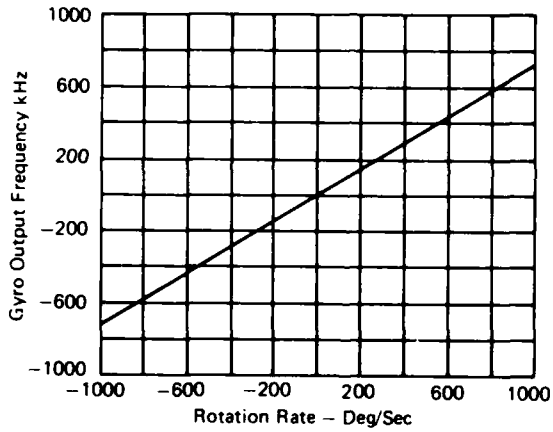

Fig. 14 Scale Factor Plot

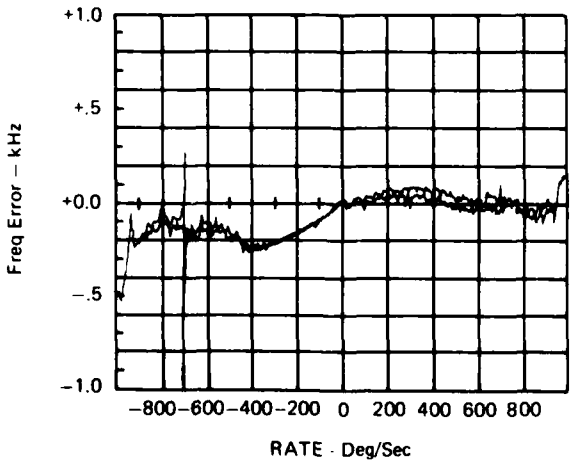

Fig. 15 Scale Factor Non-linearity

8. NEXT STAGE

Steps are being taken in the future to correct for source wavelength instability, in particular to provide temperature monitoring, and also change the source to a fibre laser [2], which has a much more stable wavelength, slightly reduced linewidth, and increased power, without the need for cooling. In addition work will continue to reduce the size of the fibre coil to a size closer to that of present-day gyroscopes. The electronics can be further integrated using custom logic arrays and customised analogue cells. The source can be integrated with its driving circuitry, and likewise the detector pre-amp can be integrated in a similar way to current PIN-FET receivers in use in the telecommunications industry.

9. CONCLUSIONS

A prototype serrodyne fibre optic gyroscope has been described which has been produced as an intermediate stage in the development of a gyroscope for missile guidance and control applications.

It has been demonstrated that the performance of the chosen architecture is suitable for this application. The use of serrodyne modulation has enabled a sensitive gyroscope to be built with a suitably high dynamic range. Careful selection of components and the chosen polarisation system together with careful alignment techniques has kept the bias to a sufficiently low level.

The architecture can be improved by the addition of a more stable light source to eliminate scale factor changes, whilst all the components can be reduced in size by utilizing well-known integration techniques.

Finally the microprocessor and the digital electronics can be used to make any necessary error corrections for output to digital guidance and control systems.

REFERENCES

1. E.J. POST. The Sagnac Effect. Review of Modern Physics Vol. 39, No. 2, April 1967, pp 475-493, section 4.

2. S. EZEKIEL. Fibre Optic Rotation Sensors: Tutorial Review. Springer Verlag, 1982, pg 2.

3. R. ULRICH, S.C. RASHLEIGH. Beam-to-fibre coupling with low standing wave ratio. Applied Optics, Vol. 19, No. 14, 15 July 1980, pp 2453-2456.

4. S-C. LIN, T.G. GIALLORENZI. Sensitivity analysis of the Sagnac Effect optical-fibre ring interferometer. Applied Optics, Vol. 18, No. 6, 15 March 1979, pp 915-931.

5. R.F. CAHILL, E. UDD. Phase nulling fibre optic laser gyro. Optics Letters, March 1979, Vol. 4, No. 3, pp 93-95.

6. R.F. CAHILL, E. UDD. Solid state phase nulling optical gyro. Applied Optics 1980, Vol. 19, pp 3054-3056.

7. M. IZUTSU, S. SHIKAMA, T. SUETA. Integrated Optical SSB Modulator/Frequency Shifter. IEEE Journal of Quantum Electronics, Vol. QE-17, No. 11, November 1981, pp 2225-2227.

8. F. HEISMANN. In-line electro-optic frequency translator for fibre optic sensors. Proc. SPIE, Vol. 517, 25 October 1984, pp 206-212.

9. C.J. KAY. Serrodyne modulator in a fibre optic gyroscope. IEE Proceedings Vol. 132, Pt. J, No. 5, October 1985, pg 259-264.

10. R.C. CUMMING. The serrodyne frequency translator. Proc. IRE, February 1957, pp 175-186.

11. C.J. KAY. Design and Performance of a Prototype Serrodyne Fibre Optic Gyro. Proc. Royal Aeronautical Society, Laser Gyros and Fibre Optic Gyros, 25 February 1987, paper 8.

12. R.A. BERGH, B. CULSHAW, C.C. CUTLER, H.C. LEFEVRE, H.J. SHAW. Source statistics and the Kerr effect in fibre optic gyroscopes. Optics Letters, Vol. 7, No. 11, November 1982, pp 563-565.

13. K. HOTATE, K. TABE. Drift of an optical fibre gyroscope caused by the Faraday effect: Influence of the earth's magnetic field. Applied Optics, Vol. 25, No. 7, 1 April 1986, pp 1086-1092.

14. R. ULRICH. Fibre Optic Rotation Sensing with Low Drift. Optics Letters, Vol. 5, No. 5, 1980, pp 173-175.

15. K. TAKADA, J. NODA, K. OKAMOTO. Measurement of spatial distribution of mode coupling in birefringent polarization-maintaining fibre with new detection scheme. Optics Letters, Vol. 11, No. 10, October 1985, pp 680-682.

16. S.C. RASHLEIGH. Origins and Control of Polarization Effects in Single-Mode Fibres. Journal of Lightwave Technology, Vol. LT-1, No. 2, June 1983, pg 312-331.

17. L. LI, G. WYLANGOWSKI, D.N. PAYNE, R.D. BIRCH. Broadband metal/glass single-mode fibre polarisers. Electronics Letters, Vol. 22, No. 19, 11 September 1986, pp 1020-1022.

18. A.J. BARLOW. Optical Fibre Birefringence Measurement Using a Photo-Elastic Modulator. Journal of Lightwave Technology, Vol. LT-3, No. 1, February 1985, pp 135-145.

19. D.M. SHUPE. Thermally Induced Non-reciprocity in the Fibre Optic Interferometer. Applied Optics, Vol. 19, 1980 pp 654-655.

20. L. REEKIE, R.J. MEARS, S.B. POOLE, D.N. PAYNE. Tunable Single-Mode Fibre Lasers. Journal of Lightwave Technology Vol. LT-4, No. 7, July 1986, pp 956-960.

AD-P005 715

AN INVESTIGATION OF STEEP DESCENT GUIDANCE FOR TERMINALLY-GUIDED SUB-MUNITIONS

by G. Trottier
Defence Research Establishment, Valcartier
P.O. Box 8800, Courcelette, Québec
Canada, G0A 1R0

ABSTRACT

The lateral acceleration requirement of a "hit-to-kill" terminally-guided sub-munition (TGSM) aimed at hitting tanks near the top is examined. An analytic development of proportional navigation against stationary targets shows that a TGSM flying level at 150 m above the ground can hit a target 150 m in front of it with near vertical impact and without acceleration saturation if it can pull an initial 13.6 g. With acceleration saturation, a hit is theoretically possible with 6.8 g. TGSM configurations capable of hitting stationary and moving targets are then defined and tested with a nonlinear 6-DOF computer simulation. The footprint of a selected configuration is provided. It is observed that the 10-g configuration is sufficient to hit most stationary and moving tanks likely to be found on the battlefield with impact angles above 60° and reasonable angles of attack.

NOMENCLATURE

A	TGSM lateral acceleration (m/s^2)	R	Range (m)
$C_{N\alpha}$	Normal force coefficient derivative (/°)	V_T	Target velocity (m/s)
$C_{N\delta}$	Normal force coefficient derivative (/°)	V	TGSM velocity (m/s)
$C_{m\alpha}$	Pitch moment coefficient derivative (/°)	x	Downrange (m)
$C_{m\delta}$	Pitch moment coefficient derivative (/°)	x^*	Static margin of the airframe (m)
C_{mq}	Pitch damping coefficient derivative	y^*	Static margin of the fins (m)
h	Altitude (m)	Z_α	Normal force derivative (N/°)
I	Transverse moment of inertia (kg-m^2)	Z_δ	Normal force derivative (N°)
K_0	Aerodynamic gain (/s)	z_α	$= Z_\alpha/mV$ (/σ)
M_α	Pitching moment derivative (N-m/°)	z_δ	$= Z_\delta/mV$ (/s)
M_δ	Pitching moment derivative (N-m/°)	α	Angle of attack (rad)
M_q	Pitch damping derivative (N-m/rad/s)	δ	Fin angle (rad)
m_α	$= M_\alpha/I$ (/s)	γ	TGSM heading (rad)
m_α	$= M_\alpha/I$ (/s)	γ_T	Target heading (rad)
m_q	$= M_q/I$ (/s^2)	μ	Damping ratio
N	Navigation constant	σ	Line-of-sight angle (rad)
q	pitch rate (rad/s)	ω_0	Weathercock frequency (rad/s)

INTRODUCTION

The requirement for ground attack aircraft to effectively engage multi-vehicle armoured targets in both close air support and battlefield interdiction roles places increasing demand on the intelligence and adaptability of the weapon system employed. One solution to the problem is the use of a weapon which consists of a flying dispenser (bus vehicle) which is released by an aircraft some distance from the target and which subsequently delivers a number of smart, autonomous terminally guided submunitions (TGSMs) into the target area.

Two weapon concepts are currently investigated as solutions to the problem: (1) "shoot-to-kill" sensor fuzed munitions which, following release from the bus vehicle, climb to provide the altitude they require for target search, deploy a parachute to stabilize vertical descent, rotate an off-set detector about the vertical while scanning the ground in a decreasing spiral scan, and fire a high velocity slug at the target upon acquisition; and (2) "hit-to-kill" aerodynamically controlled submunitions equipped with a seeker which guide to the target and detonate a shaped charge warhead at impact.

This paper considers the lateral acceleration requirement for a TGSM to hit stationary and moving targets from a near vertical dive. This approach is dictated by the improved warhead effectiveness obtained when hitting the top armour. This adds two constraints to the conventional guidance problem: steep impact, and minimum angle of attack at impact.

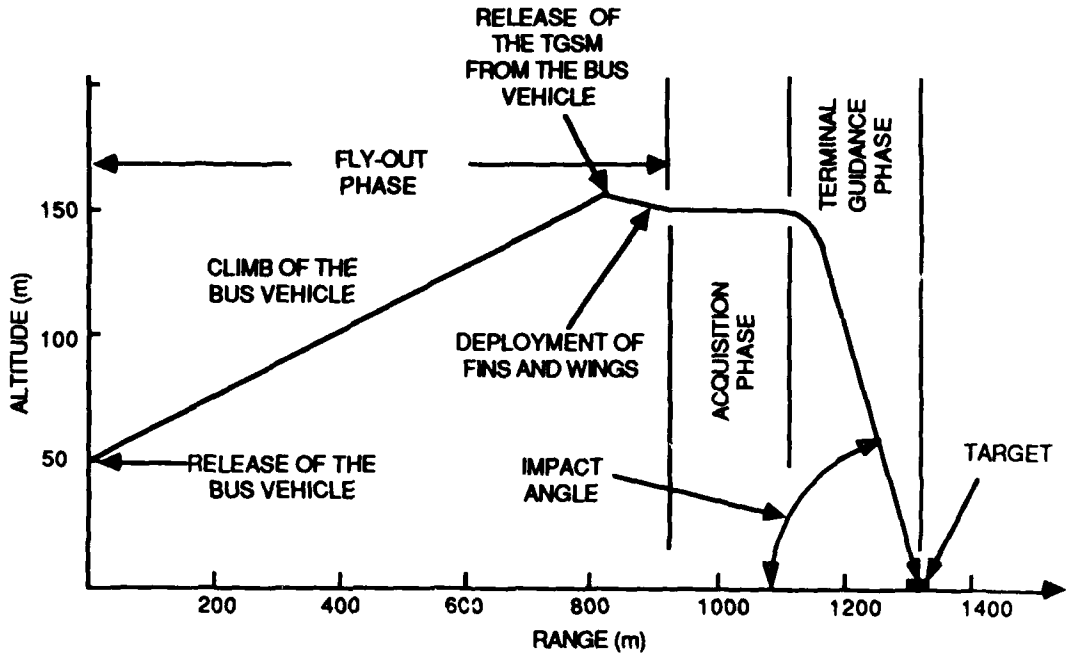

Figure 1 - Sketch of a TGSM attack scenario.

SCENARIOS

When TGSMs are released from a bus vehicle, the scenario is many-on-many in that several TGSMs have to handle several targets against various background and levels of clutter. The targets are armoured vehicles 6x3x2 m moving in columns on roads, moving in clutter, stationary in clutter (engine running) and stationary in clutter (engine off).

If one considers one TGSM only, the scenario becomes one-on-many. A typical TGSM attack scenario is shown in Fig. 1. Its flight comprises three phases: (1) the fly-out phase during which the bus vehicle is dispensed from the aircraft and flies up to reach a fixed altitude h at which the TGSM are released. Upon release, the TGSM initiates the deployment of its lifting and control surfaces

and becomes ready for target search; (2) the search phase during which it flies level (or glide) while scanning the ground for a target; and (3) the terminal homing or track phase during which it guides to hit the target. During the terminal homing guidance phase, the scenario is one-on-one.

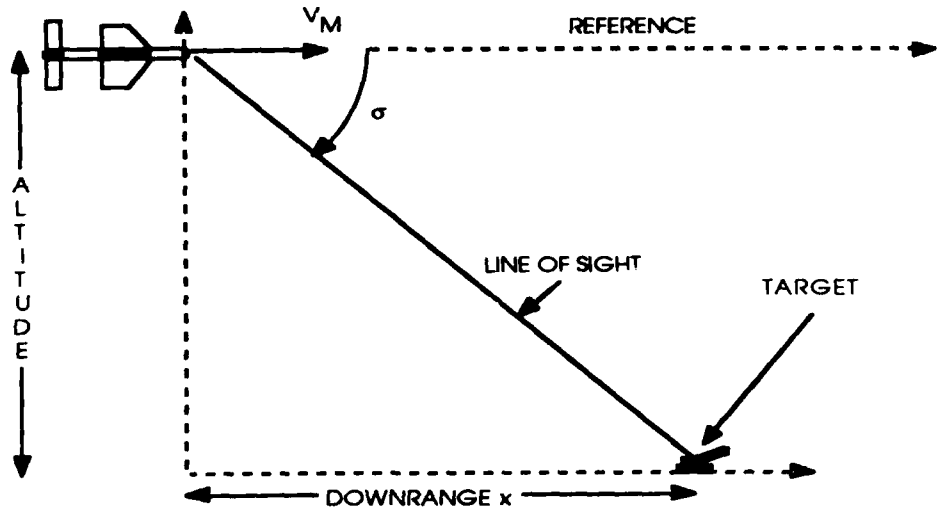

Figure 2 - Search and initial conditions for terminal homing guidance.

Search Phase

The search phase is certainly the one that demands the most from sensor and signal processing technology. The seeker located at the front end of the TGSM must search the ground, inspect all returns, take the target signatures out of the clutter, discriminate countermeasures, and make a decisition on the validity of the targets. This is a formidable problem which is not discussed here. However, there are characteristics of the search phase which impact on the terminal homing phase and these will be discussed.

It is first postulated that TGSM is equipped with only one seeker which can operate in two modes: (1) a scanning mode for the search phase, and (2) a tracking mode for the terminal homing guidance phase.

Figure 2 depicts the geometry of the search phase. The TGSM is at altitude h and flies level at velocity V. The seeker searches the ground at a look down angle σ. The maximum slant range R at which the target can be detected is limited by the detection range if the seeker uses a millimeter wave radar. The altitude h is limited by cloud cover if the seeker uses passive infrared. If the look down angle is fixed, both h and R are linked.

The velocity V of the TGSM is also limited by the characteristics of the search mode. From altitude h and level flight, any stationary object on the ground will appear as moving angularly at angular speed

$$\dot{\sigma} = \frac{V}{h}\sin^2\sigma \qquad [1]$$

If the look angle is 45° and the maximum gimbal rate of the seeker is 25°/s, then, for h = 150 m, [1] yields V/h = 0.873. Beyond this value, any attempt to eventually track a target is hopeless. Since moving targets are also considered, the relative velocity must account for some inbound component of target velocity. For h = 150 m, and inbound target velocities of 20 m/s, the TGSM velocity cannot exceed 110 m/s.

Terminal Homing Phase

A terminal homing guidance law that will guide the TGSM to a near vertical hit with the tank must now be determined. Homing guidance is a "two-point guidance"[1] and in this case, only the relative positions and velocities of the target and TGSM are important. Homing guidance uses line-of-sight angles (or rates) to home on the target. In the plane, the geometry of the homing guidance is described by the following relations:

$$\dot{\sigma} = \frac{V_T \sin(\gamma_T - \sigma) - V \sin(\gamma - \sigma)}{R} \qquad [2]$$

$$R = V_T \sin(\gamma_T - \sigma) - V \cos(\gamma_T - \sigma) \qquad [3]$$

In homing missiles, the relation between the line-of-sight direction and that of the missile velocity vector during terminal guidance is known as the navigation law. Broadly speaking, there are two fundamental ways of implementing terminal guidance: pursuit and collision homing.

In pursuit navigation, the missile always heads towards the target. If the missile attitude is maintained directed toward the target, it is attitude pursuit; if the missile velocity vector is maintained toward the target, it is velocity pursuit. In both cases, the turning rate of the missile is commanded equal to the rate of change of the line of sight so that the missile always turns during the attack unless it is head-on or tail-on. Because of the high manoeuver requirement to end the attack in a tail chase, pursuit navigation is not considered practical as a homing guidance law against moving targets, in spite of its simple implementation. One exception to this would be for a target moving very slowly compared with the missile (e.g. a ship) in which case the small miss caused by the intense last instant manoeuver would still allow the missile to hit the target.

Mariners have known for centuries that if any object, moving or stationary, appears stationary and looms larger and larger, then a collision is inevitable unless a change of course is made. In a missile-target engagement, this condition known as constant bearing navigation is realized when the missile is steered such that the line of sight does not rotate.

One obvious way to attempt implementation of constant bearing navigation is to consider the rotation rate of the line of sight as an error signal which the missile drives to zero by commanding a missile turning rate proportional to the error signal: this is proportional navigation. For a missile using proportional navigation and launched on a collision course, the initial turning rate of the missile is zero. If the target fails to manoeuver and the missile and target velocities remain the same, the missile will remain on a collision course thus achieving constant bearing navigation. If the missile is launched off a collision course, the resulting trajectory will have a curvature dependent on the navigation constant. If the navigation constant is small, the missile corrections are small early in the flight and it may require ever increasing manoeuvers as the missile approaches the target. For greater values of N, the collision course errors are corrected early during flight so that manoeuvers during the terminal phase of the flight remain at a reasonable level. $N = 1$ is pursuit guidance. $N \leq 2$ requires an infinite acceleration in the region of terminal flight[2]. $N = 2$ is therefore a lower limit whereas for N around 8, the missile steers in response to very high frequency noise as well as to lower frequency signals. As a result, there is a vast oversteering with a constant dither of the controls and high drag. Experience shows that $N = 4$ is reasonable[3].

Proportional navigation has been in use for over three decades on radar, TV and infrared homing missiles because of its effectiveness and its relative ease of implementation. Experience has shown that proportional navigation is a very powerful tool against manoeuvering targets such as aircraft. Theoretical studies have shown that it is an optimal solution of the linear guidance problem in the sense of producing zero miss distance for least integral square control effort with a zero lag guidance system in the absence of target manoeuvers[4]. This important result gave credibility to the use of modern control theory as a tool for deriving guidance laws that would prove better than proportional navigation for non-zero lag systems in presence of target manoeuvers. Most modern guidance laws tend to surpass proportional navigation in that they estimate target

accelerations and make due account of lags in the missile hardware. However, they requires more precise tracking, and more sophisticated sensors and instrumentation on-board the missile. However, modern control laws have the insuperable advantage of requiring less acceleration than proportional navigation to hit a manoeuvering target [5].

One modern guidance law worth mentioning is that proposed by Kim & Gridder[6]. It is designed to both minimize miss distance and maximize attitude angle at impact. Some prior simulations[7] of this guidance law have shown that it is very effective in achieving both constraints when a missile is launched from high altitude. In this situation, the ideal collision and vertical attitude impact courses are almost in coincidence and there is no difficulty in meeting the two constraints simultaneously. From low altitude, these ideal courses are quite distant from one another and the guidance computer has to satisfy two contradictory constraints. This causes oscillations between the two trajectories and poor homing accuracy.

As a conclusion, pursuit guidance laws are too inaccurate whereas modern guidance laws require too much input data and computing power. Proportional navigation is therefore selected as the steering law for the TGSM.

ACCELERATION AND IMPACT ANGLE

In proportional navigation, the TGSM heading rate is made proportional to the line-of-sight rate in an attempt to null it:

$$\dot{\gamma} = N\,\dot{\sigma} \quad \text{or} \quad \gamma = N\,\sigma + \gamma_0 \qquad [4]$$

When coupled with the geometry of Fig. 2 and TGSM control dynamics, equations [2], [3] and [4] become impossible to solve mathematically and require modeling on computers. The problem can be simplified and useful qualitative results can be produced by considering a linear model for the homing head (perfect information) and all TGSM characteristics. However, for a fixed target, one can solve the proportional navigation equations analytically and find a simple relation between the initial altitude and look down angle on one hand, and the maximum acceleration and the impact angle on the other hand.

Solution of the 2-D Proportional Navigation Problem

Put the reference direction in coincidence with the initial line of sight and put $V_T = 0$ in [2] and [3]. Then take the derivative of [2] with respect to time. The result is

$$R\ddot{\sigma} + (2 - N)\,\dot{R}\,\dot{\sigma} = 0 \qquad [5]$$

an exact differential that solves for

$$\dot{\sigma} = \dot{\sigma}_0 \left[\frac{R}{R_0}\right]^{N-2} \quad \text{and} \quad \dot{\gamma} = \dot{\gamma}_0 \left[\frac{R}{R_0}\right]^{N-2} \qquad [6]$$

Equation [6] shows that for $N \geq 2$, the heading rate (and therefore the acceleration) is maximum at the beginning of the flight and decreases to zero at the end of it (when R=0). Equating [2] and [6] now yields for the end of the flight

$$\gamma_f = \frac{-\gamma_0}{N-1} \qquad [7]$$

Acceleration and Impact Angle

From the perspective of the target, the final heading of the TGSM is always at an angle $\gamma_0/N-1$ above the initial line of sight. If one draws a diagram of TGSM altitude h versus the downrange x of the target when the terminal phase is initiated, curves of constant impact angle are straight lines from the origin whereas the curves of maximum acceleration are circles tangent to the origin as shown in Fig. 3 for N = 4 and V = 100 m/s. In this figure, the curves of constant impact angle are given for 20, 40, 60 and 80° whereas the curves of constant maximum acceleration are given for 3, 5, 10 and 15 g's.

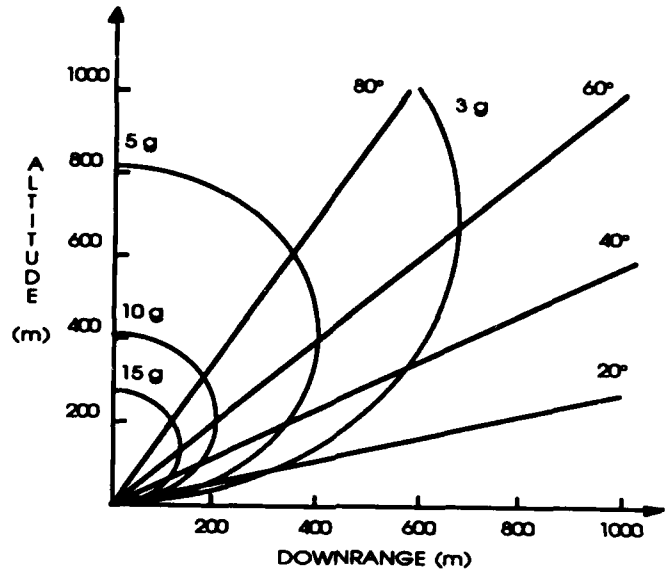

Figure 3 - Curves of constant impact angles and constant lateral accelerations.

Figure 4 is a zoom of Figure 3 in the range of operation of the TGSM where the thick line with the arrow at an altitude of 150 m shows the trajectory followed by the TGSM during the search phase. For this trajectory, impact angles from 50 to 60° are possible depending on the time required for acquisition. For the same trajectory, the acceleration requirement varies from 9.8 to 13.6 g's.

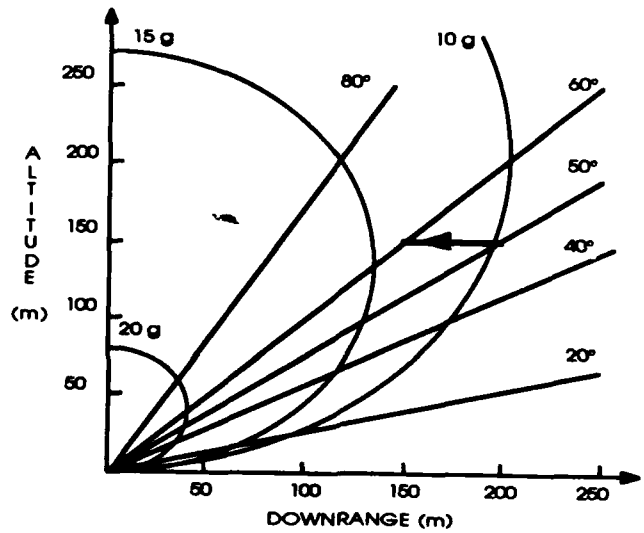

Figure 4 - Zoom of Figure 3 in the neighborhood of the target.

This development of the equations of proportional navigation is valid for a stationary target and gives the acceleration that a TGSM must pull at the beginning of the terminal guidance phase in order to hit the target without acceleration saturation. However, a hit can still be achieved even in presence of acceleration saturation.

Minimum Acceleration Capability

If 13.6 g is the acceleration capability required to hit a stationary target at x = 150 m from an altitude of 150 m without acceleration saturation, there is also a minimum acceleration below which no hit is possible. At this minimum acceleration, the TGSM will fly a circular path of 150-m radius. It will be acceleration saturated 100% of the time of flight and will hit the tank from the vertical while pulling maximum acceleration (a sizeable angle of attack). This minimum acceleration capability is 6.8 g.

PRELIMINARY DESIGN

Like missiles and aircraft, TGSMs fly aerodynamically; their velocity vectors are rotated by the application of a transverse acceleration resulting from the application of a transverse force (lift). Lift is governed by the angle of attack of the airframe in the flow field and the angle of attack is produced by the deflection of the control surfaces. Lift is produced in a non-linear proportion to the control surface deflection and so is the turning rate achieved.

It was show that the TGSM will have to execute an initial manoeuver of 13.6 g at the beginning of the track phase in order to hit a stationary target without acceleration saturation. It was also shown that this condition is not essential for a hit, and that 6.8 g is theoretically sufficient.

What is the acceleration requirement if the target is moving inbound at 20 m/s? An initial acceleration of 16.3 g will be commanded at the beginning of the flight in order to fly a N = 4 proportional navigation course without acceleration saturation. This requirement is not quite feasible for a TGSM flying at low speed (100 m/s) in a regime where the aerodynamic forces developed by the lifting and control surfaces are small. Simulations of the TGSM trajectories are necessary but, before this is done, some of its properties must be determined.

Size, Mass and Inertial Properties

The TGSM will carry a shaped-charge warhead and an impact fuze that need to be efective against tank targets. It is common knowledge that a charge diameter that can have effectiveness is 15 cm, and the diameter of the TGSM is set to 0.15 m.

Since the warhead is the heaviest component of the TGSM, there are advantages in locating it near the geometric center of the TGSM. Allowing about three charge diameter for the formation of the warhead jet, this puts the geometric center of the TGSM about .45 m behind the impact fuze. Let the length of the TGSM be 1.0 m.

By scaling down the physical properties of the Maverick airframe, the weight of the TGSM should be about 20 kg and its transverse moment of inertia ($I \sim mL^2/12$) should be about 1.6 kg-m^2.

Steering Policy

Two steering policies are used in the design of tactical missiles: "skid-to-turn" (STT) and "bank-to-turn" (BTT). BTT systems operate like airplanes and need not be of symetrical cross-section. They may have only two in-line lifting and control surfaces, and they roll their best menoeuver plane into the direction of the desired manoeuver to effect it. Though very effective, the reaction may be slow and it requires a roll demand autopilot.

In STT systems, the missile is usually cruciform with four lifting and control surfaces either in-line or interdigitated. They perform their manoeuvers in each of the two orthogonal planes, pitch and yaw. When roll-position stabilized, the motion in the pitch and yaw planes are uncoupled, and their position relation with respect to the horizontal and vertical planes in space is

simple and invariant. If the missile is allowed to roll, both instrumental and aerodynamic cross-couplings become a significant source of degradation.

For simplicity and low cost, the TGSM will be fitted with an STT cruciform configuration with in-line lifting and control surfaces. Additionally no roll autopilot will be used. If the roll damping of the airframe is insufficient, it can be increased with rollerons.

Control Location

The control surfaces can be positioned well forward (canard control), near the middle (wing control) or far aft of the airframe (tail control). Wing control is easily ruled out because of the size of the servo-systems it requires. Despites its capability of compounding the normal force produced by the lifting and the control surfaces, canard control must be ruled out too since the servo-systems would have to be located between the warhead and the seeker.

Tail control is selected because the servo-systems can easily be installed in the aft portion of the TGSM. It does not have the capability of canard control in producing acceleration but it may be quite stable in a configuration where the center of gravity does not move owing to fuel consumption.

Aerodynamics in the pitch plane

In the absence of roll, the linearized force and moment equations in the pitch plane read as follows:

$$\begin{bmatrix} s + z_\alpha & -1 \\ m_\alpha & s + m_q \end{bmatrix} \begin{bmatrix} \alpha \\ q \end{bmatrix} = \begin{bmatrix} z_\delta \\ m_\delta \end{bmatrix} \qquad [8]$$

Neglecting the contribution of m_q (it is generally a small term), [8] can be solved for α and q yielding two oscillatory modes of the TGSM. However, it is more interesting to solve for the turning rate

$$\frac{\dot{\gamma}}{\delta} = \frac{q - \dot{\alpha}}{\delta} = \frac{[(z_\alpha m_\delta - z_\delta m_\alpha) - z_\delta s^2]}{m_\alpha \left[1 + \frac{2\mu s}{\omega_0} + \frac{s^2}{\omega_0^2} \right]} \qquad [9]$$

where

$$\omega_0 = \sqrt{m_\alpha} \quad \text{and} \quad \mu = \frac{n_\alpha}{2\sqrt{m_\alpha}} \qquad [10]$$

The steady state gain of the heading rate is then

$$K_0 = \frac{z_\alpha m_\delta - z_\delta m_\alpha}{m_\alpha} \qquad [11]$$

Static Margin and Trim States

The aerodynamic forces on an airframe do not generally act on the center of gravity. Lift forces act on the airframe center of pressure whereas fin deflection forces act on the center of pressure of the fins. If x* (static margin) and y* are defined as the distances between the center of gravity and the centers of pressure of the airframe and fins, the moments are related to the normal forces as follows:

$$x^* = \frac{M_\alpha}{Z_\alpha} = \frac{mV}{I} \cdot \frac{m_\alpha}{z_\alpha} \qquad [12]$$

$$y^* = \frac{M_\delta}{Z_\delta} = \frac{mV}{I} \cdot \frac{m_\delta}{z_\delta} \qquad [13]$$

Whereas [12] and [13] relate m_α with z_α, and m_δ with z_δ, the moment equation at trim (no moment acting) provides a relation between m_α and m_δ as follows:

$$\dot{q} = -m_\alpha \alpha + m_\delta \delta = 0 \qquad [14]$$

If the total incidence is limited to 14° (and this is sound for a minimum incidence at impact), i.e., 10° in the pitch plane and 10° in the yaw plane, and if the maximum fin deflection is 20°, at trim, we have $\alpha_{trim}/\delta_{trim} = m_\delta/m_\alpha = 0.5$.

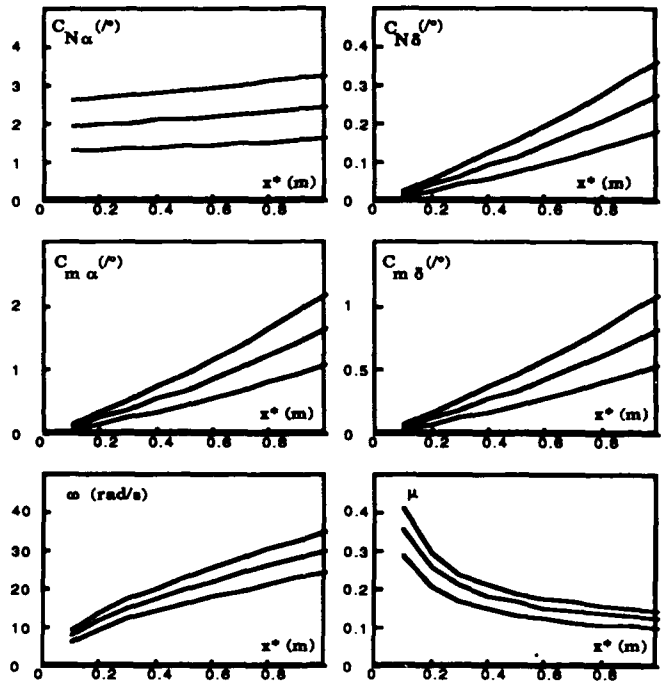

Figure 5 - Aerodynamic Parameters of the TGSM vs the static margin x*
for various values of acceleration
(from top to bottom of each graph: A = 20, 15 and 10g)

Aerodynamic Parameters

Figure 5 shows the variations of the TGSM's aerodynamic parameters as a function of the static margin x* for three configurations, namely 10-g, 15-g and 20-g. At x* = 0.01 m, the weathercock frequency is very low (7.0, 8.54 and 9.8 rad/s respectively) whereas damping is moderate (0.29, 0.36 and 0.41). This results in very slow airframe response to acceleration demands and this in inadequate for this TGSM.

At x* = 0.05 m, the airframe is faster but less well damped. The 10-g configuration has a weathercock frequency of 16.3 rad/s, a damping of 0.136 and an incidence lag of 0.25 s. For the 15-g configuration, these parameters are 20 rad/s, 0.167 and 0.168 s respectively.

There are definite advantages in selecting the 15-g configuration. It is faster, better damped and, as shown earlier, it can home without acceleration saturation. On the other hand, these advantages are paid for by an increased requirement for lift and wing size as shown in Fig. 6. In this figure, the wings and fins dimensions are drawn based on the normal force per unit area of rectangular wings with aspect ratios of two[8].

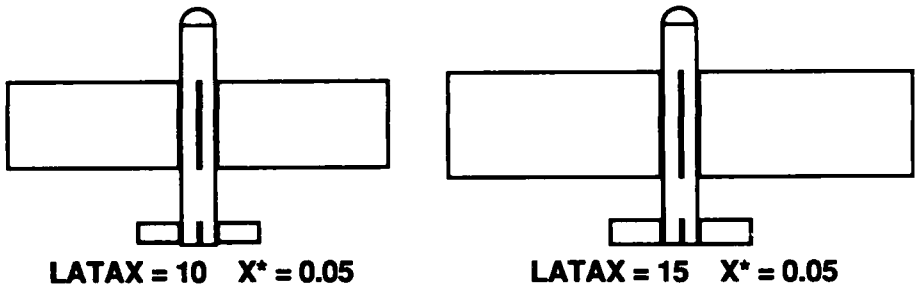

Figure 6 - 10-g and 15-g TGSM configurations showing scaled wings and fins (TGSM length = 1 m)

TGSM MODEL AND SIMULATION

The characteristics of the TGSM obtained in the preceeding sections can now be simulated if a model is made of the aerodynamics, tracking loop, actuators and autopilot, if any is required.

Aerodynamics

The aerodynamics has six degrees of freedom. The equations for the forces and moments are solved in body-fixed coordinates and gravitational acceleration is taken into account in solving them. Body-fixed velocities are transformed into inertial coordinates by the classical Euler transformations. The derivatives of the Euler angles are obtained through another classical transformation which links them with body-fixed angular rates. The aerodynamic parameters are assumed independant of Mach number. This results in 12 state variables.

The roll channel is included in the model but the derivative of the roll rate is set to zero. This implies that the roll rate is constant throughout all simulations and its instantaneous value is its initial value. Couplings due to roll rate are included in the force equations.

Tracking Loop

The tracking loop is modeled as a 1st order lag with a time constant of 0.15 s. Two tracking loops are used, one for elevation, one for azimuth line-of-sight angle. The three-dimensional model used to compute range, range rate, and line-of sight rates in elevation and azimuth is conventional. This yields three state variables for the range and the line-of-sight angles, and two state variables for the gimbal angles.

The tracking loop is nonlinear and has saturations: (1) the gimbal rate is limited to 25°/s; (2) the look angle (the angle between the line of sight and the TGSM axis) is limited to ± 50°; and (3) the field of view of the seeker is set to ±6° for the tracking mode.

Actuators

The commands to the actuators are equal to N times the gimbal rates in elevation and in azimuth. They are distributed to the pitch and yaw actuators through a rotation of coordinates that takes due account of the roll attitude. The fin actuator is modeled as a 1st order lag with a time constant of 0.05 s. Since there are two of these, two state variables are involved. The fin actuator model is also nonlinear since the fin angle is restricted to ± 20°.

Lateral Autopilots

The primary task of a lateral autopilot is to provide the lateral acceleration of the airframe in a controlled and yet responsive way. They are normally required for tail control missiles designed with a small static margin or in configurations where the center of gravity moves toward the front due to fuel consumption. They provide synthetic stability through instrument feedback. The airframe becomes more robust to changes or uncertainties in the aerodynamic parameters.

For an unpowered TGSM designed with a confortable static margin (i.e. 2-5% of length), there does not appear to be serious reasons to increase the cost with lateral autopilots.

Target Model

The target model is purely kinematic. The target has an initial position on the ground, and can move at constant acceleration. Since the model was originally developed for aircraft targets, the target model comprises 6 state variables.

Simulation Codes

The model comprises 25 state equations with nonlinearities, and integration is carried out using a Runge-Kutta integration routine of order four. For the kind of dynamics involved with the TGSM, the integration step is constant at 0.1 s. Computer codings were developed in APL for a MacIntosh computer running under STSC APL*PLUS. Each step takes about 8 s to execute.

RESULTS OF THE COMPUTER SIMULATIONS

Simulation runs were made of several TGSM configurations against stationary, constant velocity, and accelerating targets but only two were considered in depth: a 10-g and a 15-g configuration with a static margin of 0.05 m (5% of body length).

Computer Outputs

In the computer environment, every run can be inspected on a display such as shown in Fig. 7. The box marked "time" shows the total time of flight. The box marked "position" shows the positions of the TGSM and the target at the end of the flight. The box marked "velocities, accelerations" shows the initial velocities in the first column, the final velocities in the second column, and target acceleration in the third column.

The right hand side rectangle of Fig. 7 depicts the trajectory. The grid representing the ground is 200 by 200 m with lines every 50 m. In this case, the tank is stationary at a downrange of 150 m. The box in the upper left corner shows a 3 by 6 m tank and the location of the impact. In this case, it is nearly dead center. The graph that appears on the left hand side of the figure gives the position of the fins as a function of time. There is fin saturation when the graphs meet the maximum scale. In Fig. 7, the conditions of the flight is such that the TGSM pulls maximum acceleration between t = 0.3 and t = 0.7 s. The final conditions of the TGSM flight are given under the trajectory. In this case, the miss distance was 0.1 m whereas the impact angle is 57.9°. The TGSM incidence at impact is 4.8° for a lateral velocity of the warhead at impact of 6.8 m/s.

Figure 8 gives a similar computer output whose outcome is as not successful. The miss distance is 2.9 m after 2.75 s of flight. In this case, the target is initially located at the same place as in the previous case but now moves with a constant inbound velocity of 20 m/s. A loss of lock by the seeker is observed at t = 2.5 s and this is enough for a near miss. At loss of lock-on, the seeker becomes blind, the fins return to their neutral position and the TGSM impacts anywhere without guidance. When the TGSM hits the ground, the target is located at x = 95 m.

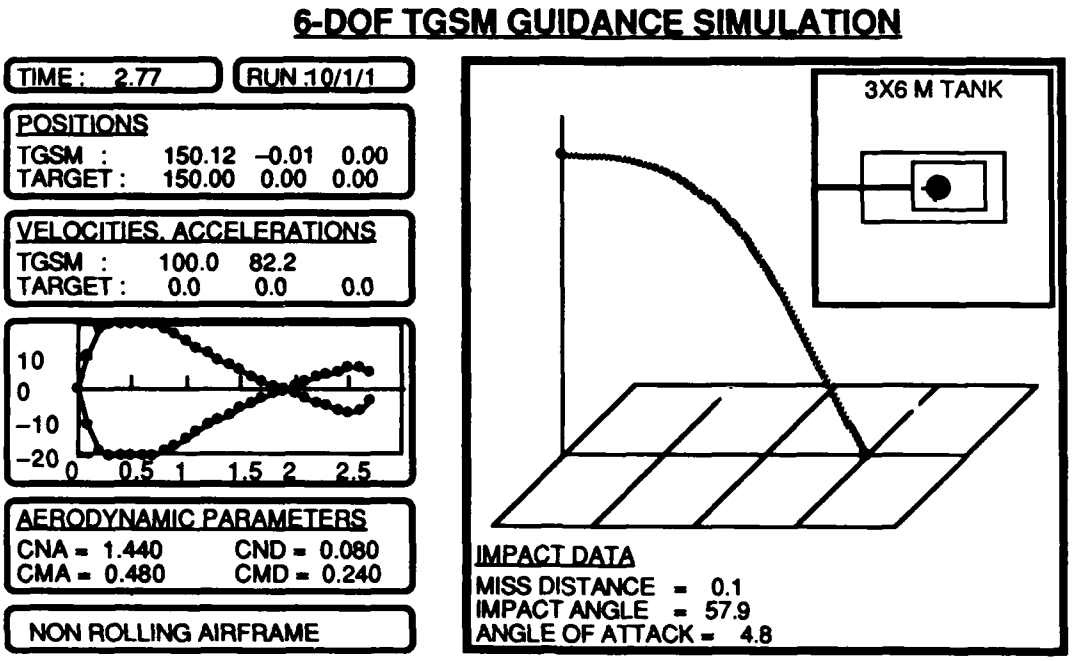

Figure 7 - Computer Output of a TGSM Flight against a Stationary Target located at a downrange of 150 m (zero cross-range).

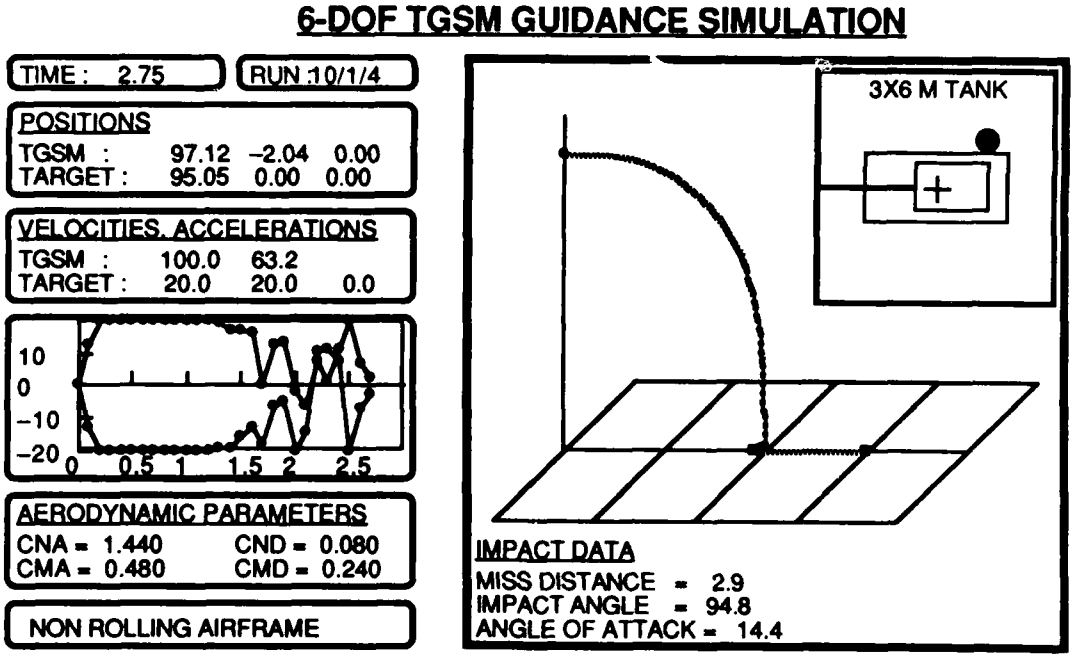

Figure 8 - Computer Output of a TGSM Flight against a 20 m/s Moving Target .

Miss Distance Footprints

At the beginning of a simulation, the TGSM is always located 150 m above the origin of the reference frame and, in principle, the target can be anywhere in a 50 by 50 m patch of ground located between x = 150 and x = 200 m. These target locations represent various degrees of guidance difficulties for the TGSM. The situation is the most difficult if the target is located at the inner boundary of the patch of ground and moves inbound. If the target is farther or moves sideways, the guidance is made easier.

One way to determine the effectiveness of a TGSM configuration is to find the limiting speeds and accelerations beyond which it will miss the target. We call this a "footprint". In this paper, the footprints are computed for the most difficult target position.

Performance of the 10-g TGSM Configuration

Figure 9 shows the footprint of the non-rolling 10-g TGSM configuration. The thick line boundary of the footprint indicates the acceleration/velocity regimes beyond which the miss distances achieved exceed 1 meter. Within the footprint, there are tags which indicate the conditions under which a miss distance under one meter was achieved. The numbers in the tags show the impact angles which were achieved.

It is observed that the impact angle increases as either the target velocity or the target acceleration increases and this increase is indicative of the difficulty of the terminal homing phase. When it becomes too difficult, the line-of-sight rate, which is equal to the local heading error divided by the time to go, becomes too high for the tracking loop to follow and loss of lock occurs. In these instances, the values of the impact angle and the angle of attack are irrelevant. No attempt was made to extend the footprint above accelerations of 7 m/s^2.

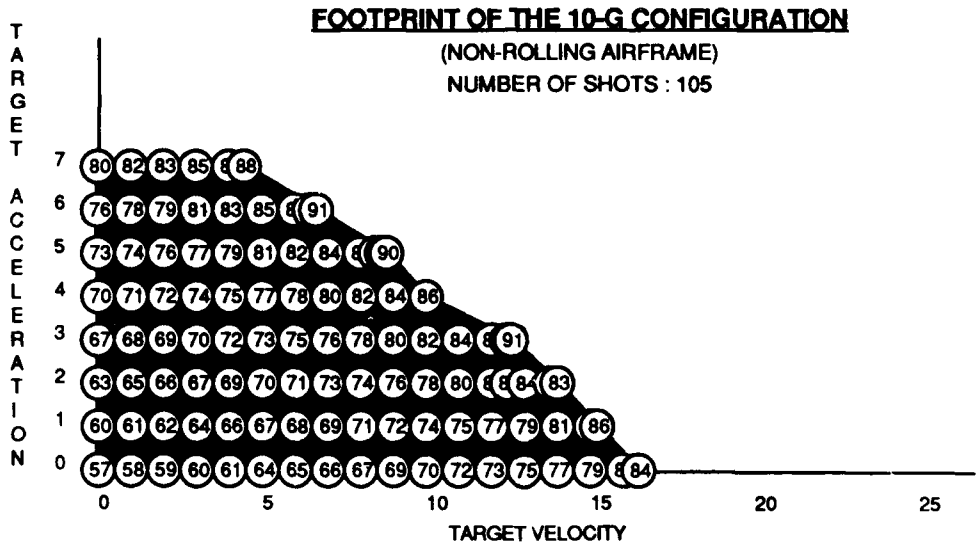

Figure 9 - Footprint of the 10-g TGSM configuration

Figure 9 shows that the non-rolling 10-g configuration can hit targets initially located 150 m in front of it and moving with constant velocities up to 16.5 m/s (60 km/hr). It also shows that it can achieve less than one meter miss distance against a tank which was initially moving at 10 m/s (36 km/hr) and accelerating at 4 m/s^2 (this tank can accelerate from 0 to 100 km/hr in 7 s!). Considering that the footprint was computed under the most severe conditions of terminal homing guidance, the 10-g configuration is considered capable to achieve hits against most armoured targets likely to be found on the battlefield.

En résumé, l'utilisation de missiles semi-actifs impose à l'avionneur des contraintes sur le radar (mode adéquat, portée, qualité et précision des informations), sur l'unité de navigation inertielle, sur l'identification des plots radar, sur les calculateurs (domaines de tir du missile, lois de navigation du chasseur) et sur la présentation des informations à l'équipage.

Figure 10 shows the distribution of the impact angles and the angles of attack observed for the shots falling in the footprint. Impact angles range from 57 to 91° whereas angles of attack at impact range from 0 to 15° with a concentration between 0 and 8°.

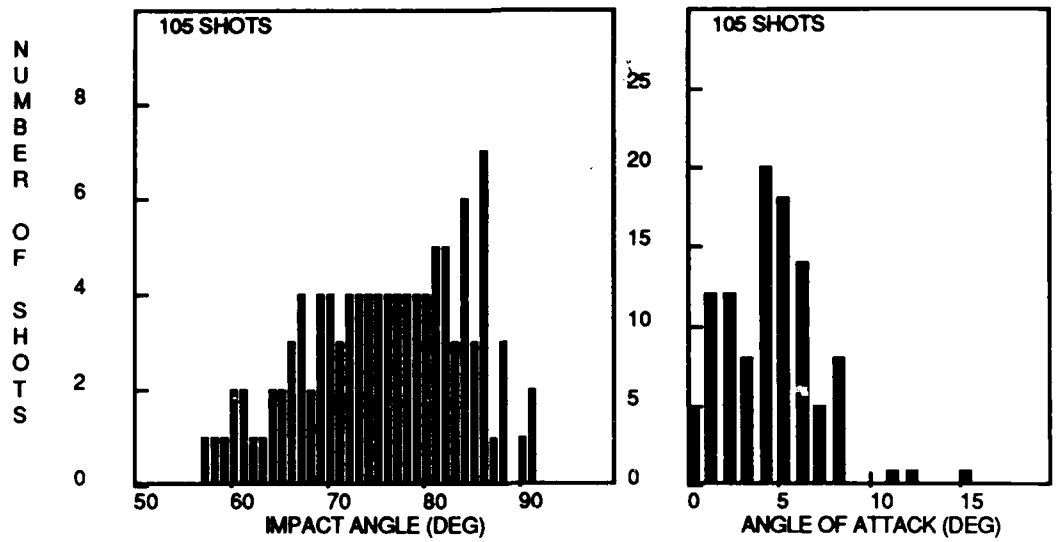

Figure 10 - Distribution of the impact angles and angles of attack at impact for the non-rolling 10-g configuration

Effect of Roll Rate on Accuracy

The simulations that were used to construct the footprints of Fig. 9 were run with a forced roll rate of zero and an initial roll position in the "lugs-up" position. However, it is important to delineate the effect of moderate roll rates on the accuracy of the TGSM. Rolling airframe simulation runs were also made with a forced roll rate of 90°/s and the footprint corresponding to the 10-g configuration is presented in Fig. 11 whereas Fig. 12 shows the distributions of impact angles and angles of attack at impact.

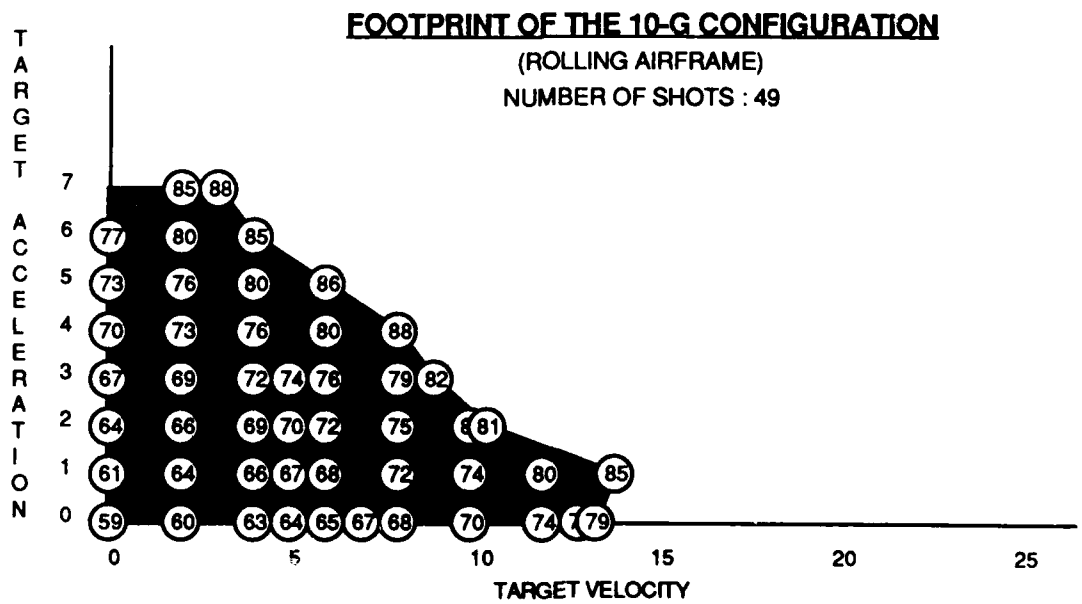

Figure 11 - Footprint of the rolling (90°/s) 10-g TGSM configuration

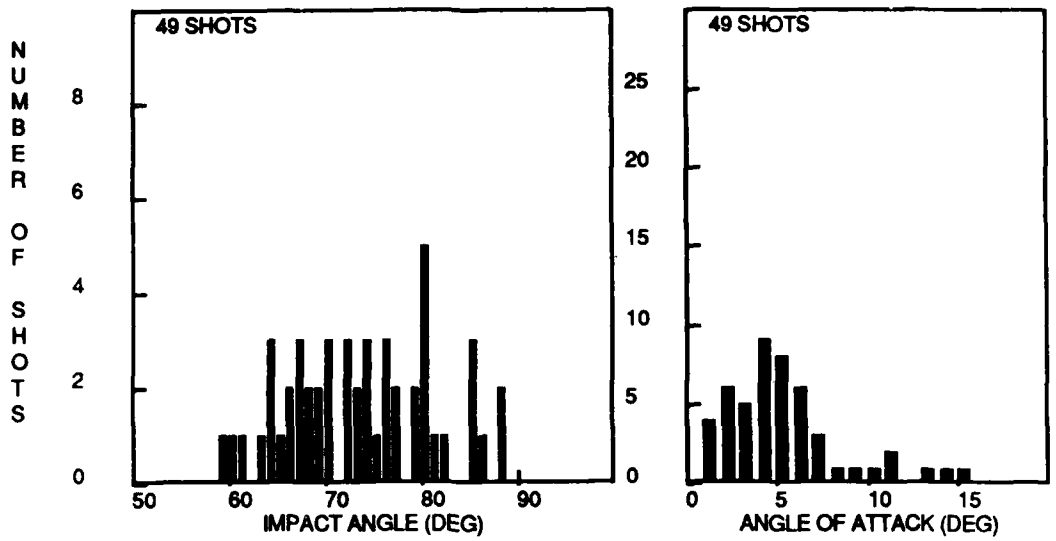

Figure 12 - Distribution of the impact angles and angles of attack at impact for the rolling (90°/s) 10-g configuration

Performance of the 15-g TGSM Configuration

Figure 13shows the footprint of the 15-g TGSM configuration. It extends much further than that of the 10-g configuration. The TGSM can hit targets moving at a constant velocity of 25-26 m/s (90-95 km/hr) whereas the 10-g configuration was limited by constant target velocities of 16.5 (60 km/hr) m/s. This configuration can also hit targets initially moving at 16 m/s (60 km/hr) and accelerating at 4 m/s^2.

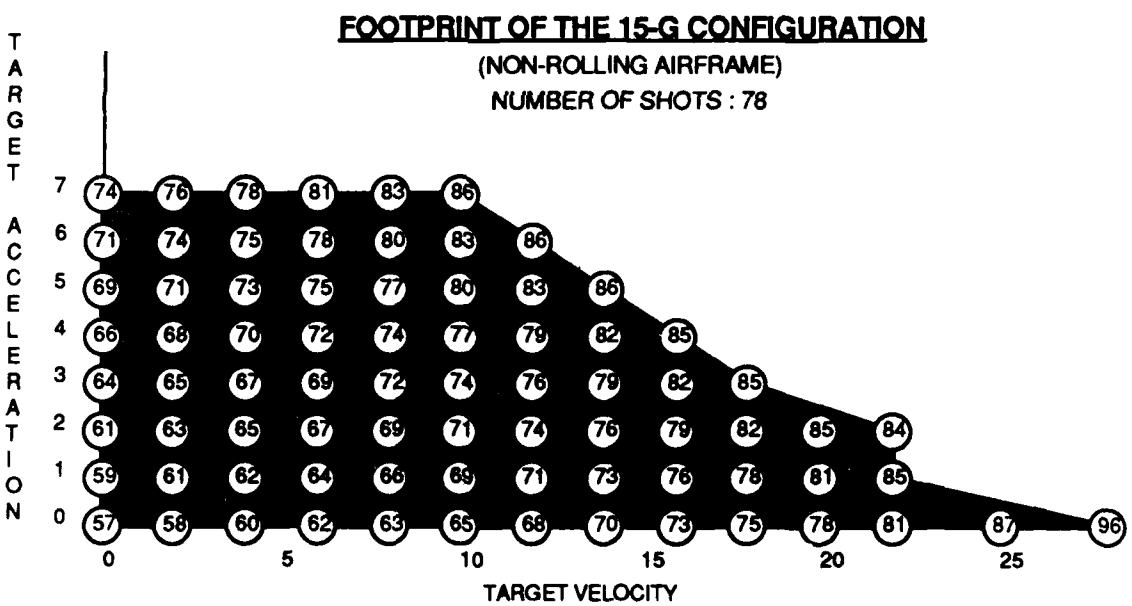

Figure 13 - Footprint of the non-roling 15-g TGSM configuration

The distribution of the impact angles is about the same as with the non-rolling 10-g configuration but the angles of attack are reduced by half.

CONCLUSION

The effectiveness of a steep impact terminally-guided sub-munition has been assessed in terms of the miss distance it can achieve against stationary and moving tank targets. Two configurations were considered and tested against the most difficult terminal guidance conditions, i.e. when the target is located 150 m in front of the TGSM. The 10-g configuration can hit tanks from the near vertical and with relatively low angle of attack at impact if the tank is not too agile. The 15-g configuration can do better but it does so at the expense of considerable wing size, and a more difficult packaging problem.

Theoretically, the 10-g configuration does not possess sufficient lateral acceleration capability to hit a stationary tank without acceleration saturation but the saturation is short enough that the TGSM can correct its flight path to a colision course before it hits. In most cases, there is still some heading error to correct, and this is shown by a non zero angle of attack at impact. The 15-g configuration has sufficient lateral acceleration capabilities to hit stationary targets without saturation but has periods of saturation against targets moving at constant velocities above 12 m/s. Simulation runs made with rolling airframes reduce the footprint without altering much neither the impact angles nor the angles of attack at impact. The 10-g TGSM configuration is considered capable of achieving hits on most targets likely to be met on the battlefield.

A word of caution! The simulation is a 6-DOF simulation which takes care of the effect of roll rate, time lags and the saturations of the seeker field of view, tracking loop and fin actuators. However, the aerodynamics is linear and no account is made for backward shifts of the center of pressure with incidence. The seeker always knows exactly where the target is, there is no blind time without guidance, and the seeker can loose lock only when its gimbal cannot follw the line of sight or when the gimbal reaches its maximum look angle. Additionally, the TGSM moves in still air. There are no wind or wind gust, no turbulence. These are ideal conditions!

This study is to be pursued to consider (1) a more realistic aerodynamics with backward shifts of the center of pressure with incidence; (2) random perturbations of the line of sight; (3) random winds; and (4) the search phase and handover from search to track.

REFERENCES

1. P. Garnell & D.J. East, "Guided Weapon Control Systems", Pergamon Press, 1977

2. F.W. Nesline & P. Zarchan, "Hardware-Software Trade-Offs for Digital Flight Control of Guided Missiles", AGARD 33rd GCP Symposium, Oct 13-15, 1981

3. L. Biberman, "Reticles in Electro-Optical Devices", Pergamon Press, Oxford, 1966

4. A.E. Bryson & Y.C. Ho, "Applied Optimal Control", Blaisdell Publishing Co., Waltham, Mass, 1969.

5. F.W. Nesline & P. Zarchan, "A New Look at Classical vs Modern Homing Missile Guidance", J. Guidance and Control, Vol. 4, No. 1, Jan-Feb 1981, pp. 78-85

6. M. Kim & K.V. Gridder, "Terminal Guidance for Impact Attitude Angle Constrained Trajectories", IEEE Transactions on Aerospace and Electronic Systems, Vol. AES-9, No. 6, November 1973, pp. 852-859

7. B.G. Neal, "Numerical Simulation of Selected Homing Guidance Laws for use with Strapdown Seekers", Master's Dissertation, Royal Military College, Kingston, April 1985

8. R.L. Stalling Jr, "Low Aspect Ratio Wings at High Angle of Attack", from "Tactical Missile Aerodynamics" edited by H.J. Hemsch & J.N. Nielsen, Progress in Aeronautics, Vol. 104, pp. 120-123

AD-P005 716

EFFECTS OF CLOSING SPEED UNCERTAINTY ON OPTIMAL GUIDANCE

by
W. W. Willman
Research Department
Naval Weapons Center
China Lake, California 93555
USA

SUMMARY

An idealized planar intercept is analyzed in which an air-to-air homing missile has angular measurements of the line of sight to a randomly maneuvering target and seeks to use a guidance law which optimizes a specific performance criterion. If the closing speed were known precisely, the optimal guidance law for this case would be proportional navigation with a certain navigation gain. There is uncertainty in the closing speed, however, because of the target maneuvers and lack of range measurements. The effect of this uncertainty on the optimal guidance law is to increase the nominal value of the navigation gain, and apparently to add a rapid weaving component if the fractional uncertainty in the inverse target range exceeds a certain level.

INTRODUCTION

A common form of homing missile guidance is "proportional navigation," meaning that the commanded missile acceleration lateral to the line of sight to the target is proportional to the observed angular rate of this line of sight in inertial space. The constant of proportionality is called the feedback gain, and is itself the product of two factors, the closing speed and the so-called navigation gain. The navigation gain must be greater than 2 for the missile to close on a constantly accelerating target.

If the closing speed is known, proportional navigation with a navigation gain of 3 is a close approximation of the optimal guidance law against a randomly maneuvering target for minimizing <u>any</u> weighted average, within wide limits, of the squared miss distance and timewise integrated drag force. Squared miss distance is approximately proportional to the probability of unsuccessful intercept, except in the uninteresting case where this probability is large, and both the speed and remaining range capability of the missile at intercept are decreasing functions of the integrated drag force. Thus this single guidance law is a natural choice for all the objectives of hitting the target, maximizing the intercept speed and maximizing the missile range, under the condition of known closing speed.

This condition is often not met, however, because only the line-of-sight direction is measured and the closing speed varies for a number of reasons, including inherently unpredictable target maneuvers. A common practice in this case is to raise the feedback gain beyond the value which would nominally provide the optimal navigation gain of 3, so that this gain will be high enough to close on the target for any plausible closing speed. Another possibility is for the missile to weave deliberately and use the resulting parallax to form a running estimate of the target's range, thereby deducing a more refined knowledge of the closing speed. This paper provides a theoretical basis for these remedies by minimizing the same kind of weighted average as described above under the assumption that the missile measures only target direction and the target maneuvers randomly in all directions, thereby producing a randomly changing closing speed. The resulting optimal guidance law is still almost independent of the weights in this average.

A PLANAR INTERCEPT PROBLEM

It suffices for this purpose [1] to consider the relative planar motion of a pursuer intercepting an evader:

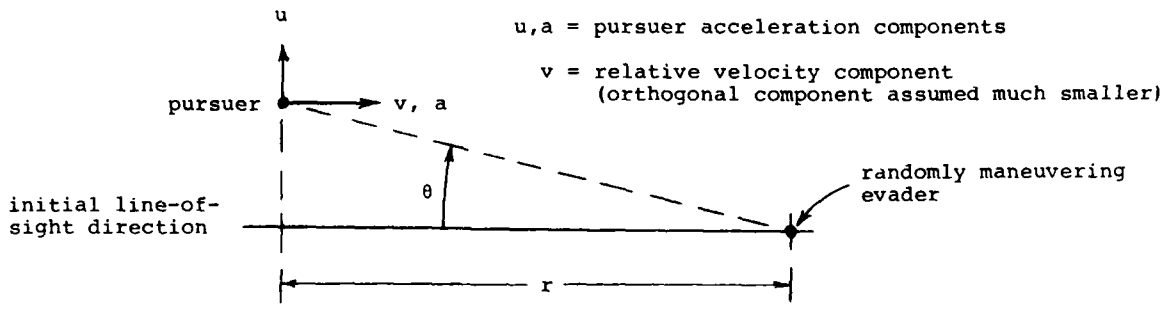

For small θ, the dynamics of the motion shown here are approximately

$$d\omega = (2v\lambda\omega + \lambda u)dt + dw_1(\lambda^2 q\, dt)$$

$$\left.\begin{aligned} d\lambda &= \lambda^2 v\, dt \\ dv &= a\, dt + dw_2(c^2 q\, dt) \end{aligned}\right\} \quad \lambda,\ v \text{ will be considered known at the initial time } t = 0$$

where:

$\omega = d\theta/dt$

$\lambda = 1/r$

dw_1, dw_2 are independent Wiener-process increments whose arguments denote their variances over time increment dt.

These Wiener-process increments are good approximations of the effects of random target acceleration components with average magnitudes A and cA, and correlation time T, if $q = A^2T$. [2] They could also represent the effects of unpredictable variations in the aerodynamic forces on both vehicles. The pursuer can measure θ and select the control acceleration u at each time instant t. There is usually a fixed relation between u and the other acceleration component a, but a is typically much smaller. Since its value is also known to the pursuer, its effects can usually be ignored as unimportant [1] as long as its (known) integral is added back to v, or estimate thereof, in using any results obtained this way. Thus we will treat only the case of a = 0 here. Predictable aerodynamic forces, such as base drag, have likewise been ignored.

The probability of intercept failure is often approximately

$$P_f = 1 - e^{-(D_c/R_L)^2} \qquad \begin{cases} D_c = \text{distance of closest approach} \\ R_L = \text{radius of effectiveness} \end{cases}$$

This can be closely approximated in the interesting range of 5% - 60% as $P_f = \dfrac{r^4\omega^2}{R_L^2 v^2}$ for any r such that

$$4R_L < r < v\sqrt{\frac{R_L}{2M}}\ , \quad M = \text{max. relative acceleration.} \tag{1}$$

Such a choice of r is possible in the usual case of $\boxed{M < \dfrac{v^2}{32\ R_L}}$.

Nonzero control accelerations u add an "induced" drag force, typically proportional to u^2, to the unavoidable base drag on the pursuer. The pursuer's airspeed and remaining range capability at intercept will be decreasing functions of the integrated total drag force, so maximizing a weighted average of the probability of successful intercept and either the pursuer's range or its airspeed in the vicinity of intercept is approximately equivalent to minimizing a performance criterion of the form

$$J = E\left\{K\left[\frac{r_f^4}{R_L^2 v^2(t_f)}\right]\omega^2(t_f) + \int_0^{t_f} u^2\, dt\right\}, \tag{2}$$

where

$K > 0$ (relative weight given to intercept probability)

E denotes prior expected value

r_f = some value of r satisfying (1)

t_f = time at which $r = r_f$.

NORMALIZED COORDINATES

It is convenient to define a nominal inverse range variable $\bar{\lambda}$ by

$$\frac{d\bar{\lambda}}{dt} = \bar{\lambda}^2 v_o\ ; \quad \bar{\lambda}(0) = \lambda_o \quad (= 1/r_o)$$

and the corresponding normalized dimensionless variables

$$\left.\begin{aligned} \alpha &= (\lambda - \bar{\lambda})/\bar{\lambda} \\ \beta &= (v - v_o)/v_o \end{aligned}\right\} \text{ fractional departures of } \lambda \text{ and } v \text{ from nominal values}$$

$$\left.\begin{aligned} \bar{\omega} &= \sqrt{\frac{v_o}{q\bar{\lambda}}}\ \omega \\ \bar{u} &= \frac{u}{\sqrt{q v_o \bar{\lambda}}} \end{aligned}\right\} \text{ normalized line-of-sight rate and control}$$

$\tau = \ln(\bar{\lambda}/\lambda_o)$ new "time" variable.

Since $d\tau = \bar{\lambda} v_o dt$, the dynamics can be expressed in terms of these new variables as

$$d\bar{\omega} = [(\frac{3}{2} + 2\alpha + 2\beta + 2\alpha\beta)\bar{\omega} + (1 + \alpha)\bar{u}]d\tau + dw_1[(1 + \alpha)^2 d\tau] \tag{3}$$

$$d\alpha = (\alpha + \beta + 2\alpha\beta + \alpha^2 + \alpha^2\beta)d\tau \; ; \quad \alpha(0) = 0 \tag{4}$$

$$d\beta = dw_2(Q\, e^{-\tau} d\tau) \; ; \quad \beta(0) = 0 \tag{5}$$

where

$$\boxed{Q = \frac{c^2 q r_o}{v_o^3} \quad \text{(typically .001 - .1)}} \; .$$

REVIEW OF SPECIAL CASE: c = 0

In the more familiar version of this problem [1], λ and v assume their nominal values with certainty at all times. This corresponds to the special case of c = 0 here, meaning that dw_2 is zero, and consequently $\alpha = \beta = 0$, for all τ. In this case, criterion (2) can be expressed as

$$\frac{J}{q} = E\left[S_f \bar{\omega}^2(\tau_f) + \int_0^{\tau_f} \bar{u}^2 \, d\tau \right] \tag{6}$$

where

$\tau_f = \ln(r_o/r_f)$, a predetermined constant, and

$S_f = K(r_f/v_o)^3/R_L^2$.

Minimizing J/q is obviously equivalent to minimizing J.

Assuming that θ is measured accurately enough to treat $\bar{\omega}$ as known (see next section), the problem of finding a control law to minimize (6) has the well-known "linear-quadratic-Gaussian" form [1] if no constraint is imposed on the control magnitude. Its solution is

$$\bar{u} = \frac{-3\,\bar{\omega}}{1 + (\frac{3}{S_f} - 1)e^{-3(\tau_f - \tau)}} \; . \tag{7}$$

If the pursuer's control acceleration is constrained to $|u| \le U$, this result is still meaningful if $K < R_L^2 U^6/q^3$, which implies [1] that the root-mean-square (r.m.s.) u corresponding to the $\bar{u}$ of (7) will always remain less than U.

The influence of the terminal boundary parameters S_f and τ_f on the optimal control decays in reverse (transformed) time $\tau_f - \tau$ with a time constant of 1/3. This corresponds to a range increase of about 40%. More generally, the choice of state and control variables used here essentially "localizes" the optimization problem to range ratios of this order. This means that, except for boundary effects near intercept, control optimality at a given current time is governed primarily by the behavior of $\bar{u}$ and $\bar{\omega}$ over the next 40% reduction in range to the evader.

The effective range of these boundary effects is determined by S_f and τ_f, and typically constitutes only a very small terminal fraction of the engagement. At longer ranges, the optimal control law (usually called a guidance law in this context) is approximately

$$\boxed{u = -3v_o\omega} \tag{8}$$

when expressed in terms of the original variables. This guidance law is an example of proportional navigation, in which the control is proportional to the line-of-sight rate ω. The navigation gain is 3 in this case. Except for the boundary effects near intercept, this single guidance law is optimal for any criterion of the form of (2), meaning for any relative weighting of integrated drag and probability of intercept failure.

APPROXIMATE CONDITIONAL DISTRIBUTION OF α AND β
(for $|\alpha|$, $|\beta| << 1$)

As a first approximation, we retain only the lowest-degree terms in (4) and (5), which gives

$$d\alpha = (\alpha + \beta)d\tau \tag{9}$$

and

$$d\beta = dw_2(Q\, e^{-\tau} d\tau) . \tag{10}$$

If the available measurements z of θ are sufficiently accurate, first and second differences over an interval Δt can be used to construct estimates of the corresponding $\bar{\omega}$ and increment $\Delta\bar{\omega}$ such that

1. the change in τ ($= \bar{\lambda} v_o \Delta t$) is << 1, so that $\bar{u}$ and $\bar{\omega}$ can be considered constant over Δt, and
2. Δt is long enough that the errors in the $\Delta\bar{\omega}$ estimate caused by z-errors are small compared to the average $\bar{\omega}$-increment caused by the random target acceleration.

For z-errors approximated as "white noise" in the usual way, i.e., with

$$dz = \theta\, dt + dw(n\, dt)$$

and

$$n = \sigma^2 \Delta$$

$$\sigma = \text{r.m.s. measurement error } (z-\theta)$$

$$\Delta = \text{error correlation time,}$$

this accuracy condition is

$$\boxed{n << .01\, q/v_o^2} \,. \tag{11}$$

This is usually satisfied for air-to-air homing missiles. In this case, $\bar{\omega}$ can be treated as precisely known and (3) can be used to construct an equivalent measurement ζ in which the target acceleration is the dominant error, with

$$d\zeta \cong [(\bar{u} + 2\bar{\omega})\alpha + 2\bar{\omega}\beta]d\tau + dw_1(d\tau) \,. \tag{12}$$

This results from using $\zeta = \Delta\bar{\omega}/\Delta\tau - 3\bar{\omega}/2 - \bar{u}$ and deleting all but the linear terms in α, β and dw_1 from (3) as relatively small. Applying standard results of Kalman filtering theory [3] to the measurement system of (9), (10) and (12) shows that the conditional *probability distribution* of α and β, given the available θ-measurements, is bivariate Normal, whose mean and covariance matrix, denoted here as

$$\begin{bmatrix} \hat{\alpha} \\ \hat{\beta} \end{bmatrix} \text{ and } \begin{bmatrix} P & B \\ B & L \end{bmatrix},$$

obey certain differential equations. When expressed in terms of the normalized covariance parameters $\bar{P} = P/Q$, $\bar{B} = B/Q$ and $\bar{L} = L/Q$, these equations assume the more instructive form

$$d\hat{\alpha} = (\hat{\alpha} + \hat{\beta})d\tau + QG_1\delta \qquad \begin{cases} G_1 = \bar{u}\bar{P} + 2\bar{\omega}(\bar{B} + \bar{P}) \\ G_2 = \bar{u}\bar{B} + 2\bar{\omega}(\bar{B} + \bar{L}) \\ \delta = d\zeta - [\bar{u}\hat{\alpha} + 2\bar{\omega}(\hat{\alpha} + \hat{\beta})]d\tau \end{cases}$$

$$d\hat{\beta} = QG_2\delta$$

with zero initial *conditions* at $\tau = 0$ and

$$\dot{\bar{P}} = 2(\bar{P} + \bar{B}) - QG_1^2 \qquad \left(= \frac{d\bar{P}}{d\tau}\right) \tag{13}$$

$$\dot{\bar{B}} = \bar{B} + \bar{L} - QG_1G_2 \tag{14}$$

$$\dot{\bar{L}} = e^{-\tau} - QG_2^2 \,. \tag{15}$$

For $Q << 1$ and $\bar{u}$ and $\bar{\omega}$ of order unity, it is clear from these equations that the θ-measurements have little effect on this conditional distribution, so that $\hat{\alpha} \cong \hat{\beta} \cong 0$ and

$$\boxed{\begin{aligned} P &\cong \frac{Q}{3} e^{2\tau}(1 - e^{-\tau})^3 && (16) \\ B &\cong \frac{Q}{2} e^{\tau}(1 - e^{-\tau})^2 && (17) \\ L &\cong Q(1 - e^{-\tau}) && (18) \end{aligned}}$$

until P becomes comparable to 1. After this it is no longer reasonable to approximate α, whose variance is P, as small compared to 1.

OPTIMAL MIDCOURSE GUIDANCE

Taking conditional expectations in (3) under the preceding conditions shows that, given the currently available θ-measurements,

$$\boxed{\begin{aligned} E(d\bar{\omega}) &= [(\tfrac{3}{2} + 2B)\bar{\omega} + \bar{u}]d\tau && (19) \\ E(d\bar{\omega}^2) &= (1 + P)d\tau && (20) \end{aligned}}$$

and

to a good approximation. If Q is not extremely small, however, (6) cannot be used as an equivalent criterion (i.e., one for which the same control law is optimal) because there would be a significant probability that the actual range r does not satisfy (1) when

$\tau = \tau_f$; in fact, intercept might already have occurred. In this case, an optimal expected cost-to-go function H* can be defined in the usual way [4], conditioned both on the available θ-measurements and on whether or not intercept has occurred yet (the cost-to-go being zero if it has). For a $\tau_1 > 1$ such that

$$e^{2\tau_1} < 3/Q \ , \tag{21}$$

which exists for the small values of Q being considered here, P, B and L will remain small compared to unity in the interval $[0, \tau_1]$. Thus the probability is negligible that r will go to zero before $\tau = \tau_1$, and the conditioning of H* on the non-occurrence of intercept can be ignored in this interval. Conditioning on the θ-measurements is also trivial there except for determining the current value of $\bar{\omega}$, so the partial function of H* restricted to $\tau < \tau_1$ and the non-occurrence of intercept is essentially a function H of $\bar{\omega}$ and τ only. Since $H(\bar{\omega}, \tau_1)$ is an even function of $\bar{\omega}$ by symmetry, expanding it in a Maclaurin series gives

$$H(\bar{\omega}, \tau_1) = \text{constant} + \tfrac{1}{2} \frac{\partial^2 H}{\partial \bar{\omega}^2} \bar{\omega}^2 + \text{higher-degree even terms in } \bar{\omega} \ .$$

The higher-degree terms are relatively small in the interesting case where the pursuer is able to keep the unnormalized line-of-sight rate small [2]; anyway, the coefficients of such terms decay to zero in reverse time, as might be expected from the "localization-in-range" property noted earlier. Thus, since the constant term has no effect, the Principle of Optimality of dynamic programming [4] implies that the optimal control law minimizes the equivalent criterion

$$\bar{J} = E\left[S_1 \bar{\omega}^2(\tau_1) + \int_0^{\tau_1} \bar{u}^2 \, d\tau \right] \ ; \quad S_1 = \tfrac{1}{2} \frac{\partial^2 H}{\partial \bar{\omega}^2} \bigg|_{\substack{\tau=\tau_1 \\ \bar{\omega}=0}} \tag{22}$$

for $\tau < \tau_1$ <u>only</u>. Also, (19) and (20) will be valid then for $\bar{\omega}$ and $\bar{u}$ of order unity.

The Bellman equation for the optimal control law of (19), (20) and (22) becomes [4]

$$-\frac{\partial H}{\partial \tau} d\tau = \min_{\bar{u}} E \left[\bar{u}^2 d\tau + \frac{\partial H}{\partial \bar{\omega}} d\bar{\omega} + \tfrac{1}{2} \frac{\partial^2 H}{\partial \bar{\omega}^2} d\bar{\omega}^2 \right]; \ H(\bar{\omega}, \tau_1) = S_1 \bar{\omega}^2 \ , \tag{23}$$

where the expectation is conditioned on $\bar{\omega}(\tau)$. For the expectations of (19) and (20), the solution is

$$H(\bar{\omega}, \tau) = S(\tau)\, \bar{\omega}^2 + \eta(\tau)$$

with

$$\bar{u} = -S\bar{\omega} \ , \tag{24}$$

$$-\dot{S} = (3 + 4B)S - S^2 \ ; \quad S(\tau_1) = S_1 \tag{25}$$

and

$$-\dot{\eta} = (1 + P)S \ ; \quad \eta(\tau_1) = 0.$$

Eq. (25) can be integrated in reverse time from τ_1 by substituting from (17) for $B(\tau)$. Defini..g

$$x = \frac{1}{S} - \frac{1}{3} \quad \text{and} \quad h = \tau_1 - \tau$$

then gives

$$\frac{dx}{dh} = -3x - 2Q(e^{\tau_1 - h} - 2 + e^{h - \tau_1})(\tfrac{1}{3} + \cancel{x}) \ ; \quad x = \frac{1}{S_1} - \frac{1}{3} \quad \text{at } h = 0.$$

If the indicated term is ignored as relatively small, this differential equation can be integrated in h to give

$$x = \left[\frac{1}{S_1} - \frac{1}{3} + \frac{Q}{3}(e^{\tau_1} - \frac{4}{3} + \tfrac{1}{2} e^{-\tau_1}) \right] e^{-3h} - \frac{Q}{3}(e^{\tau_1 - h} - \frac{4}{3} + \tfrac{1}{2} e^{h - \tau_1}).$$

This result is consistent with the ignored term being smaller than the others, except perhaps for a transient at h = 0. Thus, since $Q \ll 1$,

$$S \cong 3 \left[1 + Q \left(e^{\tau} - \frac{4}{3} + \tfrac{1}{2} e^{-\tau}\right) \right],$$

except for a transient at $\tau = \tau_1$ whose effects decay exponentially in reversed transformed time h with a time constant of 1/3 (i.e., a 40% range increase). From (17), (18) and (24), the corresponding approximation of the optimal guidance law can be expressed as

$$\bar{u} = -3(1 + 2B + \tfrac{1}{2}L + Q/6)\bar{\omega} \ . \tag{26}$$

This guidance law is consistent with the assumption of order-unity $\bar{\omega}$ and $\bar{u}$ used in solving the Bellman equation for it.

If c = 0, Q = B = L = 0 and this guidance law reduces to (8), as it should, because (26) becomes

$$u = -3(1 + 2B + \tfrac{1}{2} L + Q/6) v_o \omega$$

in terms of the original state and control variables. As in that special case, this single guidance law is a natural choice for all the objectives of successful intercept, maximizing the pursuer's range, and maximizing its airspeed at intercept. This guidance law still has the form of proportional navigation, but with a higher navigation gain than 3 for $Q > 0$ since, from (17) and (19), B and L are both positive then. For the midcourse region of $1 < \tau < \tau_1 - \frac{1}{2}$, this navigation gain becomes predominantly $3 + 6B$, which is also not a bad approximation when $\tau < 1$ for the small values of Q being considered here. With this simplification, the optimal guidance law here can be expressed as

$$\boxed{u = -3\,[\,1 + 2\,\mathrm{cov}(\lambda/\bar{\lambda},\ v/v_o)\,]\ v_o\omega}\,. \tag{27}$$

The restriction of these results to $\tau < \tau_1 - \frac{1}{2}$ and $\frac{1}{Q} > \frac{1}{3}\,e^{2\tau_1}$ ($\equiv P$) is approximately equivalent to the restriction

$$\boxed{\frac{\bar{r}}{r_o} > \sqrt{Q}}\,,$$

where $\bar{r}$ is the nominal range $1/\bar{\lambda}$. The form of (27) suggests using the factor in square brackets to compensate proportional navigation laws more generally for range and closing speed uncertainty, with an estimated λ and v used in place of $\bar{\lambda}$ and v_o. (λ is a more natural quantity than r to estimate from angle measurements [5].) The analysis here can also be carried through for nonzero P(0) and L(0), which corresponds to an uncertain initial range and closing speed. This extension leaves (27) unchanged, and only changes (26) by adding L(0) to Q. The formulas for P, B and L become more complicated than (16)-(18), however.

WEAVING AND EXTENSION OF MIDCOURSE REGION

So far, the conditioning of the α,β-distribution on the θ-measurements has been ignored in the control optimization, since this is a small effect. We now analyze this effect to a limited extent by considering the possible optimality of deliberate weaving by the pursuer to reduce the uncertainty in the evader's range and closing speed with the resulting parallax information. The normalized control $\bar{u}$ is decomposed as

$$\bar{u} = m + \phi\ , \tag{28}$$

where m varies at only a moderate rate, but ϕ alternates sign rapidly such that over any appreciable increment Δ in (logarithmic) time,

$$\int_{\tau}^{\tau+\Delta} \phi\ d\tau \cong 0 \tag{29}$$

and

$$\int_{\tau}^{\tau+\Delta} \phi^2 d\tau \cong D^2\Delta\ , \tag{30}$$

$\dot{D}$ also having only a moderate value. The analysis here will be even cruder than before, and insensitive to any detail of the alternating (i.e., weaving) control component ϕ beyond its locally averaged magnitude D. For definiteness, ϕ can be imagined as the moderately varying D multiplied by a quantity which alternates rapidly and regularly between ±1:

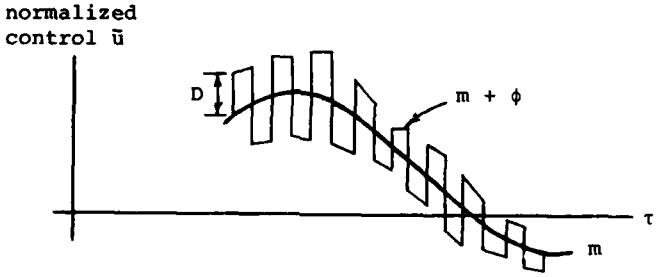

These alternations must be slow enough, however, that the assumptions underlying (13)-(15) are still valid. This constraint need not violate (29) and (30) if the pursuer's θ-measurements are accurate enough. A useful property of this weaving control component is that, over any significant increment in τ,

$$\int(\phi + A)^2\ d\tau \cong \int\phi^2\ d\tau + \int A^2\ d\tau \tag{31}$$

if A varies at only a moderate rate with τ.

Here we seek only the approximate level of the weaving component in an optimal control law of the form of (28), and proceed under the assumption that $P \gg B$ and $P \gg L$, as was true before except for boundary effects. Retaining only the dominant effects of the uncertainty in α and β, and using (19), (20), (22), (29) and (31) gives

$$d\bar{\omega} \cong [\tfrac{3}{2}\,\bar{\omega} + m]d\tau + dw[(1 + P)d\tau]$$

and

$$\bar{J} = E\,[S_1\bar{\omega}^2(\tau_1) + \int_0^{\tau_1}(m^2 + D^2)d\tau] \ .$$

If the effect of m on P is disregarded as minor here, the optimization of m is independent of D and P with the methods of the preceding section, which give $m \cong -3\bar{\omega}$ except for boundary effects. As a result, optimizing the weaving control magnitude becomes approximately the problem of finding $D \geq 0$ to minimize

$$\bar{J} = E\,[S_1\bar{\omega}^2(\tau_1) + \int_0^{\tau_1}(9\bar{\omega}^2 + D^2)d\tau]$$

with

$$d\bar{\omega} = -\frac{3}{2}\,\bar{\omega}\,d\tau + dw[(1 + P)d\tau] \tag{32}$$

and, by virtue of (31),

$$\dot{P} = 2P - P^2(\bar{\omega}^2 + D^2) \ .$$

Defining

$x = 1/P$,

Y = prior expected value of $\bar{\omega}^2$,

$F = D^2 - \bar{\omega}^2$ (used as the control variable),

and using standard methods [3] to determine $\dot{Y}$ from (32), converts this optimal control problem to that of minimizing

$$\bar{J} = S_1Y(\tau_1) + \int_0^{\tau_1}(8Y + F)d\tau$$

with

$$\dot{Y} = -3Y + 1 + 1/x \ , \tag{33}$$

$$\dot{x} = -2x + F \ , \tag{34}$$

and the control constraint $F \geq \bar{\omega}^2$. This constraint is a-priori random, so as a further approximation, we will use the deterministic constraint $F \geq 0$ and interpret any resulting $F < \bar{\omega}^2$ as specifying a weaving magnitude of approximately zero.

If a Hamiltonian is defined as $H = F + 8Y + \lambda_x(F - 2x) + \lambda_y(1 + 1/x - 3Y)$, then [1] equations for F minimizing $\bar{J}$ are (34),

$$-\dot{\lambda}_y = -3\lambda_y + 8 \ ; \quad \lambda_y(\tau_1) = S_1 \ , \tag{35}$$

$$-\dot{\lambda}_x = -2\lambda_x - \lambda_y/x^2 \ ; \quad \lambda_x(\tau_1) = 0 \tag{36}$$

and

$$F = \begin{cases} 0 \text{ for } \lambda_x < -1 \\ \text{value keeping } \lambda_x = -1 \text{ otherwise (singular arc)} \end{cases}$$

The effects of the terminal boundary conditions on the solution again decay in reverse transformed time. From (35), λ_y is always positive and approaches the steady-state value of 8/3. Substituting this and the singular arc conditions into (36) gives $x = 2/\sqrt{3}$, for which (34) gives $F = 4/\sqrt{3}$. Using (13)-(15) then gives approximately

$$\boxed{\begin{aligned} P &= \frac{1}{x} = \tfrac{1}{2}\sqrt{3} \\ B &= L \\ \dot{L} &= Q\,e^{-\tau} - \bar{u}^2L^2 \\ D &= \sqrt{4/\sqrt{3} - \bar{\omega}^2} \end{aligned}} \qquad \begin{aligned} &(37) \\ \\ \\ &(38) \end{aligned}$$

for the singular arc solution away from the terminal boundary. This is consistent with the earlier assumption of $P \gg B$ and $P \gg L$. Finally, (33) shows that Y, the variance of $\bar{\omega}$, approaches a steady-state value of only $(1 + \tfrac{1}{2}\sqrt{3})/3$ under these conditions. Since $\bar{\omega}$ is a zero-mean Normal random variable [3], $\bar{\omega}^2$ has mean Y and variance $2Y^2$, which implies that the optimal magnitude of the (normalized) weaving control in (38) is meaningful with high probability by the Chebychev inequality.

The basic result here is that no amount of weaving is ever optimal under the conditions of the preceding section, because τ_1 was defined there so that P remains considerably less than 1, meaning that the above singular arc conditions never arise. However, the singular arc solution provides a reasonable basis for extending the results of that section beyond such τ_1, which, as (21) shows, can cover a considerable portion of

flight before the terminal boundary region is reached. The high probability of (38) being positive reflects the fact that the weaving component dominates the effect of the control on the conditional α, β - distribution. Thus it is a good approximation in this context as well to optimize the homing control component without regard for its effect on this distribution. If done in the presence of a weaving component with magnitude (38), P would be kept below $\frac{1}{2}\sqrt{3}$, so an estimated current range (or inverse range) would remain a somewhat meaningful quantity. An optimal current homing control component could then be determined as before by using the estimated current inverse range and closing speed as nominal in place of $\bar{\lambda}_o$ and v_o, and by restricting consideration to the next half-unit or so in τ by virtue of the localization-in-range property. The approximation would be poorer in this case because it ignores a more significant probability of the actual r going to zero over the next halving of estimated range. Also, P and B would be large enough that $\hat{\alpha}$ and $\hat{\beta}$ would vary somewhat from zero, although such variations would be comparatively minor over this short a τ-interval according to the Kalman filter equations. This optimization procedure gives the (normalized) homing control as $\bar{u}$ of (24) and (25), with B as specified by the singular arc conditions rather than (17). If the relatively small variation of B is ignored in the integration of (25), $S = 3 + 4B$ in this case away from the terminal boundary. The corresponding optimal control law approximation is given by (28), (38) and

$$\boxed{m = -(3 + 4B)\bar{\omega}} ,$$

which is fairly close to (27) with the weaving component added.

CONCLUSION

The main effect of the closing speed uncertainty on the optimal guidance law is to raise the apparent value of the navigation gain by approximately the factor in (27) - and possibly superimpose some rapid weaving. Significant weaving is not optimal, however, until the range uncertainty grows to a certain level. This level, and the resulting optimal short-term average magnitude of the weaving component, appear to be approximately those given by (37) and (38) in terms of normalized variables. The analysis here is not accurate enough to specify the optimal weaving in any further detail, however. On the average, this weaving is somewhat smaller in magnitude than the other component (proportional navigation) of the optimal guidance law. It nevertheless provides most of the parallax information about the radial relative motion because proportional navigation actually suppresses parallax by acting to null out the line-of-sight rate. These results are subject to the restrictions of (1) and (11), and also do not apply inside a small terminal boundary region near intercept.

LITERATURE

[1] A. E. Bryson and Y.-C. Ho, Applied Optimal Control, Washington, D.C., Hemisphere, 1975.

[2] W. W. Willman, "Some Formal Effects of Nonlinearities in Optimal Perturbation Control," J. Guidance and Control, Vol. 2, No. 2, Mar.-Apr. 1979, pp. 99-100 (see NTIS document #N78-33820).

[3] A. Gelb (ed.), Applied Optimal Estimation, Cambridge, Mass., M.I.T. Press, 1974.

[4] S. E. Dreyfus, Dynamic Programming and the Calculus of Variations, New York, Academic Press, 1965.

[5] V. J. Aidala and S. E. Hammel, "Utilization of Modified Polar Coordinates for Bearings-Only Tracking," IEEE Trans. Aut. Control, Vol. AC-28, No. 3, Mar. 1983, pp. 283-294.

[6] F. W. Nesline and P. Zarchan, "A New Look at Classical vs Modern Homing Missile Guidance," J. Guidance and Control, Vol. 4, No. 1, Jan.-Feb. 1981, pp. 78-85.

[7] A. E. Bryson, "Linear Feedback Solutions for Minimum Effort Interception, Rendezvous, and Soft Landing," AIAA J., Vo. 3, No. 8, Aug. 1965, pp. 1542-1544.

[8] Y.-C. Ho, A. E. Bryson and S. Baron, "Differential Games and Optimal Pursuit-Evasion Strategies," IEEE Trans. Aut. Control, Vol. AC-10, No. 4, Oct. 1965, pp. 385-389.

GUIDAGE ET PILOTAGE DES ARMEMENTS TIRES D'AVION :

POINT DE VUE DE L'AVIONNEUR

PAR

P. PAGNIEZ

F. CHIVOT

AVIONS MARCEL DASSAULT - BREGUET AVIATION

78 quai Marcel Dassault

92214 SAINT-CLOUD

1. RESUME

Les constructeurs d'armements aéroportés conçoivent et développent des produits de plus en plus sophistiqués ; il ne faut cependant pas oublier que l'obtention de manière opérationnelle des performances optimales de ces armes est une conséquence de l'homogénéité de l'association "avion-équipage-arme". Ils imposent ainsi à l'avionneur de résoudre un nombre croissant de problèmes dont la sévérité augmente avec la sophistication de l'armement.

L'avionneur doit donc réaliser un compromis de plus en plus compliqué entre les besoins de l'arme, la vulnérabilité de l'avion (discrétion, signature radar, distance de passage par rapport à l'objectif,...), la charge de travail de l'équipage,... pour assurer la meilleure adéquation possible "avion-équipage armement".

Les contraintes varient selon le type de l'arme mais peuvent se regrouper en familles :

- contraintes d'évolution avant, pendant et après tir,
- contraintes de performance du système de navigation et d'attaque,
- contraintes de compatibilités entre les différents armements,
- contraintes mécaniques,
- actions de l'équipage.

Notre conférence se propose de montrer quelles sont les contraintes posées à l'avionneur et précise quelles sont les indispensables relations entre celui-ci et le fabricant d'armement pour arriver à la meilleure association possible "avion-équipage-arme" avec des armements de plus en plus sophistiqués.

2. INTRODUCTION

Les fabricants d'armes conçoivent et développent des produits de plus en plus sophistiqués, mais dont l'adaptation sur avion impose à l'avionneur de réaliser des compromis de plus en plus compliqués pour assurer, grâce à l'homogénéité de l'association "avion (s) - équipage (s) - arme", l'efficacité de ces armes.

Notre conférence se propose de montrer successivement sur les armements AIR/AIR puis sur les armements AIR/SOL et AIR/MER quels sont les problèmes que l'avionneur doit résoudre pour réaliser ce compromis.

En conclusion, nous proposerons le point de vue des AVIONS MARCEL DASSAULT-BREGUET AVIATION sur la manière de réduire ces problèmes et d'optimiser l'homogénéité de l'association avion (s) - équipage (s) - arme.

3. CAS DES ARMEMENTS AIR/AIR

Il est possible de classer les armements AIR/AIR tirés d'avion en trois familles :

- autodirecteurs passifs,
- autodirecteurs semi-actifs
- autodirecteurs actifs.

Cet ordre correspond à la fois à un ordre chronologique et à un nombre croissant de contraintes imposé à l'avionneur pour obtenir la meilleure adaquation "avion-équipage-arme" possible. Nous nous proposons d'étudier successivement ces trois types d'armements AIR/AIR.

3.1. Cas des autodirecteurs passifs

L'autodirecteur de ces missiles est du type infrarouge ; l'arme est donc attirée par les points chauds de la cible. Le MAGIC (FRANCE) et le SIDEWINDER ou AIM9 (USA) sont des exemples de ce type d'armement. Ces armes sont du type "TIRE ET OUBLIE" et sont plutôt utilisées en combat rapproché ou en autodéfense (la différence entre ces deux actions réside dans le caractère offensif de la première et dans le caractère défensif de la seconde).

Les missiles passifs peuvent être utilisés en autonome et dans ce cas ils ne nécessitent pas d'apport d'information de la part du Système d'Armes de l'avion, si ce n'est l'ordre de tir venant du pilote. En effet, la mission se réalisant dans le champ visuel du pilote, aucun calcul de domaine de tir, aucune identification autre que visuelle ne sont strictement nécessaires. Si le missile est utilisé en mode intégré, il faut alors lui transmettre la direction d'accrochage du radar et les exigences quant à ce capteur deviennent identiques à celles que nous développerons pour les missiles semi-actifs dans le paragraphe suivant.

Par ailleurs, les armements passifs n'imposent aucune contrainte d'harmonisation mécanique sur l'avion. Les principaux problèmes mécaniques que doit résoudre l'avionneur sont une cryogénie de l'arme et l'adaptation d'un lance-missile au point d'emport considéré.

En conclusion, nous pouvons dire que les missiles passifs, du fait de leurs exigences réduites, sont des armements pouvant s'adapter sur tous les avions et sur tous les Systèmes d'Armes. Le MAGIC en est une preuve du fait de sa présence sur une vingtaine d'aéronefs au moins.

3.2. Cas des autodirecteurs semi-actifs

Les missiles semi-actifs représentent un ensemble d'armement dont le but est de réaliser des interceptions à moyenne portée. L'autodirecteur de l'arme est du type électromagnétique. Le SPARROW ou AIM7 (USA), la famille des 530, SUPER 530 F, SUPER 530 D (FRANCE) ou encore le SKYFLASH (ROYAUME UNI) sont des exemples de ce type d'armement. Ces missiles sont plus contraignants pour l'avionneur que les missiles passifs pour deux raisons majeures :

- leur principe de fonctionnement
- leur philosophie d'emploi

Le principe de fonctionnement de ces missiles impose à l'avionneur d'embarquer un moyen permettant d'illuminer continuellement la cible et d'assurer pour les missiles utilisant l'effet Doppler (SUPER 530 D par exemple) une référence arrière du missile. Ceci impose donc :

- de posséder un radar et un mode de fonctionnement de ce radar permettant l'illumination continue de la cible (poursuite sur information continue)
- de posséder dans certains cas un illuminateur continu
- de boucher les trous du diagramme d'antenne du radar pour illuminer la référence arrière de l'arme

Ce principe de fonctionnement a également pour conséquence, du fait de la nécessité d'illuminer de manière continue la cible pendant le vol complet du missile, d'augmenter la vulnérabilité de l'avion par perte de toute information sur la situation tactique (apparition d'autres plots radar par exemple) pendant ce laps de temps (de 20 à 50 secondes) mais aussi par la limitation des évolutions de l'avion.

Par ailleurs, certains missiles nécessitent de recevoir un niveau minimal de signal comme référence arrière, ce qui impose une certaine puissance d'émission du radar en dehors du lobe principal.

La philosophie d'emploi des missiles semi-actifs étant de réaliser des interceptions moyenne portée, la cible se trouve par définition hors du domaine visuel du pilote. Ceci impose donc à l'avionneur de concevoir un Système d'Armes possédant :

- un radar permettant de détecter les cibles suffisamment loin pour utiliser les capacités maximales de l'armement (généralement on considère qu'il existe au moins un facteur 1,8 entre la portée de l'arme et la distance de détection minimale du radar)
- un moyen d'identification sûr car le tir est effectué sur un plot radar
- un moyen de calculer les domaines de tir du missile et les lois de navigation du chasseur
- des informations de bonne qualité sur la position, sur la vitesse relative chasseur-cible pour calculer les domaines et lois précédents, ce qui impose une classe de performances de l'unité de navigation inertielle et du radar du chasseur
- une symbologie adéquate pour une présentation synthétique des informations à l'équipage.

Le fait que l'arme, outre des informations angulaires sur la cible, des informations de distance avion-cible ou de vitesse relative avion-cible si le missile utilise l'effet Doppler, reçoive un échantillon de fréquence, a pour conséquence de constituer des couples radar-arme, ce qui est une contrainte supplémentaire imposée à l'avionneur.

Par ailleurs, si on désire avoir la possibilité de réaliser des tirs d'armements semi-actifs ayant leur autodirecteur déjà accroché sous l'avion, l'avionneur doit étudier les problèmes de découplage avec le radar et de réaliser un système de créneaux temporels par exemple pour éviter tout problème.

En résumé, l'utilisation de missiles semi-actifs impose à l'avionneur des contraintes sur le radar (mode adéquat, portée, qualité et précision des informations), sur l'unité de navigation inertielle, sur l'identification des plots radar, sur les calculateurs (domaines de tir du missile, lois de navigation du chasseur) et sur la présentation des informations à l'équipage.

3.3. Cas des autodirecteurs actifs

Les armements actifs représentent la dernière génération d'armes AIR/AIR tirés d'avion. Les seules études en cours actuellement sont l'AMRAAM (USA) et le MICA (FRANCE). Pour ce dernier, la plage d'utilisation possible couvre le domaine du combat aérien et s'étend jusqu'à celui de l'interception longue portée. De plus, parallèlement à l'augmentation des performances et des capacités de ces armes, la possibilité de faire du tir multicible apparait.

Suivant le type d'utilisation, le vol du missile se déroule de manière différente comme le montrent les trois cas de tir suivants :

- tir à longue portée : trois phases de vol
  - 1 : vol inertiel avec liaison avion-missile pour rafraichissement des informations
  - 2 : vol inertiel pur
  - 3 : accrochage de l'autodirecteur actif
- tir à moyenne portée : deux phases de vol
  - 1 : vol inertiel pur
  - 2 : accrochage de l'autodirecteur actif
- tir à courte portée de combat : une ou deux phases de vol suivant le dépointage
  - (0 : réduction du dépointage si il est important)
  - 1 : accrochage de l'autodirecteur actif

Les trois exemples précédents montrent que le cas de tir le plus contraignant est celui du tir à longue portée. Dans ce cas, l'avionneur doit :

- réaliser une liaison avion-missile, c'est-à-dire qu'il doit implanter dans l'avion un émetteur ayant des performances telles qu'à tout instant, le bilan de liaison soit assuré
- assurer à l'avion et au missile un repère de référence commun
- assurer un alignement par recopie du missile de l'ordre de 30 mrd, ce qui impose d'avoir une bonne datation des informations inertielles issues du Système d'Armes de l'avion
- assurer une détection suffisamment lointaine des cibles et donc d'intégrer au Système d'Armes un radar aux performances adéquates
- assurer une identification sûre des plots radar détectés
- calculer un domaine de tir de plus en plus complexe du fait de l'augmentation des performances des armements et donc de disposer de paramètres issus du Système d'Armes de l'avion de plus en plus précis (radar et centrale à inertie)
- assurer, du fait de la capacité multicible, la gestion de plusieurs missiles, de plusieurs désignations d'objectif, de plusieurs liaisons avion-missile et de présenter de la manière la plus synthétique possible toutes ces informations à l'équipage
- assurer des critères de choix dus au multicible (quel missile sur quelle cible ?)
- prendre en compte dans la définition du Système d'Armes les charges et débits de calcul nécessités par l'emploi de ces armements.

En ce qui concerne le tir à moyenne portée de missiles actifs, les problèmes à résoudre sont les mêmes, à l'exception de ceux liés à la liaison avion-missile qui disparaissent.

Le tir à courte portée ou le combat nécessitent quant à eux la présence de capteurs (optroniques ou viseur de casque par exemple) supplémentaires pour pouvoir effectuer des désignations d'objectifs à des gisements par rapport à l'avion allant jusqu'à ± 90 degrés.

Si l'on considère un système global de plusieurs avions amis (les combats AIR/AIR sont rarement du un contre un), les armements à autodirecteur actif du fait de la capacité multicible qu'ils apportent, accroissent les problèmes posés à l'avionneur pour rendre la coopération efficace :

- établissement d'un repère commun entre les avions
- établissement d'une liaison data link protégée pour les échanges d'informations
- recherche des informations nécessaires à présenter à chaque pilote
- prise en compte de paramètres externes à l'avion dans les critères de choix multicible

On détermine ensuite une représentation d'état récurrente à partir de la représentation d'état continue que nous venons de présenter ; après avoir envisager les critères d'observabilité et de gouvernabilité du système ainsi obtenu, il ne reste plus qu'à appliquer la théorie classique du filtrage de KALMAN discret pour déterminer un filtre de houle numérique optimal (au sens d'une variance d'erreur minimale).

En résumé, l'emploi de missiles actifs impose à l'avionneur de résoudre un nombre élevé de problèmes. Du fait que ce concept soit en cours de développement et afin de minimiser ces contraintes pour ne pas privilégier un aspect au détriment d'un autre, le dialogue doit être permanent entre le fabricant de l'arme et l'avionneur qui possède une vue globale du problème.

4. CAS DES ARMEMENTS AIR/SOL ET AIR/MER TIRES D'AVION

Autant il est simple de classer les armements AIR/AIR tirés d'avion en un nombre réduit de famille (trois en l'occurrence), autant cette classification est difficile pour les armements AIR/SOL et AIR/MER tirés d'avion du fait de leur grande variété (bombes lisses, bombes freinées, bombes superfreinées, bombes modulaires, missiles à autodirecteur laser, missiles à autodirecteur TV, missile à autodirecteur radar, roquettes,...) et des particularités de chacun. C'est pourquoi nous avons préféré faire une étude des différents types de problèmes posés à l'avionneur en l'illustrant par des exemples.

Ces problèmes peuvent se regrouper en quatre thèmes principaux mais non totalement distincts comme nous le verrons dans la suite de l'exposé. Ces thèmes sont :

- contraintes imposées au niveau du Système d'Armes de l'avion
- contraintes au niveau des évolutions de l'avion pendant la mission
- contraintes au niveau des actions de l'équipage
- contraintes au niveau de la vulnérabilité de l'avion

4.1. Contraintes au niveau du Système d'Armes

L'évolution des performances et de la complexité des armes impose d'une part une qualité toujours plus grande des paramètres élaborés dans le Système d'Armes de l'avion et d'autre part parfois la présence de capteurs externes sans lesquels l'emploi de l'arme serait impossible.

L'évolution des performances des armes a pour conséquence de donner aux conditions initiales d'utilisation des armes une part de plus en plus importante dans le budget d'erreur final de ces armements. Ainsi par exemple, si l'on considère des tirs sur coordonnées où une phase de vol de l'arme est une phase de navigation inertielle et c'est une tendance actuelle afin d'augmenter les portées, l'avionneur doit résoudre les problèmes suivants :

- problèmes d'harmonisation mécanique de plus en plus précise de l'arme sur son pylône et du pylône sur l'avion, ce qui augmente les coûts de fabrication
- problèmes de procédure d'alignement de la centrale de l'arme sur la centrale de l'avion, ce qui a pour conséquences d'imposer des contraintes d'évolution de l'avion, des contraintes sur la qualité et la précision des informations issues de la centrale avion, des contraintes sur la qualité de datation de ces informations, des contraintes sur la qualité des recalages précédant l'alignement
- problèmes de compensation par logiciel des modes souples de l'avion

Si l'on considère maintenant qu'une liaison data link mono ou bidirectionnelle entre l'avion et le missile soit nécessaire comme cela pourrait être le cas pour un missile tiré sur coordonnées dont on voudrait rafraichir la désignation d'objectif ou encore le cas d'une arme de type MAVERICK à guidage TV dont on doit transmettre l'image vidéo vers l'avion et à qui on doit retourner des ordres de pilotage, un certain nombre de contraintes apparait pour l'avionneur :

- contrainte d'avoir à tout instant quel que soit l'environnement (brouillé ou non) un bilan de liaison satisfaisant
- contrainte d'assurer une protection de cette liaison
- contrainte d'assurer un champ de la liaison suffisant pour ne pas imposer de surcroit un domaine d'évolution à l'avion.

Dans le cas particulier de certaines armes, l'avionneur est contraint de disposer dans son Système d'Armes de capteurs supplémentaires. C'est le cas par exemple des armes guidées laser qui imposent la présence d'un pod de désignation laser ou d'un écartomètre laser si le tir se fait en coopération avec un autre avion ou tout moyen permettant d'illuminer la cible. C'est le cas également de certains missiles qui nécessitent la présence d'un mode radar particulier.

L'avionneur se trouve aussi contraint du fait de la complexité des armes et du volume d'informations qui leur est nécessaire toujours plus grand, de dimensionner son Système d'Armes en fonction du volume de données transitant entre l'avion et les armes (paramètres inertiels, cartes prédictives, images vidéo,....) et de résoudre de manière satisfaisante le problème de la datation de ces informations.

Par ailleurs, du fait de ce dialogue de plus en plus complexe qui s'établit entre l'avion et l'armement et de la diversité de ce dialogue en fonction des armes, l'avionneur ne pouvant privilégier telle ou telle arme, se trouve contraint de standardiser à la fois les interfaces (norme 1760 B) mais aussi les postes de commandes de ces armes en multiplexant les commandes par exemple.

Enfin, de la même manière que pour les armements AIR/AIR, l'avionneur doit calculer des domaines de tir de plus en plus pointus en prenant en compte des modélisations de plus en plus compliquées (la balistique n'a rien à voir avec celle d'une bombe lisse par exemple) mais aussi des paramètres issus de capteurs précis (centrale inertie, radar, moyen de télémétrie, moyens de recalages,...). Cette étape franchie, l'avionneur se trouve confronté au problème de la présentation synthétique des informations à l'équipage.

En résumé, les principaux problèmes posés par les armements AIR/SURFACE modernes au niveau du Système d'Armes et que doit résoudre l'avionneur sont :

- contraintes de performances capteurs nécessaires
- contrainte d'équipements supplémentaires nécessaires à l'utilisation de certains armements
- contrainte de volume d'échange entre lar armes et le système d'armes
- contrainte de standardisation des points d'emports et des postes de commande de ces emports
- contrainte de datation des informations transmises aux armes
- contrainte de présentation simple des informations à l'équipage

Ces contraintes peuvent être diminuées en nombre et en sévérité si le contact s'effectue le plus tôt possible entre l'équipementier et l'avionneur et non quand tous les choix sont verrouillés. En effet, si le dialogue s'effectue le plus en amont possible, il est alors moins compliqué de changer le débattement d'un autodirecteur, moins compliqué de faire évoluer sa sensibilité, moins compliqué de modifier la méthode de guidage ou la méthode de recalage d'un missile par exemple.

4.2. Contraintes au niveau des évolutions de l'avion

L'utilisation de certaines armes AIR/SOL (armes guidées laser, armes à guidage TV par exemple) impose à l'avionneur dans la réalisation de sa conduite de tir associée, de réduire le domaine des évolutions possibles de l'avion pendant certaines phases de la mission, ce qui va parfois à l'encontre des problèmes de réduction de la vulnérabilité de l'avion (discrétion, distance de passage par rapport à la cible).

Avant tir, le domaine d'évolution peut, du fait de la nécessité d'un certain type d'alignement de la centrale inertielle du missile sur celle de l'avion, être réduit en facteur de charge, en pente, voire même imposé si cela est nécessaire. Des contraintes d'évolutions avant tir existent également quand l'équipage doit faire une désignation de l'objectif par un capteur quelconque.

Pendant le tir, des contraintes d'évolutions liées à la réussite du tir existent également. Certaines armes ne se tirent qu'en palier, d'autres imposent le tir en piqué.

Après tir, les contraintes d'évolutions de l'avion peuvent être imposées par :

- le fait que la cible doive toujours être illuminée (cas des armes guidées laser par exemple)
- le fait que la cible doive renvoyer un niveau minimal d'énergie vers l'autodirecteur de l'arme pour qu'il accroche
- le fait que l'on doive garder le missile dans le champ de la liaison data link avion-cible

Ces contraintes d'évolutions après tir ont pour conséquence de réduire la distance de passage de l'avion à la cible et donc d'augmenter la vulnérabilité de l'avion. Elles pourraient être réduites dans le cas où pour une nouvelle arme la coopération entre l'avionneur et l'équipementier commencerait suffisamment en amont. Ainsi l'augmentation de la sensibilité d'un autodirecteur décidée en commun pourrait avoir pour conséquence d'augmenter al distance de passage avion-cible et donc de réduire la vulnérabilité de l'avion. C'est pourquoi le concept de travail en coopération de plusieurs avions, l'un en basse altitude assurant le tir du missile, l'autre en haute altitude plus éloigné de la cible assurant son guidage ou l'illumination de la cible est à développer car cela permet de réduire la vulnérabilité des avions et la charge de travail des pilotes.

4.3. Contraintes au niveau des actions de l'équipage

L'évolution des armes, la complexité toujours croissante de leur mise en oeuvre, font que l'avionneur se voit contraint de trouver des solutions pour réduire la charge de travail de l'équipage. L'avionneur est alors contraint, soit :

- de privilégier certains actes de l'équipage au détriment d'autres (cas du missile à autodirecteur TV que el pilote dans un avion monoplace doit guider tout en pilotant ; le guidage est privilégié par rapport au pilotage)
- de multiplier les membres de l'équipage (avion biplace ou dans l'exemple précédent, le poste avant assurerait le pilotage de l'avion, le poste arrière le guidage du missile) mais c'est une solution chère
- de sécuriser certaines informations pour que le pilote n'ait pas à les vérifier.

4.4. Contraintes au niveau de la vulnérabilité des avions

La réussite d'une mission dépend de l'efficacité de l'arme, mais aussi du fait que l'avion ait été dans de bonnes conditions au moment du tir afin que l'arme ait son efficacité maximale. Ceci impose de réduire la vulnérabilité potentielle de l'avion. Pour cela, l'avionneur est contraint d'augmenter les contre-mesures (pour, entre autres, protéger l'avion pendant les solutions nécessaires às l'alignement du missile) ou encore d'essayer de plaquer au maximum les emports à l'avion pour réduire la Surface Equivalente Radar. L'avionneur est aussi contraint de solutionner les problèmes de compatibilité entre les armements et les équipements du Système d'Armes (contre-mesures par exemple).

5. CONCLUSIONS

Les exemples que nous venons de donner aussi bien pour les armements AIR/AIR tirés d'avion que pour les armements AIR/SOL et AIR/MER tirés d'avion montrent que la sophistication toujours plus grande de ces armes augmente le nombre de problèmes que l'avionneur doit résoudre en effectuant le meilleur compromis possible entre l'avion, l'arme et l'équipage souvent après qu'un bon nombre de paramètres aient été fixés. C'est pourquoi, les "AVIONS MARCEL DASSAULT -BREGUET AVIATION" estiment que le dialogue "avionneur-fabricant d'armes" doit être initialisé le plus tôt possible.

Ainsi par exemple, l'avionneur, le fabricant d'armes, les équipementiers, avant même d'avoir défini l'avion, doivent réaliser des études de concepts en commun pour tenir compte des évolutions possibles de l'avion, des armements et des capteurs. Si certains points paraissent plus difficiles, des études de prédéveloppement précises sont alors nécessaires (développement exploratoire multicible par exemple).

Au moment de la définition d'un programme avion, les AMD-BA estiment que l'étude système qui introduit par rapport aux études précédentes des paramètres supplémentaires comme la vulnérabilité avion, sa polyvalence, les problèmes d'interface homme-machine, de standardisation (ce qui implique aussi des contraintes sur l'arme) doit être réalisée en commun et que les équipementiers doivent ensuite participer au développement complet de l'avion. Il faut aussi souligner que toutes ces études doivent être réalisées en n'oubliant pas que l'armement considéré doit également s'adapter sur plusieurs avions.

SYSTEME DE CONTROLE AUTOMATIQUE DU VOL POUR HELICOPTERES MODERNES

par

J.C.Derrien
S.F.I.M.
13 Av. Marcel Ramolfo-Garnier
91301 Massy, France

et

P.Cauvy
Aérospatiale — Division Hélicoptères
France

RESUME

Cet article a pour but de présenter l'état de l'art à la SFIM et à l'AEROSPATIALE - DIVISION HELICOPTERES en matière de conception et de développement de systèmes de pilotage automatique utilisant les techniques numériques.

Dans une première partie, nous aborderons plutôt les aspects opérationnels des missions relatives aux hélicoptères en général et nous essaierons de déterminer leurs relations avec le système de contrôle automatique du vol au travers de quelques exemples.

Dans la deuxième partie de cet exposé, nous insisterons plus particulièrement sur les aspects théoriques qu'il est nécessaire de maîtriser afin de déterminer les meilleures lois de pilotage de l'hélicoptère, compatibles avec les exigences opérationnelles de sa mission. Nous choisirons pour cela quelques exemples représentatifs.

Enfin dans une troisième et dernière partie nous présenterons le système de contrôle automatique du vol AP 165, actuellement en cours de développement à la SFIM, et qui intègre tous les besoins recensés à l'heure actuelle par les trois armes (air, terre, mer) relativement aux missions que l'on confère aux hélicoptères. L'application au cas du SUPER PUMA MK2 de l'AEROSPATIALE - DH (Marignane - FRANCE) servira de support à cette présentation.

1 - SYSTEME DE CONTROLE AUTOMATIQUE DU VOL ET ASPECTS OPERATIONNELS RELATIFS A L'UTILISATION DE L'HELICOPTERE

1.1. CONSIDERATIONS GENERALES

Nous allons nous attacher à mettre en évidence dans ce premier chapitre les relations très fortes qui existent entre la définition opérationnelle de la mission de tout hélicoptère et les caractéristiques qu'il est alors nécessaire d'associer au système de contrôle automatique du vol afin que l'hélicoptère puisse réaliser cette mission dans les meilleures conditions et avec une charge de travail aussi allégée que possible en ce qui concerne l'équipage.

D'une manière générale, la fonction pilotage automatique de n'importe quel hélicoptère peut être décomposée en deux parties.

Une première partie concerne le contrôle des attitudes, du cap et des vitesses angulaires autour du centre de gravité de l'hélicoptère. La seconde partie concerne la trajectoire de l'hélicoptère dans l'espace et par conséquent le contrôle de l'altitude, des vitesses et accélérations linéaires dans les trois dimensions. Par la suite, on utilisera la terminologie "stabilisations de base" pour la première partie et "modes supérieurs" pour la seconde partie.

L'hélicoptère possède un comportement naturel relativement instable et est un véhicule dont les caractéristiques de fonctionnement sont fortement non linéaires dans l'ensemble de son domaine de vol. C'est par ailleurs un aéronef qui présente de très fortes intéractions entre ses différents axes de pilotage, avec des dynamiques assez rapides. Par exemple un mouvement de la commande de pas collectif (puissance moteurs) génère des mouvements importants sur les autres axes (en tangage, roulis et lacet), lorsque l'hélicoptère est laissé aux mains du seul pilote humain, et ce bien que des précautions aient été prises dans la conception mécanique de l'hélicoptère lui-même. On conçoit alors aisément qu'afin de diminuer la charge de travail du pilote humain, et pour que sa mission puisse être accomplie, il sera nécessaire de lui adjoindre un système de contrôle automatique, ce système devenant d'autant plus complexe et d'autant plus perfectionné que l'hélicoptère est plus difficile à piloter et que les missions qui lui sont dévolues sont de plus en plus sophistiquées.

Cependant, la façon dont on va définir le système de pilotage ne peut être fait ni dans l'absolu, ni de manière unique (comme on pourrait le concevoir pour un asservissement linéaire traditionnel). Il s'agit la plupart du temps d'un ensemble de contraintes qu'il faut prendre en compte, tout en alliant les objectifs de sécurité et de performance qui sont nécessaires pour réaliser la mission de l'hélicoptère.

Nous avons abordé précédemment le problème de l'interactivité entre les différents axes de pilotage : vouloir faire en sorte que l'action du pilote humain sur un axe de pilotage ne touche systématiquement que les paramètres de pilotage associés à cet axe, en admettant que ce soit possible, ne serait pas obligatoirement satisfaisant car il est des situations opérationnelles où de tels couplages naturels sont tout à fait bénéfiques.

Par exemple, lorsque à grande vitesse pour des raisons de confort et de sécurité on désire piloter le paramètre altitude barométrique par l'axe de tangage, alors que pour plus de précision et à vitesse plus faible on voudra contrôler ce même paramètre par l'axe collectif (puissance moteurs). Par contre, dans d'autres situations, il est impératif de minimiser ces mêmes couplages lorsque, par exemple, le pilote humain veut effectuer au travers du système de pilotage une commande manuelle qui contrôle un seul paramètre et de manière aussi pure que possible.

De la même façon nous avons parlé du caractère très instable de l'hélicoptère autour de son centre de gravité. Si dans beaucoup de situations on cherche avant tout à obtenir au niveau des stabilisations de base des tenues de paramètres à long terme qui soient très performantes, il est des cas, en vol tactique par exemple, où l'on veut conserver ou modifier la trajectoire et les assiettes d'un hélicoptère par de faibles déplacements des commandes de vol, et où l'on cherchera plutôt à utiliser (voire à amplifier), tout en la contrôlant, l'instabilité naturelle de l'hélicoptère, afin que ce dernier réponde plus vite aux sollicitations du pilote humain en vitesse angulaire et en accélération. Là encore, on constate que pour chaque situation opérationnelle, on peut déterminer un système de contrôle automatique qui réagisse de manière tout à fait adaptée, et ceci aussi bien au niveau des stabilisations de base qu'au niveau des modes supérieurs : ce sont les modes supérieurs qui le plus souvent caractérisent la mission propre à l'hélicoptère.

Dans cette présentation nous ne passerons pas en revue tous les rôles que peut jouer l'hélicoptère en ce qui concerne les aspects opérationnels, aussi bien pour les missions civiles que pour les missions militaires. Cependant, afin de bien mettre en lumière les quelques réflexions que nous venons de proposer, nous allons choisir plusieurs exemples assez caractéristiques qui montrent comment l'on va passer du contexte opérationnel à la synthèse des lois de pilotage, et surtout avec quelles techniques et quels moyens.

1.2. ETUDE DE QUELQUES FONCTIONALITES PARTICULIERES D'UN SYSTEME DE PILOTAGE POUR HELICOPTERE

1.2.1. Missions envisagées

Nous allons illustrer notre propos en choisissant quelques modes supérieurs de pilotage que l'on rencontre dans les missions de type "Marine" comme le sauvetage en mer (SAR = Search And Rescue) ou la lutte ASM (Anti Sous-Marine), ou bien encore dans les missions du type "Terrestre" comme le tir canon, le tir de roquettes ou la surveillance du champ de bataille. Cependant, avant d'entrer plus directement dans la description des besoins opérationnels relatifs à ces différentes missions, nous allons traiter plus particulièrement le cas des stabilisations de base de l'hélicoptère, fonctions qui présentent certaines difficultés qu'il faut avoir résolues avant d'aborder l'aspect mode supérieur pour une mission déterminée.

1.2.2. Problèmes liés aux stabilisations de base

Le pilotage d'un hélicoptère par l'intermédiaire d'un système de contrôle automatique du vol est un problème complexe dans la mesure où, contrairement à l'avion, l'hélicoptère présente des dynamiques rapides, des non-linéarités marquées dues aux interactions entre les différentes parties de l'appareil (fuselage, rotor principal, rotor arrière), de forts couplages entre axes et des instabilités prépondérantes aux basses vitesses.

Les systèmes actuels de pilotage automatique permettent de stabiliser l'appareil dans tout son domaine de vol avec des performances correctes, mais ne résolvent pas complétement le problème des couplages entre les 4 axes de pilotage dans ce même domaine. Par ailleurs, et en conséquence, ils ne diminuent pas suffisamment la charge de travail de l'équipage, compte tenu des missions de plus en plus sophistiquées que l'on fait réaliser à l'hélicoptère.

L'évolution des techniques numériques dans le domaine aéronautique a ouvert de nouvelles voies dans la maîtrise des qualités de vol des hélicoptères possédant des systèmes de contrôle automatique. Les critères qu'il est nécessaire de prendre en compte aujourd'hui dans l'élaboration des lois de pilotage concernent non seulement la stabilité (statique et dynamique) du véhicule en cas de perturbations, mais ce sont aussi ceux qui permettent d'assurer par ailleurs une bonne maîtrise du découplage des commandes et des états selon les modes de fonctionnement envisagés, une maniabilité accrue de l'aéronef et surtout qui permettent de conférer une robustesse maximale au système de contrôle automatique, et ce dans tout le domaine de vol de l'hélicoptère, c'est-à-dire de - 10 kt à + VNE (vitesse maximale admissible).

Par ailleurs, le système de contrôle automatique du vol d'un hélicoptère au niveau de ses stabilisations de base doit pouvoir être surpassé à tout moment par le pilote humain de manière "transparente", c'est-à-dire sans que cela ne provoque d'à-coups, ni de discontinuités sur l'état de l'hélicoptère, y compris sur les mouvements de ses servo-commandes. Pour cela, les critères de passage de la phase pilotage automatique/pilotage humain à la phase pilotage humain/pilotage automatique doivent être déterminés de manière très précise.

On imagine aisément, compte tenu de tous les problèmes énoncés précédemment, que seules des techniques avancées de l'automatique nous permettront de définir les "meilleures" stabilisations de base pour un hélicoptère donné. Ce sera l'objet d'une partie du chapitre 2, où nous présenterons rapidement les études qui ont été faites sur ce point particulier.

1.2.3. Cas des missions du type "Marine"

La SFIM et l'AEROSPATIALE - DH se sont efforcées ces dernières années de définir et de mettre au point en vol des fonctions liées aux opérations de sauvetage en mer et de lutte anti sous-marine. Tous les modes supérieurs correspondant à ces missions ont été intégrés dans le système Coupleur De Vol CDV 155 sur les hélicoptères Dauphin 365 N1 et Super Puma 332. Ce système est actuellement en production série.

La fonction dont nous allons présenter maintenant les principaux aspects opérationnels est la "Transition automatique vers le bas". C'est un mode de pilotage complexe qui nécessite le contrôle des 4 axes simultanément.

La mise en place d'une telle fonction suppose que les problèmes liés aux stabilisations de base soient parfaitement résolus en tout point, car ce mode de pilotage met en jeu tout le domaine de vol de l'hélicoptère. En effet, à partir d'un état initial quelconque (vitesse longitudinale, vitesse verticale, hauteur radio-sonde), le système de navigation ayant amené auparavant l'hélicoptère face au vent, par un simple appui sur la touche (T.DWN) du poste de commande, le système de contrôle du vol doit pouvoir, à cap constant, amener l'hélicoptère au stationnaire (vitesses Doppler stabilisées à zéro) et à une hauteur radio-sonde (min. 40 ft) préaffichée par l'équipage avant l'engagement du mode. Cette transition vers le bas au-dessus de la mer doit être possible de jour comme de nuit, dans de mauvaises conditions météo, et pour des états de mer allant jusqu'à force 5-6. Par ailleurs la transition automatique doit avoir un comportement parfaitement reproductible en terme de distance au naufragé pour des conditions initiales identiques, s'effectuer en temps minimal et respecter un grand nombre de contraintes, pour des raisons de confort mais aussi de sécurité. Les contraintes principales portent sur les accélérations et décélérations longitudinales admissibles, sur les vitesses verticales que l'hélicoptère peut prendre au fur et à mesure qu'il descend et au fur et à mesure que sa vitesse longitudinale (air ou sol) diminue.

En outre, le profil de descente doit être optimal et nécessite un couplage paramétrique temporel entre les axes. D'autres contraintes peuvent également apparaître, notamment afin d'éviter tout recul final lors de la mise à plat au stationnaire et pour limiter les évolutions d'assiettes en tangage et roulis. Par ailleurs, le pilotage en altitude et en vitesse doit être précis. Au départ de la transition vers le bas à grande vitesse, un cabré à pas constant ayant tendance à faire remonter l'hélicoptère, le couplage entre les axes tangage et collectif doit être minimum. Cette brève description des aspects opérationnels liés à un tel mode montre qu'il sera nécessaire là encore de mettre en oeuvre un certain nombre de techniques de l'automatique, comme nous le verrons dans le chapitre 2.

1.2.4. Cas des missions du type "Terrestre"

A l'heure actuelle, plusieurs expérimentations sont menées par AEROSPATIALE-DH et SFIM en ce qui concerne la mise au point en vol de fonctions telles que le tir canon et le tir de roquettes, destinées au Dauphin 365 M "Panther", ou la surveillance du champ de bataille à l'aide d'une antenne radar aéroportée sur Puma 330 (système pré-ORCHIDEE).

Nous avons volontairement regroupé ces différentes fonctions car elles présentent du point de vue opérationnel des similitudes assez proches en ce qui concerne l'interaction du système d'armement avec l'hélicoptère porteur et nécessitent la mise en oeuvre de techniques de l'automatique qui, contrairement aux autres fonctions que nous avons abordées dans les paragraphes précédents, n'entrent pas véritablement dans un cadre théorique conventionnel.

a) Relativement au tir canon, il est nécessaire que le pointage de l'arme soit extrêmement précis et que l'hélicoptère soit en configuration stationnaire, ou en virage à grande vitesse, ou encore en vol de translation rectiligne avec l'axe du canon situé selon un autre axe en site et gisement. Or dans de telles conditions, le tir en rafale de cette arme est de nature à induire sur l'hélicoptère lui-même des mouvements qui vont dégrader considérablement la précision du tir.

b) Pour ce qui est du tir de roquettes, le problème est sensiblement le même encore que, l'armement étant fixe en gisement par rapport à l'hélicoptère, il peut exister des situations qui induisent des mouvements dissymétriques en lacet au niveau du porteur. Par ailleurs la précision du tir est aussi fortement liée à celle des informations du sytème de visée et de télémétrie laser éventuelle. Or sous l'action d'un tir de roquettes en rafale, les mouvements subis par l'équipage réduisent considérablement le confort de visée.

c) Enfin en ce qui concerne le fonctionnement de l'antenne radar tournante aéroportée, il existe également un compromis à trouver entre la précision de stabilisation du faisceau de l'antenne et les effets aérodynamiques induits sur l'hélicoptère en translation rectiligne de 80 kts à 120 kts, par le fonctionnement de l'antenne elle-même : une telle antenne peut en effet prendre des configurations très variées relativement au site et au gisement de son axe principal, par rapport à l'axe principal du porteur, et en ce qui concerne son balayage par rapport à son axe principal.

Dans les trois cas que nous venons d'aborder, on conçoit aisément que le système de pilotage automatique aura un rôle prépondérant à jouer afin de conférer à l'ensemble (système d'armes, porteur) une précision suffisante dans toutes les configurations opérationnelles relatives à la mission de l'hélicoptère sur lequel il sera monté. Cependant, comme nous allons le voir dans le chapitre suivant, les techniques de l'automatique utilisées pour résoudre ce type de problèmes sont relativement pauvres et appartiennent à la catégorie des "précommandes" en boucle ouverte.

2 - TECHNIQUES DE L'AUTOMATIQUE ET ETUDE DE LOIS DE PILOTAGE POUR HELICOPTERE

2.1. INTRODUCTION

Les principales techniques de l'automatique que nous avons été amenés à utiliser ces dernières années découlent directement des spécificités opérationnelles relatives aux quelques exemples que nous avons présentés précédemment. Par ailleurs, leur introduction dans l'élaboration des systèmes de contrôle automatique du vol a été grandement facilitée par l'utilisation des techniques numériques.

Les quelques théories que nous avons retenues pour réaliser certaines lois de pilotage ont fait l'objet de nombreux travaux à la SFIM et à l'AEROSPATIALE-DH, travaux qui ont été soutenus par la Direction Générale pour l'Armement (DRET et STTE). Dans la suite de cette présentation, nous n'entrerons pas de manière explicite dans un développement théorique quelque peu rébarbatif mais nous insisterons plutôt sur les méthodes qui ont servi à la détermination de lois de pilotage performantes.

En particulier, nous aborderons l'utilisation des techniques de commande multivariable en ce qui concerne la définition des stabilisations de base d'un hélicoptère, et l'utilisation des techniques de commande optimale et de filtrage de KALMAN en ce qui concerne la synthèse de certaines lois, comme celles relatives au mode "Transition automatique vers le bas". La détermination des précommandes relatives au fonctionnement particulier de certains systèmes d'armes sera également abordée. Pour chacun des exemples choisis, nous présenterons brièvement les résultats obtenus. Par ailleurs, sans toutefois entrer dans le détail, nous parlerons dans ce chapitre des outils informatiques qui supportent les quelques méthodes présentées.

2.2. EXEMPLE DES STABILISATIONS DE BASE POUR HELICOPTERE

2.2.1. Position du problème

Ayant choisi un cas de vol donné et un type d'hélicoptère, les paramètres que l'on peut fixer a priori étant l'altitude, la vitesse-air longitudinale, la masse, le centrage, la vitesse verticale et le dérapage initiaux de l'appareil, un modèle linéaire tangent d'ordre 8 peut être généré à partir du modèle non-linéaire S80, représentatif du comportement de l'hélicoptère, modèle développé par AEROSPATIALE-DH et que nous utilisons pour la mise au point des systèmes de pilotage actuels.

Dans une première phase, les modèles linéaires sur lesquels nous travaillons se présentent sous une forme d'état classique :

$$\begin{cases} \dot{X} = AX + BU \\ Y = CX \end{cases}$$

où

X est le vecteur des états de l'hélicoptère,

Y est le vecteur des mesures effectuées à bord,

U est le vecteur des commandes de pas (cyclique longitudinal, collectif, cyclique latéral, palonnier), relatives au rotor principal et au rotor anti-couple.

Quelques remarques s'imposent en ce qui concerne les matrices A et B, qui justifient la nécessité de l'introduction d'un système de stabilisation de l'hélicoptère :

- Les valeurs propres de la matrice A qui caractérisent les modes de l'hélicoptère "naturel" ne sont pas satisfaisantes en termes de stabilité : parties réelles positives (modes instables), amortissements insuffisants (pour les modes stables).

- Les matrices A et B ont un caractère "complet", c'est-à-dire peu de coefficients nuls, témoignant d'une forte interaction entre les différents états et entre les différentes commandes, ce qui traduit un fort couplage entre les mouvements sur les différents axes pour l'hélicoptère naturel.

- Ces matrices ont par ailleurs des évolutions extrêmement non-linéaires lorsque l'on parcourt le domaine de vol de l'hélicoptère, c'est-à-dire principalement du stationnaire à la croisière à vitesse maximale, la vitesse-air longitudinale étant le paramètre prépondérant. L'analyse de ces évolutions correspond à une seconde phase de travail mais cette fois en utilisant le modèle non-linéaire de l'hélicoptère.

Finalement il s'agit donc de déterminer des lois de pilotage qui permettent :

a) la stabilisation de l'appareil en boucle fermée, avec une dynamique imposée,

b) un découplage statique aussi bon que possible des axes de pilotage,

c) le découplage dynamique des commandes à la disposition de l'équipage,

d) une réjection maximale des perturbations extérieures agissant sur l'état de l'hélicoptère,

e) et l'adaptation de l'appareil en tout point de son domaine de vol (robustesse).

Pour atteindre cet objectif, nous avons essayé plusieurs méthodes que nous avons ensuite comparées entre elles, afin de retenir autant que possible celles qui présentent le meilleur compromis "performance/facilité de mise en oeuvre et d'optimisation".

2.2.2. Présentation des méthodes multivariables retenues pour cette étude

Elles appartiennent essentiellement à deux groupes :

- le groupe des méthodes fréquentielles, qui permettent la conception de systèmes de contrôle robustes à partir de modèles non exacts,

- le groupe des méthodes géométriques, qui permettent de dominer la structure interne du système à contrôler, mais qui nécessitent des modèles relativement éprouvés si l'on veut obtenir des lois de commande robustes.

a) Méthodes fréquentielles

Elles permettent une extension au cas multivariable des notions classiques en monovariable à savoir : lieu de Nyquist/Bode, marge de gain et marge de phase, lieu des pôles.

Nous rappelons ci-après les principes généraux de l'analyse fréquentielle des systèmes :

Méthode des lieux caractéristiques

Considérons un système propre φ (A, B, C) décrit par sa représentation d'état :

$$\begin{cases} \dot{X} = AX + BU \\ Y = CX \end{cases}$$

X est le vecteur d'état de dimension n,

U et Y sont respectivement le vecteur des commandes et le vecteur des mesures de dimension m.

A, B, C sont des matrices de dimensions appropriées.

Etudions le système en boucle ouverte : soit g(s) la fonction algébrique définie par l'équation caractéristique :

$$\text{(i) dét } (g\, \dot{I}_m - G(s)) = \text{dét } (g\, \dot{I}_m - C\,(s\, \dot{I} - A)^{-1}\, B)) = 0$$

où G(s) est la fonction de transfert du système en boucle ouverte.

Les m branches de g(s) forment l'ensemble des fonctions analytiques $\{g_i(s)\}$ distinctes localement, appelées fonctions de gains caractéristiques (GC) ; les vecteurs propres $\{W_i(s)\}$ associés aux valeurs propres $\{g_i(s)\}$ sont les Directions Caractéristiques (DC). Les lieux des $\{g_i(s)\}$ obtenus lorsque s décrit le contour de Nyquist dans le sens horaire sont appelés Lieux Caractéristiques (LC).

L'introduction de g(s) permet de généraliser au cas multivariable le critère de stabilité de Nyquist et l'approche Nyquist/Bode classique.

En effet, considérons la forme dyadique de G(s) :

$$G(s) = \sum_{i=1}^{m} g_i(s)\, W_i(s)\, V_i^{\,t}(s)$$

où $\left\{V_i^{\,t}(s)\right\}$ est l'ensemble des vecteurs propres duals de $\left\{W_i(s)\right\}$.

Si R(s) est la matrice de fonction de transfert du système en boucle fermée, elle admet la décomposition dyadique suivante :

$$R(s) = \sum_{i=1}^{m} \frac{g_i(s)}{1 + g_i(s)}\, W_i(s)\, V_i^{\,t}(s) = \sum_{i=1}^{m} r_i(s)\, W_i(s)\, V_i^{\,t}(s)$$

Les directions caractéristiques sont donc conservées par retour unitaire et les gains caractéristiques $\{r_i(s)\}$ s'écrivent simplement :

$$r_i(s) = \frac{g_i(s)}{1 + g_i(s)} \quad \text{, pour } i = 1, \ldots m$$

ce qui permet de caractériser aisément le comportement en boucle fermée du système à partir de son comportement en boucle ouverte, de la même façon qu'en monovariable.

D'autre part, l'introduction de la notion d'Angle d'Alignement (AA), qui mesure l'angle des directions propres par rapport à la base naturelle, permet de donner une bonne évaluation du degré d'interaction du système.

Méthode du lieu des pôles multivariables

Considérons l'équation caractéristique duale de la précédente (i) :

$$\text{(ii) det } (s\, \dot{I} - S(g)) = \text{det } (s\, \dot{I} - (A + g^{-1}\, BC)) = 0$$

définissant la fonction de fréquence caractéristique S(g). Il s'agit d'étudier systématiquement la variation de S(g) en posant $g = -\frac{1}{k}$ avec k variant de 0 à l'∞, de façon analogue au cas monovariable. Le lieu des fréquences caractéristiques S(g) définit le Lieu des Pôles Multivariables (LPM).

Les points de départ du LPM (k = 0) sont les pôles du système en boucle ouverte.

Pour $k \longrightarrow \infty$, un certain nombre de fréquences caractéristiques tendent vers des positions finies ou zéros finis (ZF). Sous réserve de complète contrôlabilité et d'observabilité, on montre que les ZF sont les zéros invariants du système. Les fréquences caractéristiques restantes tendent asymptotiquement vers l' ∞ (ou zéros infinis (ZI)).

Approche hybride : lieu des pôles/lieux caractéristiques

Une telle approche intègre à la fois les techniques multivariables classiques (diagrammes de Nyquist/Bode) et les techniques du lieu des pôles. En effet, il a été prouvé que ces deux techniques mathématiquement duales peuvent être utilisées de manière complémentaire : on utilise dans un même temps une description interne (variables d'état) et une description externe (matrice de fonctions de transfert). Cette démarche, qui est beaucoup plus efficace que l'une ou l'autre des deux méthodes appliquées séparément, comporte en fait deux étapes importantes :

- un bouclage interne rapide exploitant au maximum tous les états accessibles du système,

- une boucle externe utilisant les méthodes fréquentielles afin d'atteindre les performances dynamiques et découplages requis.

Cependant, la complexité du problème posé et notamment pour l'application à l'hélicoptère, nécessite l'utilisation d'un logiciel d'aide à la conception (CAO).

Pour les méthodes décrites précédemment, il s'agit du logiciel U.M.I.S.T. développé par l'Université de Manchester. Cet outil informatique est implanté sur VAX/VMS. Un vaste ensemble de programme FORTRAN permet l'analyse en ligne et l'introduction aux méthodes de conception et simulation de systèmes mono et multivariables. Les programmes de conception sont utilisés dans un mode interactif, en conversationnel sur console graphique.

b) Méthodes géométriques

Nous nous proposons de présenter ici les grandes lignes de ces méthodes sur l'exemple d'un retour d'état.

On considère le système :

$$\dot{X} = AX + BU \tag{1}$$

à n états (vecteur X) et m entrées (vecteur U): A matrice n lignes x n colonnes, B matrice n lignes x m colonnes.

On cherche à réguler le système par un retour d'état : $U = KX$ (K matrice m lignes, n colonnes) tel que le système en boucle fermée (la matrice $A_f = A + BK$) admette comme valeurs propres l'ensemble $\left\{s_i,\ i = 1 \ldots n\right\}$ de notre choix.

Les vecteurs propres du système en boucle fermée V_i associés un par un aux valeurs propres s_i sont caractérisés par :

$$(A + BK)\ V_i = s_i\ V_i \text{ pour } i = 1, \ldots, n \tag{2}$$

soit en tout n systèmes linéaires (un par valeur propre s_i) à n équations (V_i de dimension n).

D'une manière générale, le principe de l'approche géométrique consiste à formuler les objectifs de commande (cahier des charges) en termes de contraintes sur les V_i mises sous formes d'équations. Ces équations, alliées aux équations de définition des V_i, permettent de les calculer tous puis d'en déduire le retour d'état K. Pour cela, on a recours au théorème suivant : pour une valeur propre s_i souhaitée en boucle fermée, l'ensemble des vecteurs propres V_i associés vérifie le système :

$$\left[A - s_i\ \dot{I},\ B\right] \cdot \begin{bmatrix} V_i \\ W_i \end{bmatrix} = 0$$

Ainsi on associe à chaque s_i (donc à chaque V_i) un vecteur de dimension m appelé "direction d'entrée" et défini par $W_i = KV_i$. Ceci permet de décomposer la recherche de K en n problèmes vectoriels portant chacun sur un couple (V_i, W_i). En effet, en l'absence d'objectifs de commande les (V_i, W_i) doivent seulement satisfaire (2), que l'on écrit :

$$(A - s_i\ \dot{I})\ V_i + B\ W_i = 0 \tag{3}$$

soit pour chaque s_i, n équations linéaires à n + m inconnues. Ces systèmes sont donc sous-déterminés et il nous est alors possible d'introduire dans chacun d'eux m équations linéaires de notre choix, sur lesquelles nous exprimerons les objectifs de commande.

Supposons que nous ayons fait cela et résolu en V_i et W_i chaque système ainsi complété, associé à chaque valeur propre, nous déduirons alors le retour d'état en remarquant que d'après (3) :

$$\underbrace{\left[W_1, W_2, \ldots, W_n\right]}_{W} = K \underbrace{\left[V_1, V_2, \ldots, V_n\right]}_{V} \tag{4}$$

(où $\left[X_1, X_2, \ldots, X_k\right]$ désigne la matrice formée par les vecteurs colonnes $X_1, \ldots, X_k$). On a donc :

$$K = W.V^{-1} \tag{5}$$

(l'inversibilité de V est garantie par le fait que les V_i, étant associés à des valeurs propres s_i supposées distinctes, forment alors une base).

Jusqu'ici il ne s'agit que d'une façon de poser le calcul de K. Mais l'intérêt de formuler le problème en terme d'équations sur les composantes de V_i, réside dans le rôle que jouent les V_i dans la réponse du système en boucle fermée soumis à une condition initiale X_0 sur l'état X.

Rappelons la forme de cette réponse. Le système en boucle fermée obéit à :

$$\dot{X} = A_f X \tag{6}$$

dont la solution est :

$$X(t) = \exp\,(A_f.t)\; X_0 \tag{7}$$

Cette dernière expression se décompose en somme de contributions des différents modes :

$$X(t) = \sum_{i=1}^{n} q_i \exp\,(s_i t)\, V_i \qquad (\text{avec } X_0 = \sum_{i=1}^{n} (q_i\, V_i))$$

Une telle écriture permet de se rendre compte que la réponse du système en boucle fermée dépend :

- des valeurs propres qui fixent le caractère convergent ou divergent de la réponse,

- de la décomposition de la condition initiale sur la base propre (q_i), qui fixe l'intensité avec laquelle chaque mode est excité,

- des vecteurs propres eux-mêmes qui indiquent dans quelle proportion un mode apparaîtra sur telle ou telle variable d'état.

En particulier, on remarque que si l'on excite le système par une condition initiale X_0 située sur une direction propre ($X_0 = \lambda V_i$ ou encore $q_j \neq i = 0$), l'évolution ultérieure de l'état ne mettra en jeu que le mode s_i et sera toujours située sur la direction V_i. Dès lors, un bon moyen de découpler les axes d'un hélicoptère est de forcer chaque vecteur propre à n'appartenir qu'à un seul axe : ainsi une perturbation d'état sur cet axe n'aura de conséquences que sur ce même axe.

Malheureusement, pour obtenir ce résultat, il faut imposer plus de contraintes linéaires que les m contraintes dont nous disposons.

Toutefois, il est possible d'y parvenir de manière approchée, et il existe ainsi plusieurs méthodes pour exprimer le découplage approché par seulement m équations linéaires supplémentaires.

L'une d'elles consiste à définir m "sorties" représentatives de m axes à découpler, puis à imposer la répartition des modes sur chacune de ces sorties, en utilisant les m degrés de liberté du sytème (3).

Une autre approche consiste à résoudre le problème sur-contraint initial au sens des moindres carrés, en minimisant pour chaque vecteur propre un multi-critère quadratique relatif aux objectifs désirés (exemple : découplage, robustesse, ...).

On est souvent amené dans ce multi-critère à combiner un critère quadratique de découplage avec un critère quadratique d'insensibilité des vecteurs propres et valeurs propres à des petites erreurs de modélisation.

Toutes les opérations mathématiques associées à l'utilisation de ces méthodes géométriques sont supportées par des outils informatiques interactifs très puissants, qui ont été développés à la SFIM et à l'AEROSPATIALE-DH dans le cadre de contrats DRET.

2.2.3. Résultats obtenus

Les méthodes présentées ont été appliquées à la détermination des stabilisations de base pour les hélicoptères Dauphin et Super Puma. Elles se sont révélées en final relativement bien adaptées à notre problème assez contraignant, compte tenu des caractéristiques particulières de l'hélicoptère. Les résultats obtenus en simulation montrent que les performances du système de pilotage sont supérieures à celles d'un pilote automatique classique, au prix d'une complexité à peine plus importante.

Cependant, c'est plutôt l'utilisation d'une combinaison des méthodes abordées, supportées par des outils informatiques très puissants, qui ont permis d'obtenir un résultat global satisfaisant. En particulier l'introduction de pré-commandes pour le découplage dynamique des commandes pilote subsiste et joue toujours un rôle important.

D'autre part, l'application de méthodes relatives à la théorie des systèmes linéaires s'est révélée efficace pour traiter le cas fortement non-linéaire de l'hélicoptère.

En résumé, les performances sur les stabilisations de base ont été notablement améliorées avec des commandes tout à fait admissibles et ne dépassant pas l'autorité des servo-commandes, ce point étant fondamental.

Les algorithmes obtenus grâce à l'application de ces méthodes vont faire l'objet d'une mise au point en vol sur le SUPER PUMA MK2, puisqu'ils vont être intégrés dans le système AP 165 actuellement en cours de développement à la SFIM (cf. chapitre 3).

2.3. EXEMPLE DU MODE SUPERIEUR "TRANSITION AUTOMATIQUE VERS LE BAS"

2.3.1. Position du problème et théories utilisées

La description opérationnelle de ce mode supérieur (cf. § 1.2.3), nous conduit naturellement à envisager l'utilisation de techniques de l'automatique qui permettent de prendre en compte les spécificités de cette mission de l'hélicoptère.

Pour la partie guidage sur trajectoire descendante, nous avons retenu la théorie de la commande optimale sous contraintes et pour la partie filtrage des fortes houles, nous avons retenu la théorie du filtrage de KALMAN. Ces théories sont tout à fait classiques et nous ne ferons pas de rappels à leur sujet.

Néanmoins, nous poserons le problème en termes mathématiques afin de donner au lecteur une bonne idée de la relative complexité de conception d'un tel mode.

a) Guidage sur trajectoire

On suppose que l'hélicoptère est modélisé par la représentation d'états discrets suivante :

$$X_{n+1} = f(X_n, U_n)$$

où f est une fonction linéaire qui représente de façon correcte l'hélicoptère en phase de transition descendante dans le plan (x, z) avec des variables astucieusement choisies et où l'on néglige le vent en première approximation. On suppose par ailleurs que le cap est correctement tenu par la fonction stabilisation de base correspondante.

$$\begin{cases} X_n \text{ est le vecteur des états } (V_{Xn}, Z_n, V_{Zn})^T \\ U_n \text{ est le vecteur des commandes } (\gamma_{Xn}, \gamma_{Zn})^T \end{cases}$$

On cherche ensuite la commande optimale comme une suite de N échelons de commande, qui permettent de passer de l'état initial $X_1 = (V_{X1}, Z_1, V_{Z1})^T$ à l'état final $X_N = (0, Z_{AFF}, 0)^T$ en temps minimum (ou en temps imposé, ou en distance de transition imposée, au choix) tout en respectant l'ensemble des contraintes principales suivantes :

$$\forall_n \in [1, N] \quad \begin{cases} |V_{Zn}| \leq g_1(Zn) \quad , Zn \in [40 \text{ ft}, 2500 \text{ ft}] \\ |V_{Zn}| \leq g_2(V_{Xn}) \quad , V_{Xn} \in [0, VNE] \\ |\gamma_{Xn}| \leq g3 \quad = \text{cte ou fonction d'un critère supérieur (temps ou distance de transition)} \end{cases}$$

g_1 et g_2 étant des fonctions définies par morceaux, et en minimisant le critère R de la forme :

$$R = \sum_{i=1}^{N} \alpha_i \cdot \gamma^2_{Zi},$$

où les coefficients de pondération α_i permettent de moduler les phases d'accélérations verticales selon la situation de l'hélicoptère dans son domaine de vol (exemple, favoriser de plus fortes accélérations verticales en début de transition vers le bas plutôt qu'à la fin de l'évolution = aspect sécurité). Les α_i sont choisis comme une fonction des Zi.

Ce type de critère est lié à la puissance nécessaire au mouvement ainsi qu'au "confort" de l'évolution. Un principe analogue, mais plus simple, est également mis en oeuvre sur l'axe longitudinal.

On montre par ailleurs qu'il est nécessaire d'optimiser le nombre N des commandes admissibles, si l'on veut respecter à la fois les exigences de performance de la loi de pilotage et les exigences liées à son implémentation dans un calculateur numérique temps réel.

b) Filtrage de houle

Dans une première étape, l'hélicoptère est supposé au stationnaire sur mer forte. Le filtre de houle sur l'axe z est donc déterminé dans cette configuration. Il est possible dans une seconde étape de l'étendre à une phase dynamique (V_Z, V_X) d'arrivée au stationnaire, au cours de la transition vers le bas (cf. a)). Dans cette présentation, nous n'aborderons que le problème simplifié du filtrage de houle au stationnaire, selon l'axe z.

Les deux informations à notre disposition sont :

- une mesure de la hauteur radio-sonde $\tilde{Z}_{RS}(t)$,

- une mesure de l'accélération verticale $\tilde{\gamma}_Z(t)$.

La radio-sonde mesure instantanément la distance entre l'hélicoptère et la surface de la mer, mais par contre l'accéléromètre vertical mesure l'accélération selon z de l'hélicoptère, lui-même asservi à tenir la hauteur de stationnaire dans le cadre du mode supérieur qui nous intéresse (stationnaire automatique, en fin de transition descendante).

Si l'on utilise la mesure $\tilde{Z}_{RS}$ sans filtrage de houle, on asservira la hauteur de l'hélicoptère à la surface de la mer et par conséquent ce dernier montera et descendra au rythme de la houle, plaçant ainsi les membres de l'équipage dans une situation inconfortable.

Afin d'éviter cet inconvénient, l'introduction d'un filtre de houle utilisant la théorie du filtrage de KALMAN nous a paru bien adaptée. Un tel filtre utilisera donc les deux informations $\tilde{Z}_{RS}$ et $\tilde{\gamma}_Z$. Il s'agit en fait de déterminer un modèle de reconstitution des signaux de mesure qui caractérise aussi bien que possible les aspects physiques du problème posé.

Le schéma ci-après résume clairement la situation.

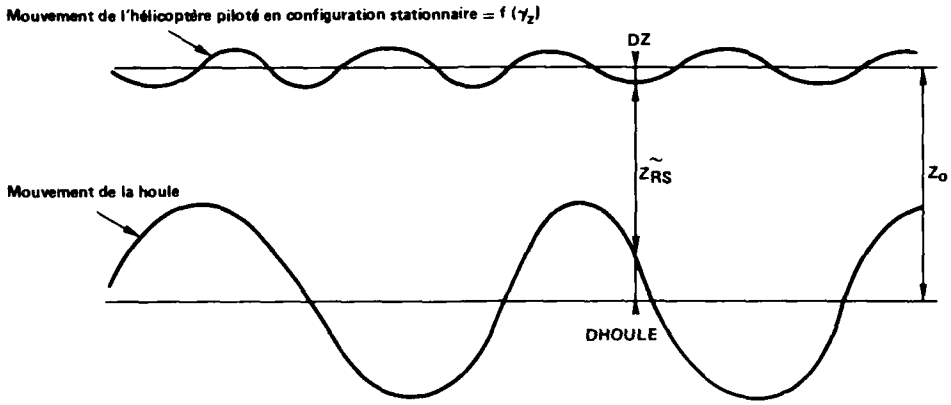

A partir des mesures $\tilde{\gamma}_Z$ et $\tilde{Z}_{RS}$, il s'agit de déterminer la meilleure estimation de Z_0.

$$\text{On pose } \tilde{Z}_{RS} = Z_0 + \text{DHOULE} + \text{DZ} + V_1$$

où
- Z_0 est la grandeur à estimer,
- DHOULE représente la variation de hauteur de houle par rapport à son mouvement moyen, supposé nul dans cette configuration de stationnaire,
- DZ représente la variation de hauteur de l'hélicoptère par rapport à son mouvement moyen, supposé nul dans cette configuration de stationnaire,
- V_1 est le bruit de la radio-sonde apparaissant sur la mesure $\tilde{Z}_{RS}$.

Par ailleurs on pose :

$$\tilde{\gamma}_Z = D\ \gamma_Z + V_2$$

où
- $D\ \gamma_Z$ est une variation de l'accélération verticale de l'hélicoptère par rapport à sa valeur moyenne, supposée nulle dans cette configuration de stationnaire,
- V_2 est le bruit de l'accéléromètre vertical apparaissant sur la mesure $\tilde{\gamma}_Z$.

Le modèle de reconstitution des signaux de mesure que nous avons retenu implique la détermination de deux modèles d'état caractérisant le premier les mouvements d'une houle établie et le second les mouvements de l'hélicoptère au stationnaire.

Il nécessite par ailleurs la détermination d'un modèle caractérisant les bruits de mesure.

En ce qui concerne la houle, nous avons choisi un modèle stochastique qui représente au mieux la densité spectrale de celle-ci. La houle sera donc restituée par un bruit blanc bo passé dans un filtre de forme :

$$G_0(p) = \frac{p}{p^2 + 2\zeta\omega_4 p + \omega_4^2}$$

$\Phi_{bobo}(p)$ est la densité spectrale du bruit blanc d'état, bo

Les valeurs optimales de ζ, ω_4 et $\Phi_{bobo}(p)$ ont été déterminées statistiquement à partir d'une collection de 45 spectres de houle (Atlantique). On montre par ailleurs que $\Phi_{bobo}(p)$ est un paramètre très variable, dépendant directement du carré de l'amplitude de la houle et aussi du coefficient ζ.

En ce qui concerne la modélisation d'un hélicoptère au stationnaire, configuration qui correspond à la phase de vol qui suit une transition descendante, nous avons utilisé une représentation d'état classique d'ordre 3.

La variable de commande est un bruit blanc d'état bl, dont la densité spectrale $\Phi_{blbl}(p)$ dépend de la densité spectrale $\Phi\ \tilde{\gamma}_Z\ \tilde{\gamma}_Z(p)$ du signal $\tilde{\gamma}_Z$, mesuré à partir d'un enregistrement réel d'hélicoptère au stationnaire.

Enfin la modélisation des bruits de mesure a été faite grâce à des bruits blancs Gaussiens dont les écarts types ont été définis à partir des caractéristiques techniques des capteurs associés à ce mode de pilotage.

Pour l'ensemble des phénomènes physiques pris en compte, on aboutit alors à la représentation d'état suivante :

$$\begin{cases} \dot{X} = AX + BW \\ Z = HX + V \end{cases}$$

où X, W, V sont des vecteurs fonction du temps.

$X = (DZ, DVZ, D\gamma Z, Z_0, DX5, DHOULE)^T$ est le vecteur d'état.

W est le vecteur des bruits d'état

V est le vecteur des bruits de mesure

HELICOPTERE

$$\text{matrice d'état } A = \left[\begin{array}{ccc|c|cc} -\omega_1 & 1 & 0 & & & \\ 0 & -\omega_2 & 1 & 0 & \multicolumn{2}{c}{0} \\ 0 & 0 & -\omega_3 & & & \\ \hline \multicolumn{3}{c|}{0} & 0 & \multicolumn{2}{c}{0} \\ \hline \multicolumn{3}{c|}{0} & 0 & 0 & 1 \\ & & & & -\omega_4^2 & -2\zeta\omega_4 \end{array}\right]$$

HOULE

$$\text{matrice de commande } B = \left[\begin{array}{cc} 0 & 0 \\ 0 & 0 \\ 1 & 0 \\ \hline 0 & 0 \\ \hline 0 & 0 \\ 0 & 1 \end{array}\right] \qquad \text{matrice de mesure } H = \begin{bmatrix} 1 & 0 & 0 & 1 & 0 & 1 \\ 0 & 0 & 1 & 0 & 0 & 0 \end{bmatrix}$$

On détermine ensuite une représentation d'état récurrente à partir de la représentation d'état continue que nous venons de présenter ; après avoir envisager les critères d'observabilité et de gouvernabilité du système ainsi obtenu, il ne reste plus qu'à appliquer la théorie classique du filtrage de KALMAN discret pour déterminer un filtre de houle numérique optimal (au sens d'une variance d'erreur minimale).

Le filtre ainsi obtenu a été essayé en Méditerrannée, dans l'Atlantique et en mer d'Irlande, et s'est comporté partout de manière tout à fait correcte. Il est donc relativement robuste compte tenu du modèle de houle "Atlantique" utilisé pour estimer l'état de la mer.

c) Toutes les opérations mathématiques et tous les tests de simulation qu'il faut effectuer pour aboutir à la détermination de tous les algorithmes concernant le mode "Transition automatique vers le bas" sont supportés par des outils informatiques interactifs bien adaptés et fonctionnant sur VAX/VMS (logiciel "OPTSYS" programmé en FORTRAN).

2.3.2. Résultats obtenus

Les algorithmes associés au mode "Transition automatique vers le bas" ont été validés en vol avec le système de pilotage CADV 155, et notamment sur deux hélicoptères d'AEROSPATIALE-DH (DAUPHIN N1-IAC et SUPER PUMA). Les résultats obtenus ont été jugés tout à fait performants dans des conditions opérationnelles réelles et parfois très difficiles (vol de nuit au-dessus de la mer, par force 5 à 6).

En particulier, la précision du stationnaire automatique (Doppler, Radio-sonde) au-dessus d'une mer très agitée a pu être évaluée.

Par ailleurs, la répétitivité et la souplesse d'utilisation du mode "Transition automatique" ont été fortement appréciées, notamment en ce qui concerne la possibilité d'engager ce mode quelle que soit la vitesse de l'appareil et dans une plage de hauteur allant de 2500 ft à 40 ft, tout en étant assuré d'une arrivée au stationnaire rapide, sans aucun recul, avec des dépassements en-dessous de la hauteur affichée inférieurs à 2 ft et des dérives Doppler inférieures à 1 kt sur les axes cycliques.

Il faut également signaler que de telles performances ont été obtenues avec des capteurs analogiques tout à fait conventionnels. L'ensemble de ces algorithmes que nous avons ainsi validés en vol seront repris dans le cadre du système AP 165 actuellement en cours de développement et que nous présenterons dans le chapitre 3. En particulier, ce système devrait voir ses performances s'accroître encore, compte tenu de la nouvelle génération de senseurs à sorties numériques dont nous disposerons pour réaliser ces modes de pilotage.

2.4. ELABORATION DES PRECOMMANDES NECESSAIRES AU TIR CANON, AU TIR DE ROQUETTES ET A LA STABILISATION D'ANTENNE DE SURVEILLANCE AEROPORTEE

2.4.1. Problème posé

Pour les trois exemples que nous avons abordés au paragraphe 1.2.4. à propos des missions du type "Terrestre", le problème est pratiquement le même : il s'agit, par l'intermédiaire du système de pilotage automatique, de contrer les effets induits sur la mécanique du vol de l'hélicoptère par l'activation du sytème d'armes considéré (tir canon, tir de roquettes ou fonctionnement de l'antenne de surveillance en rotation). Cependant la rapidité des dynamiques mises en jeu lors d'un tir (canon ou roquette) d'une part et la difficulté de modélisation des perturbations provoquées par les rafales du canon, le départ des roquettes ou le balayage de l'antenne d'autre part, font qu'il est difficilement envisageable pour contrer ces phénomènes d'utiliser les techniques classiques de l'automatique en boucle fermée. Néanmoins, dans tous les cas, on utilisera le pilote automatique en boucle fermée dans son mode "amortisseur", mais il sera toujours nécessaire d'augmenter l'avance de phase au niveau du déplacement des commandes de vol en y ajoutant des termes de précommande en "boucle ouverte" judicieusement calculés.

2.4.2. Approche mise en oeuvre

Afin de déterminer la forme mathématique de ces précommandes, nous avons retenu l'approche systématique suivante :

- par utilisation d'un modèle de simulation simplifié du système d'armes à l'étude, on tente de recréer dans un premier temps les effets observés sur le porteur réel,

- les paramètres prépondérants qui sont nécessaires à l'élaboration de cette simulation étant déterminés, on obtient par inversion la forme mathématique générale des précommandes et ce pour les différentes configurations envisagées au niveau du système d'armes,

- on suppose ensuite que les ordres à envoyer vers les commandes de vol sont des termes proportionnels que l'on vient sommer par l'intermédiaire de gains sur les sorties du système de pilotage fonctionnant dans un mode bien déterminé,

- ces gains sont ensuite réglés dans un environnement de simulation non linéaire par approximations successives et pour toutes les configurations de l'ensemble (hélicoptère + système d'armes), de façon à obtenir la précision voulue sur les paramètres à stabiliser.

Cette approche est du type "boucle ouverte", mais l'introduction des techniques numériques a grandement favorisé de telles solutions (qui parfois sont les seules envisageables) car il est alors possible de rendre ces précommandes fonction d'un grand nombre de paramètres mesurés par le système de pilotage lui-même (vitesse de l'hélicoptère, site et gisement de l'arme, durée de la rafale, intensité de l'effort de tir, site et gisement de l'axe de l'antenne, vitesse de balayage de l'antenne, ...), les gains étant tabulés par ailleurs selon l'état de booléens de configuration (tir en cours, antenne descendue, ...).

De plus il faut noter que dans une telle approche les aspects liés à la sécurité ne sont absolument pas négligés (autorité limitée des commandes de vol) car c'est le meilleur compromis (sécurité/précision/confort de maniement du système d'armes) que l'on cherche à obtenir.

2.4.3. Résultats obtenus

A partir d'une telle approche, la mise au point en vol des précommandes de stabilisation d'antenne de surveillance a été effectuée en 1983 sur un hélicoptère PUMA (SA 330) à l'aide d'un calculateur numérique SFIM, le CAS 1000.

Les résultats obtenus ont été jugés tout à fait corrects et le temps de mise au point a été relativement court, compte tenu du fait que la simulation au sol a dû être recalée régulièrement à l'issu des vols de l'hélicoptère. Ceci était impératif étant donné la méthode proposée, et également de par la relative complexité des précommandes élaborées pour stabiliser le faisceau de l'antenne.

En ce qui concerne les précommandes de tir canon, les essais sont en cours sur un Dauphin 365 M1 "Panther", mais d'ores et déjà la détermination des précommandes en simulation a montré qu'il était possible de diviser au moins par deux les effets du tir sur les mouvements de l'hélicoptère, en tangage et en roulis, sans avoir besoin d'accroître l'autorité des commandes de vol, donc avec le même niveau de sécurité en ce qui concerne le système de pilotage. L'axe de lacet par contre devra voir son autorité augmenter, mais il n'y a pas de problème relatif à la sécurité sur cet axe.

Toutes les lois obtenues dans le cadre des missions "Terrestre" envisagées ici se retrouveront intégrées dans le système de pilotage AP 165 que nous allons présenter dans le chapitre suivant.

3 - INTEGRATION DE L'ENSEMBLE DES FONCTIONS DE PILOTAGE DANS UNE ARCHITECTURE D'AVIONIQUE MODERNE - SYSTEME AP 165

3.1. PRESENTATION GENERALE DU SYSTEME AP 165 ET CARACTERISTIQUES PRINCIPALES

Le système AP 165 (ou AFCS 165) est un système totalement numérique de pilotage/guidage/directeur de vol "4 axes" pour hélicoptère.

Il se compose de deux calculateurs, de deux postes de commande dédiés aux modes de pilotage dits basiques (stabilisations 4 axes, modes de croisière et d'approche ILS), et dans certains cas de postes de commande dédiés aux missions spécifiques (militaires, terrestres ou marines).

Le système AP 165 est destiné à équiper la nouvelle génération d'hélicoptères lourds (type AS 332 - MK2) et peut s'adapter aux futures versions d'hélicoptères de tonnage moyen (type AS 365 M).

Chaque calculateur constituant l'AFCS 165 comporte deux voies de traitement à microprocesseurs associées à une électronique de désactivation des pannes multiaxes sur les sorties vers les commandes de vol. Une telle architecture permet d'assurer la passivation sur toute panne d'un calculateur, les pannes des capteurs redondants étant couvertes par des tests de surveillance.

En ce qui concerne la poursuite de la mission, l'opérationnalité après panne d'un calculateur est assurée sans aucune perte de performance sur le calculateur restant. Relativement aux applications civiles, le système ainsi conçu permet également d'effectuer des approches en catégorie 2 et autorise le vol en IFR monopilote. L'AFCS 165 appartient à la famille des systèmes "dual - dual".

3.2. FONCTIONS DE PILOTAGE DISPONIBLES

Concernant les stabilisations de base, on trouve toutes les fonctions classiques de tenue des assiettes et du cap à long terme, ainsi qu'un amortisseur de pas collectif.

De nombreux modes de pilotage "au travers" du système de contrôle automatique du vol, dont le mode contrôle de maniabilité, font partie de ce premier groupe de fonctions, au même titre d'ailleurs que les termes de découplage d'axes et la coordination de virage.

Pour ce qui est des modes supérieurs permettant le suivi de trajectoire, on trouve tous les modes suivants, actifs selon la configuration et la mission de l'hélicoptère équipé du système AFCS 165.

Pour les modes civils :

- tenue de vitesse-air actuelle,
- tenue d'altitude barométrique actuelle,
- acquisition et tenue d'altitude barométrique affichée,
- acquisition et tenue de cap affiché,
- acquisition et tenue de vitesse verticale affichée,
- acquisition et tenue d'altitude radio-sonde affichée,
- approche ILS cat. 1 et cat. 2,
- approche MLS,
- remise automatique de gaz,
- navigation (route navigation ou VOR).

Pour les modes militaires terrestres :

- tenue de stationnaire automatique (avec ou sans Doppler),
- vol tactique (maniabilité),
- asservissement sur une ligne de visée,
- pré-commandes d'antenne de surveillance aéroportée,
- pré-commandes de tir canon et de tir roquettes,
- tenue de poste hélicoptère (vol de patrouille).

Pour les modes militaires marines (SAR) :

- over-fly,
- acquisition et tenue de stationnaire automatique sur mer forte,
- tenue de hauteur de stationnaire radio-sonde affichée,
- transition automatique vers le bas (avec ou sans couplage à la navigation),
- transition vers le haut,
- tenue de vitesses-vol actuelle,

et (ASM) :

- tenue du stationnaire câble SONAR.

Ce système possède par ailleurs plusieurs autres fonctions telles que :

- surveillance de l'enveloppe de vol de l'hélicoptère (marge de puissance, VNE, etc.),

- surveillance des capteurs et reconfiguration, lorsque c'est possible, selon les demandes de l'équipage,

- surveillance des organes de commande,

- fonctions de sécurité (Fly-up, écarts excessifs sur les quatre axes, test avant vol),

- fonctions d'autotest des calculateurs et de maintenance intégrée (1er et 2ème échelons, en ligne).

Tous les modes que nous venons de lister très brièvement ont fait l'objet d'évaluations en vol sur divers hélicoptères de l'AEROSPATIALE-DH et ce aussi bien avec des systèmes analogiques classiques qu'avec des systèmes numériques (tels que le CDV 155).

L'intégration dans une architecture "tout numérique" de l'ensemble des besoins recensés à l'heure actuelle par les différentes armées (air, terre, mer) est en cours de réalisation dans le cadre du développement concernant la nouvelle génération de systèmes de contrôle de vol type AFCS 165.

Dans le paragraphe ci-après, nous allons présenter succintement l'architecture externe de ce système pour l'application au SUPER PUMA MK 2.

3.3. DESCRIPTION DE L'ARCHITECTURE EXTERNE DU SYSTEME AP 165

Le système AP 165 s'insère dans un système de conduite du vol intégré, totalement Duplex (cf. synoptique n° 1). Autour des deux calculateurs composant le coeur du système de pilotage sont articulés plusieurs sous-ensemble :

- 2 postes de commande basiques PA, faisant office de concentrateurs de données pour toutes les commandes situées sur les manches (cyclique et collectif) ainsi que pour les logiques d'engagement de modes, issues des postes de commandes optionnels. Ces deux postes de commande basiques sont situés en planche de bord, l'un sur la planche pilote et l'autre sur la planche copilote, au voisinage des écrans de visualisation et à côté des postes de commande de visualisation.

- 2 Centrales de Références Primaires (CRP), qui outre les informations d'assiettes, de vitesses angulaires et d'accélérations linéaires, élaborent par ailleurs les informations baro-anémométriques, à savoir la vitesse-air, la vitesse verticale et l'altitude barométrique, ainsi que l'information de température extérieure. Ces centrales peuvent aussi fournir en option les informations relatives à l'anémométrie basse-vitesse.

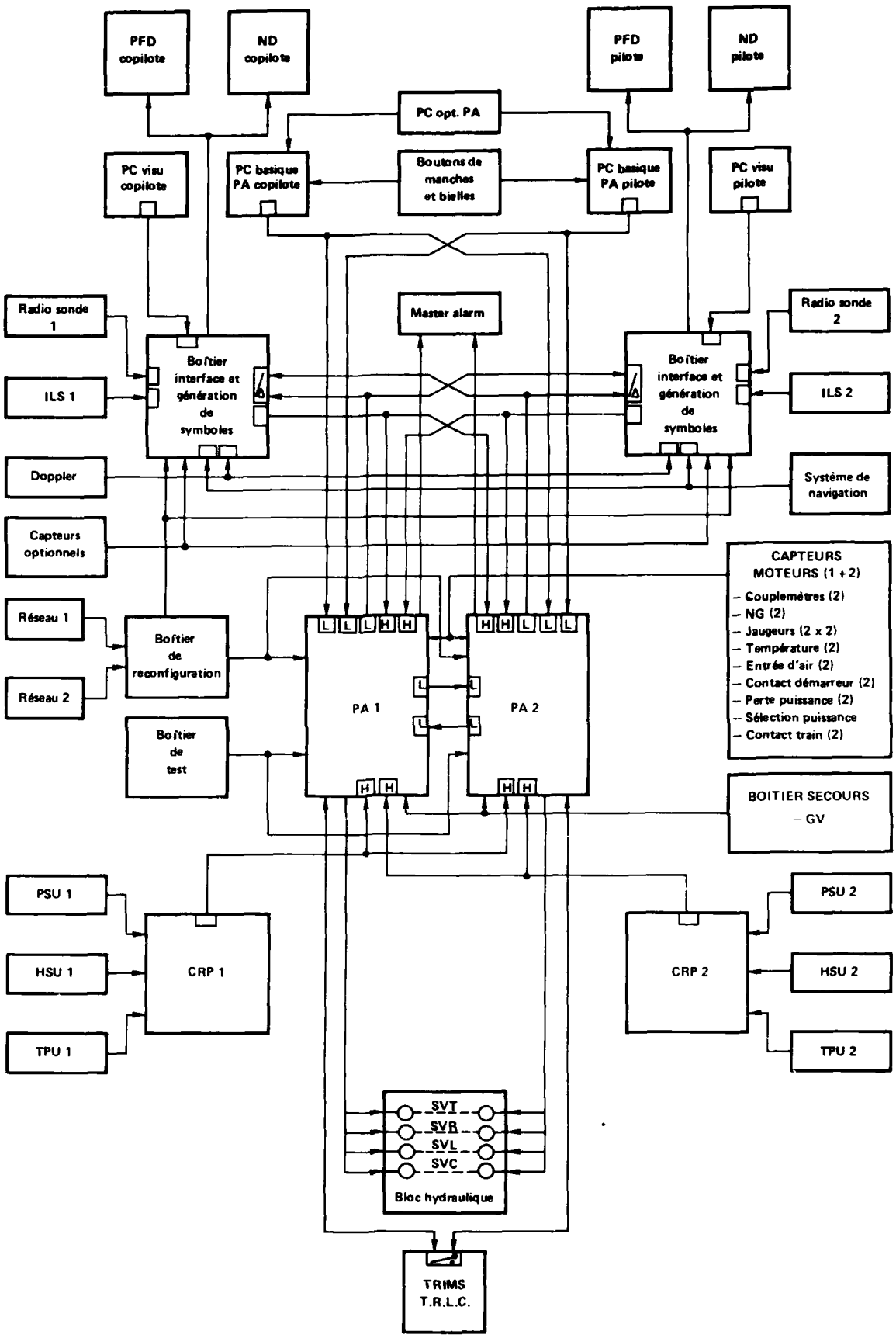

SYNOPTIQUE N° 1 : ARCHITECTURE DU SYSTEME DE CONTROLE DU VOL AP 165

- 2 "Boîtiers Interface et Génération de Symboles" ayant les rôles suivants :

* concentration des capteurs de radio-navigation et radio-altimétriques ainsi que des capteurs nécessaires à la réalisation des modes optionnels (exemple SAR, ASM, ...),

* couplage à un BUS 1553 (en option),

* acquisition des postes de commande de visualisation,

* concentration des mots de maintenance issus de chacun des sous-ensembles (PA, CRP, ...) dans un système de mémorisation centralisée,

* acquisition des CRP (une par boîtier) pour affichage sur les écrans de visualisation,

* génération des signaux de visualisation et d'alarme sur les écrans de visualisation à partir des informations fournies par les calculateurs de pilotage.

- 2 ensembles de visualisation pilote et copilote, composés chacun d'un poste de commande de visualisation, d'un PFD (Primary Flight Display) et d'un ND (Navigation Display). Chaque planche (pilote ou copilote) reçoit l'une des centrales de références primaires pour affichages. Chacun des deux postes de commande de visualisation contrôle directement sa planche associée (via le "Boîtier Interface et Génération de Symboles").

a) Sur la visualisation PFD sont affichées outre la hauteur de décision, les informations suivantes en provenance des calculateurs de pilotage, via les boîtiers "Interface" :

* les barres de tendance pour la fonction directeur de vol,
* les sélections de cap affiché, d'altitude barométrique affichée et de vitesse verticale affichée,
* les modes actifs, armés, désengagés, de même que les interdictions d'engagement,
* les informations concernant les possibilités de reconfiguration du système de pilotage,
* la visualisation de l'enveloppe de vol (sur l'échelle des vitesses),
* les alarmes d'ordre de reprise en main,
* l'activation de la sécurité "Fly-up",
* les écarts excessifs liés au suivi de trajectoires,
* les dissemblances capteurs,
* Les mots d'état enregistrés dans la mémoire centralisée, en phase de maintenance seulement.

b) Sur la visualisation ND sont présentées :

* les informations de cap, de route et de navigation, avec la possibilité d'y superposer la carte météo,

* la hauteur radio-sonde actuelle et la hauteur affichée,

* la marge de puissance disponible (sur une échelle de pas collectif).

- 1 ensemble de capteurs de secours comprenant deux gyroscopes de verticale et permettant de surveiller l'attitude de l'hélicoptère après perte d'une CRP.

- 1 ensemble de capteurs permettant d'élaborer les informations "marge de puissance" et "enveloppe de vol". Il s'agit essentiellement de capteurs effectuant des mesures au niveau des ensembles tournants (BTP, moteurs).

- 1 boîtier de reconfiguration, situé sur le pylône central à disposition des pilote et copilote.

- 1 boîtier de maintenance, permettant également d'initialiser le test pré-vol, le test de maintenance approfondie et la comande de visualisation sur écran des mots d'état de maintenance stockés dans le dispositif de mémorisation centralisée.

- 1 dispositif de visualisation d'alarmes (Master Alarm), afin de pouvoir reprendre en mains le contrôle de l'appareil en toute sécurité.

- 1 ensemble (trims et servo-commandes) permettant le pilotage automatique de l'hélicoptère sur ses 4 axes.

Il s'agit là d'une description assez succinte du système de pilotage AP 165, intégré dans une architecture d'avionique moderne, et dont nous venons de présenter les éléments principaux. Il n'est pas question dans ce papier de développer tout le contexte opérationnel d'un tel système, car cela serait bien trop long. Néanmoins nous renvoyons le lecteur aux chapitres 1 et 2, où nous avons développé quelques exemples qui donnent une très bonne idée des capacités de ce système, aussi bien sur le plan opérationnel qu'au niveau de ses performances et de sa sûreté de fonctionnement.

3.4. PRINCIPES DE REALISATION ET TECHNOLOGIE DU SYSTEME AP 165

3.4.1. Méthodes de conception et de développement

De part sa complexité importante, le développement d'un tel système de pilotage nécessite l'utilisation de méthodes de conception qui permettent de maîtriser l'approche descendante/montante (Top-Down/Down-Top) classique : une démarche méthodologique cohérente entre l'Avionneur et l'Equipementier est le garant d'un bon déroulement de tout programme . Dans ce but la SFIM a été amenée à développer certains outils informatiques ou à en utiliser d'autres déjà existants sur le marché.

La plupart des outils SFIM fonctionnent sur VAX-VMS ; on peut citer plus particulièrement l'outil de spécification SPECIF, qui est utilisé essentiellement au niveau de la conception globale système et logiciel de l'AP 165 lui-même et qui sert principalement à définir les flots d'informations de façon externe entre ce système de pilotage et les différents sous-ensembles participant à l'avionique de l'hélicoptère. Cet outil permet également de définir les flots d'informations de façon interne, au niveau des sous-ensembles matériels et logiciels constituant le système de contrôle automatique du vol.

Connecté à SPECIF, nous avons développé par la suite un outil particulier (INTERCO) permettant de générer automatiquement l'interconnexion physique du sous-système de pilotage placé dans son environnement.

Par ailleurs, un ensemble de programmes de simulation très sophistiqués permet d'observer ce que sera le comportement du système AP 165 une fois monté dans l'hélicoptère de servitude.

La particularité de notre approche réside dans le fait qu'il s'agit d'observer, de tester et de valider en simulation le comportement du logiciel "cible" lui-même, tel qu'il sera implanté dans les calculateurs de pilotage lorsque ceux-ci fonctionneront en temps réel en vol. Ce logiciel cible est développé en PASCAL, le reste de l'environnement étant écrit en FORTRAN.

Un certain nombre d'Outils spécifiques de Définition de Tests (ODT) et d'outils graphiques (PAGOS), permettent de faciliter le dialogue entre les ingénieurs de conception (système, logiciel) et l'environnement de simulation représentatif de l'application en cours de développement.

Dans une première étape, tous ces travaux sont réalisés en temps différé ; par la suite et dans une prochaine étape, il sera possible d'effectuer les mêmes tâches mais cette fois en temps réel, grâce à l'outil SILENE 3 en cours de réalisation à la SFIM. Ce simulateur temps réel est organisé autour d'un ordinateur GOULD (SEL 32). Il sert principalement à la validation du sous-système de pilotage avant sa livraison au client AEROSPATIALE-DH, ce dernier réalisant ensuite la validation de toute l'avionique de l'hélicoptère sur son banc de simulation temps réel SISYPHE.

Enfin tous les produits issus du développement de ce système de contrôle automatique de vol sont pris en gestion de configuration grâce à l'outil GCF.

3.4.2. Principes de réalisation du logiciel de l'AP 165

Dès lors que les fonctions du système de pilotage présenté sont réalisées par logiciel, des précautions architecturales sont à prendre en compte relativement à sa sûreté de fonctionnement. Celles-ci sont traduites non seulement au niveau de l'architecture des deux calculateurs numériques embarqués (structure "dual - dual"), mais également au niveau de leur programmation respective. Ainsi à l'intérieur de chacun des deux calculateurs, toutes les fonctions de pilotage jugées critiques sont réalisées deux fois, de façon dissymétrique, avec des logiciels de niveau 2 (au sens de la DO 178A) et exécutées par deux ensembles de ressources matérielles identiques mais distincts, et possédant leurs propres moyens de communication avec l'extérieur. Ces deux ensembles de ressources sont également capables d'échanger des informations de consolidation, sans risque de pollution mutuelle.

Dans le système AP 165, tous les traitements logiciels sont réalisés par utilisation du langage de haut niveau PASCAL. La dissymétrie, lorsqu'elle est nécessaire, est assurée depuis la conception des logiciels jusqu'à leur programmation, en imposant l'emploi de deux compilateurs différents (BSO et OREGON) à deux équipes différentes.

3.4.3. Technologie du système AP 165

Pour la réalisation de ce système nous avons décidé, après étude des différentes familles de microprocesseurs à notre disposition sur le marché, d'utiliser la technologie MOTOROLA (68020 + 68881). Chacun des deux calculateurs numériques est constitué de deux entités de calcul "68020 + 68881" fonctionnant à 12,5 MHz, qui confèrent au système AP 165 une grande puissance de calcul.

Les composants électroniques utilisés sont pris dans la gamme étendue (- 45°, + 85°), la compatibilité étant assurée à terme pour les applications nécéssitant l'emploi de composants électroniques militaires.

CONCLUSION

Au cours de cette présentation, nous avons essayé de montrer comment à partir d'une définition la plus précise possible des besoins opérationnels, il est envisageable de synthétiser des lois de pilotage relatives à une application sur hélicoptère pour une mission donnée, grâce à l'utilisation de techniques particulières de l'automatique théorique. Après une rapide présentation de l'AP 165 actuellement en cours de développement à la SFIM, nous avons abordé ensuite les principes de la réalisation du sytème de contrôle de vol lui-même, et notamment nous avons mis l'accent sur l'utilisation d'une technologie électronique avancée ainsi que sur les méthodes de développement d'un système tel que l'AP 165. Il ne reste plus désormais qu'à valider toute notre approche en vol et c'est ce qui est envisagé à court terme, puisque le système AP 165 va faire l'objet d'une évaluation complète sur le SUPER PUMA MK2 de l'AEROSPATIALE-DH (Marignane - France).

AD-P005 717

COMPUTER AIDED TACTICS FOR AIR COMBAT

by
N. Mitchell
British Aerospace
Military Aircraft Division
Warton Aerodrome, Preston, Lancashire PR4 1AX

SUMMARY

In order to achieve maximum operational effectiveness with an acceptable crew workload, the new generation of NATO fighter aircraft will contain a significant degree of automation and computer support to the crew. One key area of support is computer aided tactics, which help the crewman to assess the complex air battle situation, select appropriate targets, and plan the best method of attack. This paper describes a microcomputer tactical aid called MITAC, which has been produced by British Aerospace as part of a ~~wider~~ programme ~~of work~~ on mission management aids. By computing a range of possible aircraft and missile flight paths and processing the results through a sequence of tactical rules, MITAC can offer the crewman useful advice on recommended attacks and their consequences. It provides a good insight into the sort of facility that could be available in next generation fighter cockpits.

INTRODUCTION

Over the past few years there has been a growing recognition of the need for onboard automation and computer aids to support the crew of new combat aircraft. To address this need, British Aerospace has been involved in a number of initiatives aimed at clarifying the requirements and identifying areas of interest (see, for instance, reference 1.).

In parallel with this general activity, it was decided to produce a number of specific demonstrators, which would show more clearly what such computer aids were and how they could support the crew. An initial demonstrator was produced called MITAC, a microcomputer tactical aid, to illustrate how the crew might be given tactical assistance. It also provided a useful vehicle for the development of algorithms and new ideas on tactical reasoning.

This paper first discusses the need for automation and computer aids, in particular computer aided tactics, then it describes MITAC and how it functions. Finally it indicates the further developments that are underway to produce a new more powerful computer tactical aid called COMTAC, from which it should be possible to specify tactical algorithms for an airborne system.

THE NEED FOR COMPUTER AIDS

The current trend in fighter aircraft design is towards more complex systems operated by a single crewman. The EAP (Experimental Aircraft Programme) Technology Demonstrator, which mades it first highly successful flight from Warton last year, is a forerunner of this new breed of fighter. They will be highly manoeuvrable and equipped with sophisticated attack and defence systems and with intelligent fire-and-forget missiles. These aircraft will have to operate in an increasingly severe air/land battle environment, containing many threats from enemy air and ground units (Figure 1.), which will demand maximum performance from the aircraft, its weapons and its crewman.

In order to achieve full performance, the crewman is required to perform the following functions simultaneously:-

* Maintain an awareness of the total air battle scene.
* Plan the best method of attack.
* Fly complex attack manoeuvres.
* Closely control multiple weapon release.
* Organise self defence against arriving threats.
* Communicate with other friendly forces.
* Manage all on-board systems.
* Respond to onboard emergencies/failures.

Even with a two man crew and present generation systems, these tasks are very demanding. The new more complex systems, to be handled by a single crewman, will require the introduction of more automation and computer assistance if the crew workload is to be kept to an acceptable level.

FORMS OF COMPUTER AID

There are two main types of computer assistance that could be provided to the crew: tactical and non-tactical. The non-tactical computer aids involve the automation of sub systems management and housekeeping functions. This could include automated sensors, automated flight path control, automated weapon control, and automated defensive aids. Housekeeping functions to be automated could include fuel, power, hydraulics and air. Hand in hand with such automation would go an appropriate monitoring system.

This non-tactical automation would relieve the crewman of much of the detailed and demanding systems management and control tasks, thus allowing him more time to concentrate on overall mission management. However, although the non-tactical automation is very important and complementary, this paper is concerned with the tactical forms of computer assistance. Such computer aided tactics will assist the crew throughout all phases of the mission. In the context of an air combat mission, the computer aided tactics could provide particular assistance to the crew in four main areas:

1. Understanding the complex air battle situation.
2. Identification of important targets and threats.
3. Planning the best method of attack and self defence.
4. Execution of the attack sequence.

A key part of all such aids is the man/machine interface between the computer and the crew. This will be operating at a much more 'intelligent' level than in the past and will involve voice conversation as well as new pictorial displays.

MITAC

Although there has been much general discussion on the topic of mission management aids, which provide computer support to the crew, it requires the design and implementation of actual systems to give a clear understanding of what they are and what they can do. In order to progress along this path, a microcomputer tactical aid called MITAC has been produced, to give initial experience in the design and development of tactical decision aids; Figure 2 shows MITAC in operation. Such an approach has allowed the rapid implementation of new ideas for algorithms and tactical reasoning, and is one element in a wider ongoing programme of work to develop computer aids and automation for use in combat aircraft.

The list of mission management aid (MMA) features provided by MITAC is shown in Figure 3. These will be discussed in more detail later. MITAC has a user option to introduce pauses between each of its processes, which is useful for demonstrations. Normally, however, the sequence of processes is completed, through to the recommended attack, without stopping.

The user first defines all of the elements in his scenario. This includes the position, speed, heading and status of all aircraft, plus the position, engagement range and status of all surface to air missile batteries. This total scenario is often referred to as the alpha scene, which would be produced by correlation of all sensor and intelligence data onboard the aircraft. A typical alpha scene is shown in Figure 4, containing line vectors for aircraft and circles for surface-to-air missile engagement zones. All displays are shown relative to own aircraft, which remains at the origin and heading left to right.

. Situation assessment

The first MITAC function is Situation Assessment, in which it processes the whole of the alpha scene to identify the most important elements in the scene; these may be targets or threats or both. The processing algorithms include a number of criteria, e.g. friend or foe, range to go, time to go, but are less detailed than subsequent processes, because situation assessment has to operate on the whole alpha scene and computer power will be limited. A head-on attack algorithm is used to compute missile launch times from which the eight most immediate targets are selected (Figure 5).

This reduced group of eight targets, known as the beta scene, will be subjected to further processing. As the attack sequence develops, in particular when own aircraft changes heading, the relative importance of the elements in the alpha scene will change, and so will the selected beta scene.

. Attack and counter-attack assessment (Figure 6)

The next MITAC process computes collision course attacks against each of the eight enemy aircraft in the beta scene, calculating the aircraft approach path and the missile launch and trajectory data. Then for each of these attack profiles, the corresponding enemy counter-attacks and missile launch points are evaluated. This process takes a little longer, because for each attack against one of the enemy aircraft, MITAC has to examine eight potential enemy counter-attacks, i.e. sixty four counter-attacks in all. The surface to air missile batteries engage all aircraft coming within their range and more than one missile may be fired at an aircraft depending on how long it takes to pass through the zone. Each one of these attack and counter-attack profiles is known as a gamma option. MITAC has now reached the situation where all of the attack options and their counter-attack consequences are known including the crucial missile launch data.

. Target prioritisation (ranking)

The important thing that the user wishes to know, of course, is which is the best target to go for. This is computed by MITAC in the next process called target prioritisation or ranking. To do this it uses a series of tactical rules in order to rank the targets in a preferred tactical order, using data from the attack and counter-attack assessment. These tactical rules attempt to maximise your advantage by achieving the most target kills with the least number of counter-attacks. An example of such tactical rules are shown in Figure 7. The first ranking criteria is 'lowest number of counter-attacks'. For profiles with the same number of counter-attacks, priority is given to those where the first counter-attack occurs latest. Further ranking criteria are applied until all of the attack options are placed in a preferred order. The recommended attack, at the top of the list, is called the gamma star option. MITAC has now completed its cycle of computations and is ready to present its results to the user.

. Display options

MITAC presents the results of its tactical assessment on the screen, first showing the 'no manoeuvre situation', which indicates whether continuing on the present course will expose you to attack within a specified time interval. By the repeated pressing of a key, the full list of attack options can be displayed, in order of priority, starting with the recommended attack. A recommended attack option display is shown in Figure 8, where it will be seen that the track from self has two legs: the first is the aircraft flight path to missile launch and the second is the missile trajectory from launch to impact. Note that the impact point is on the target track projected some time ahead. As there are no similar tracks from any of the enemy aircraft towards self, this indicates that no counter-attacks will occur before you launch a missile at the selected target.

A read out line at the bottom of the display indicates heading change and attack time to the selected target. Progressing through the options shows an increasing number of counter-attacks, with the worst option, number 8, showing six counter-attacks. (Figure 9).

MITAC offers the user the choice of selecting any one of its ranked options or suggesting alternatives for it to assess. The user can examine the effect that changes in his speed or height will have on the attack and counter-attack situation. When a course of action has been decided upon, MITAC progresses the air battle forward in time by a selected timestep. The new situation is then displayed and all of the procedures are repeated on the full alpha scene.

ATTACK SEQUENCE USING MITAC

To illustrate how MITAC could be used to execute an attack sequence, let us start by accepting the recommended attack option against a/c 15, shown in Figure 8.

MITAC first checks whether you are likely to be attacked, then updates to the next scene, which is the missile launch point against aircraft 15 (Figure 10). Notice that the display is still centred on self, so the impression is that the whole scene has rotated and moved relative to self. MITAC has worked on the whole alpha scene again and computed a full set of gamma options for the new situation. The recommended attack is, of course, against aircraft 15, and as the target is in range, MITAC asks for missile launch instructions. One missile is selected and launched at aircraft 15; the missile in flight will be shown as a small circle. The second option is against aircraft 11 and the display (Figure 10) shows that, in the course of this attack, the aircraft in close proximity to 11 could turn and launch a missile at us. We attack, nevertheless.

MITAC now advances to the missile launch point against aircraft 11, shown in Figure 11, where a missile launch option has been selected. At least one counter-attack is possible in the near future on all of the gamma options, so we launch a missile at aircraft 11 and turn 80 degrees to port to avoid retaliation. Figure 12 shows the no manoeuvre situation sometime later, indicating no counter-attacks. Our two missiles can be seen in flight towards aircraft 15 and 11.

As a final illustration of MITAC facilities a simpler scenario is used, as shown in Figure 13, with only two targets; a high speed medium level fighter (number 6) and a slower low level strike aircraft. MITAC recommends attacking the fighter, because the second option against the strike aircraft, (Figure 13), shows a risk of counter attack. If it is important that the strike aircraft is destroyed, then it would be useful to find out how to achieve that without being attacked in the process. MITAC examines the effect of changing speed and height and shows that it is possible to attack the strike aircraft with no counter-attacks (Figure 14).

FURTHER DEVELOPMENTS

Although MITAC uses a relatively simple model, it nevertheless is a program with over 2000 statements and does thousands of computations each cycle. It has been an extremely effective tool for the initial investigation of new ideas in the area of computer aided tactics.

Further developments are now underway using more complex models with greater tactical reasoning, which provide more extensive tactical assistance. They are running on more powerful computers with high resolution colour graphics displays and provide the basis for significant development of tactical algorithms. The display shown in Figure 15 is from the first development phase of a new computer tactical aid called COMTAC.

Parallel work is also underway on the application of artificial intelligence techniques in this area, and on the integration of computer aided tactics into future combat aircraft.

The time is right for the introduction of such computer aids and they offer the prospect of major improvements in the operational effectiveness of combat aircraft.

REFERENCES

1. Powell, J.H., and Adams, B.H., "A Mission Management Aid for High Performance Fixed Wing Aircraft", AGARD, 51st Avionic Panel Symposium, May 1986, Norway.

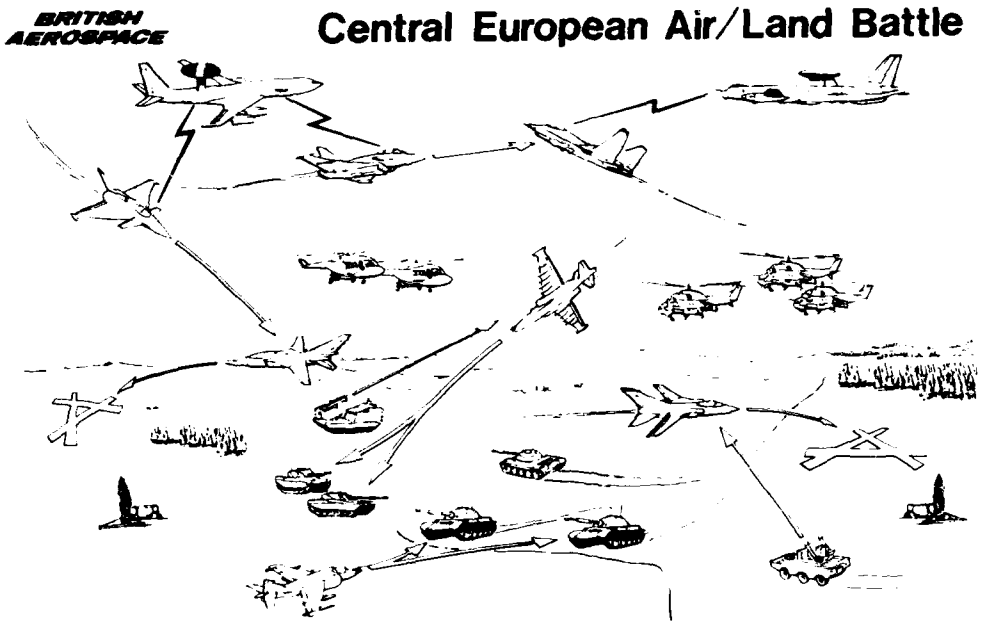

Figure 1

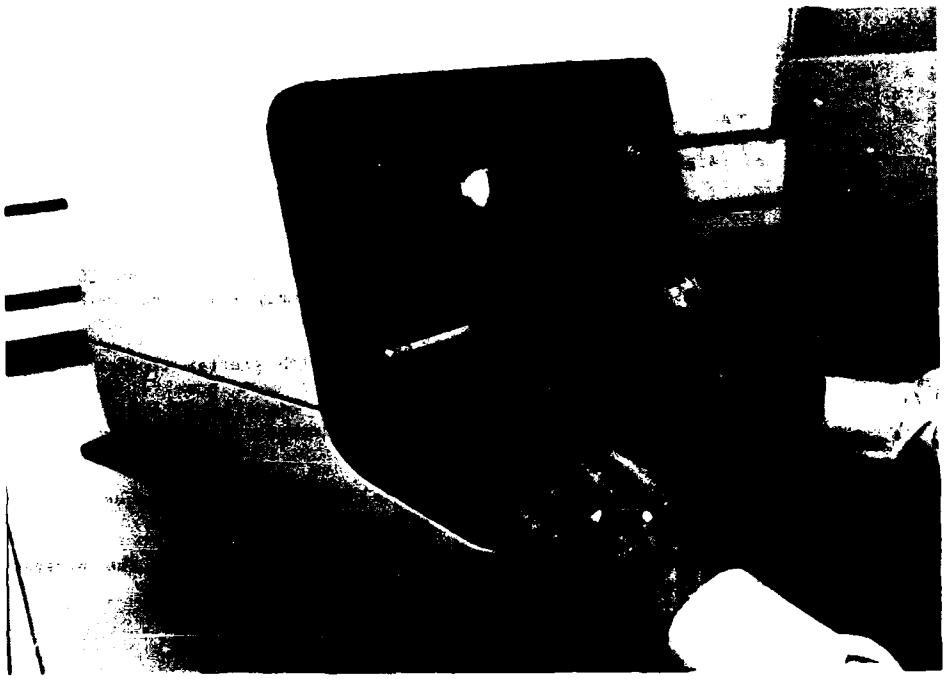

Figure 2 MITAC in Operation

COMPUTER AIDED TACTICS	
MMA	MITAC
CORRELATION	–
ALPHA SCENE	√
SITUATION ASSESSMENT	√
BETA SCENE	√
ATTACK/COUNTER ATTACK ASSESSMENT	√
GAMMA OPTIONS	√
TARGET PRIORITISATION (RANKING)	√
RECOMMENDED ATTACK (GAMMA STAR OPTION)	√
CREW ALTERNATIVES ASSESSMENT	√
OPTION CHOICE	√
ATTACK EXECUTION	√
WEAPON SELECTION AND LAUNCH	√

Figure 3

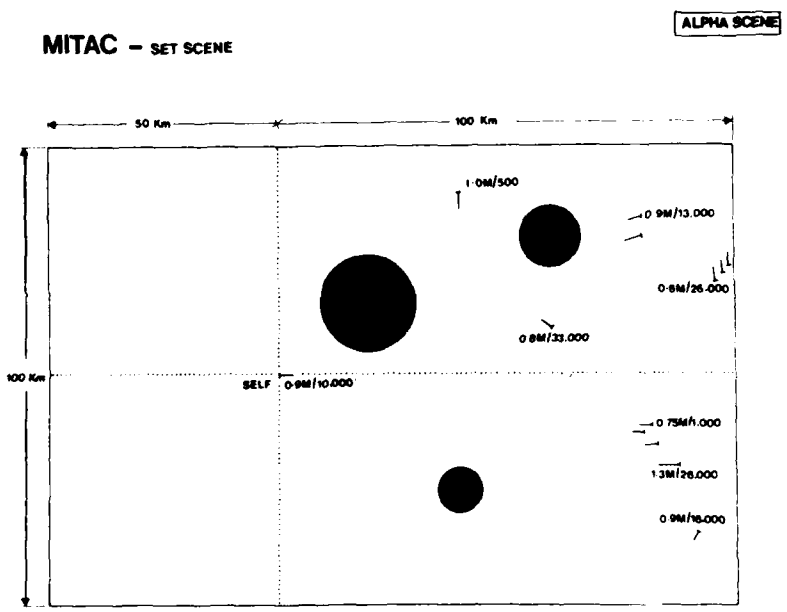

Figure 4

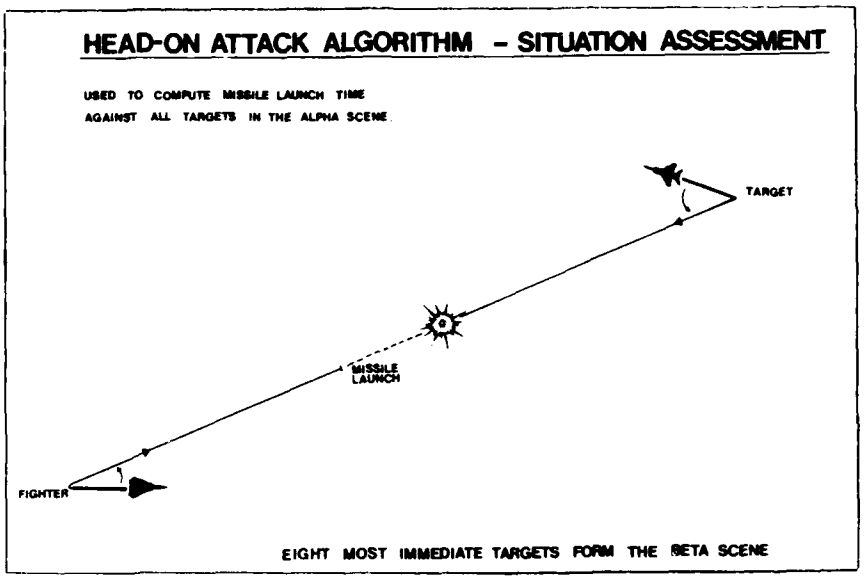

Figure 5

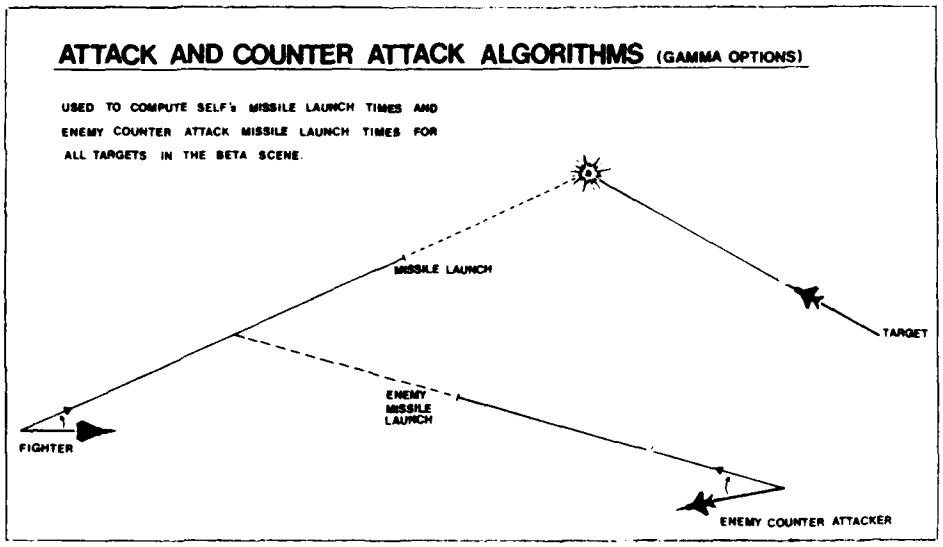

Figure 6

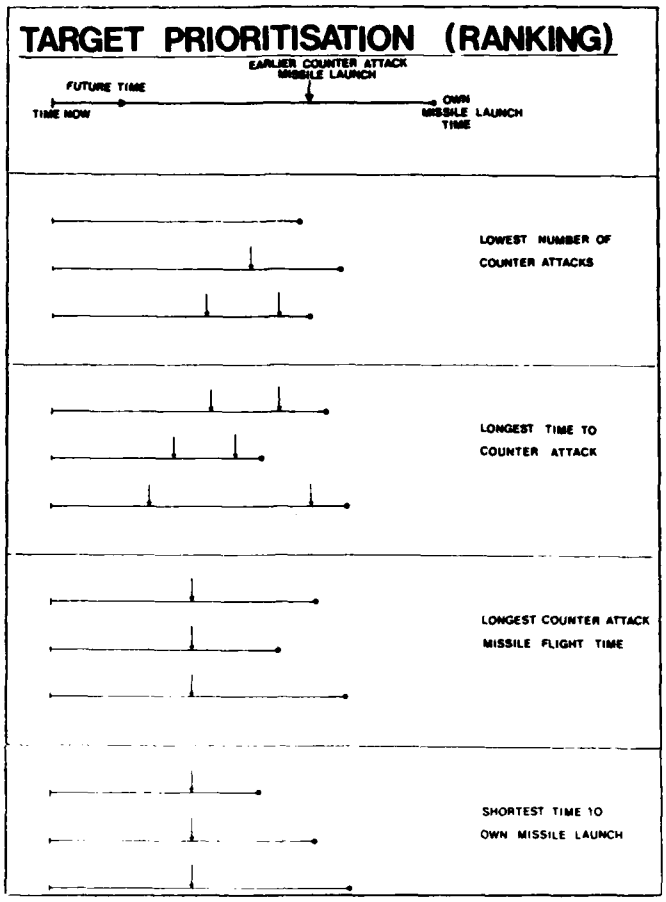

Figure 7

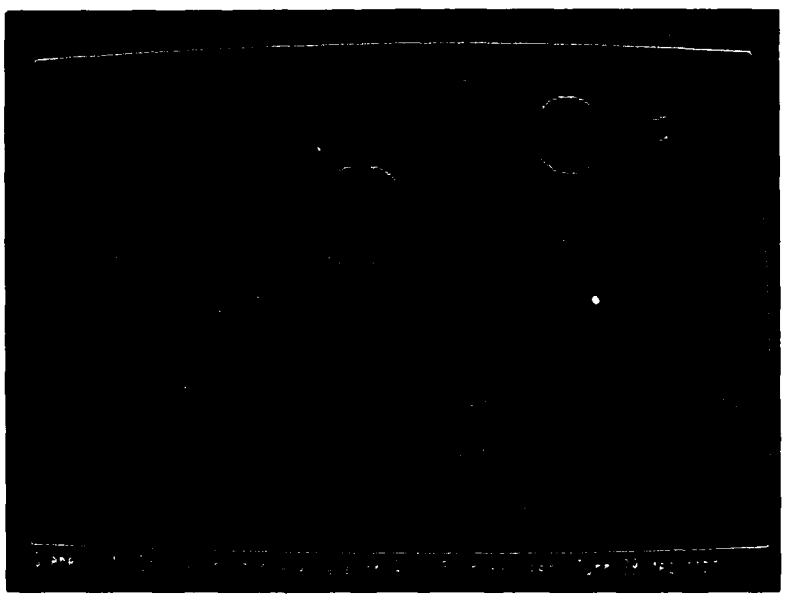

Figure 8 Recommended Attack Option

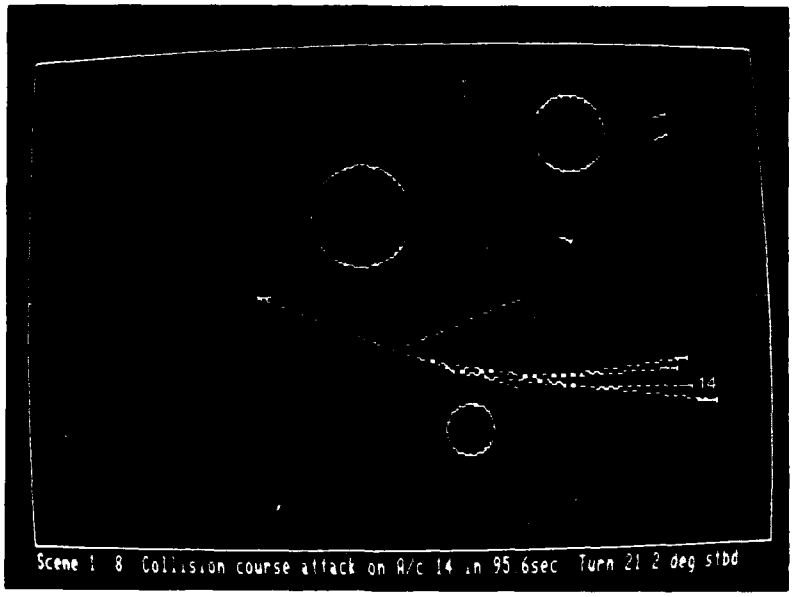

Figure 9 Worst Option

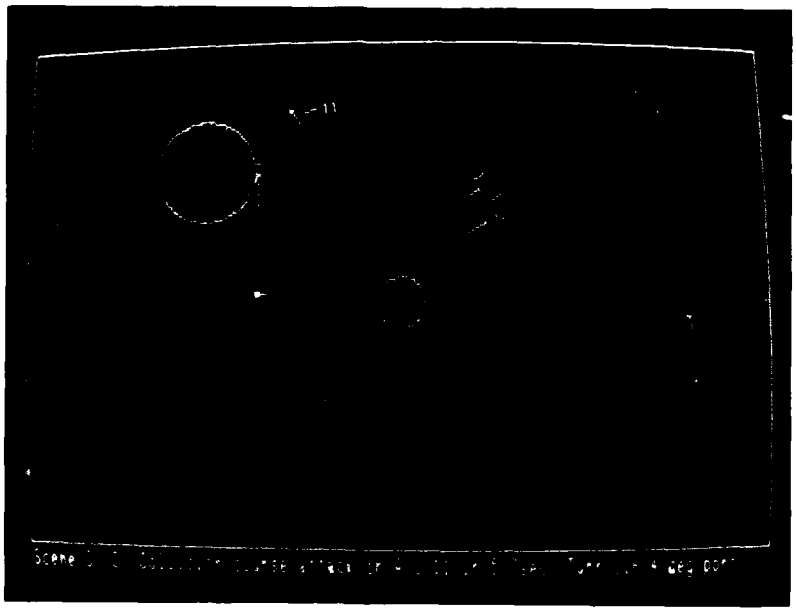

Figure 10 Launch Point Against Aircraft 15

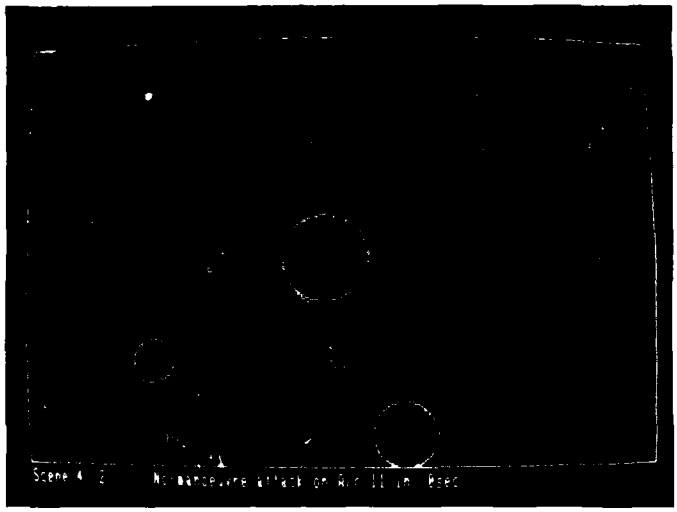

Figure 11 Launch Point Against Aircraft 11

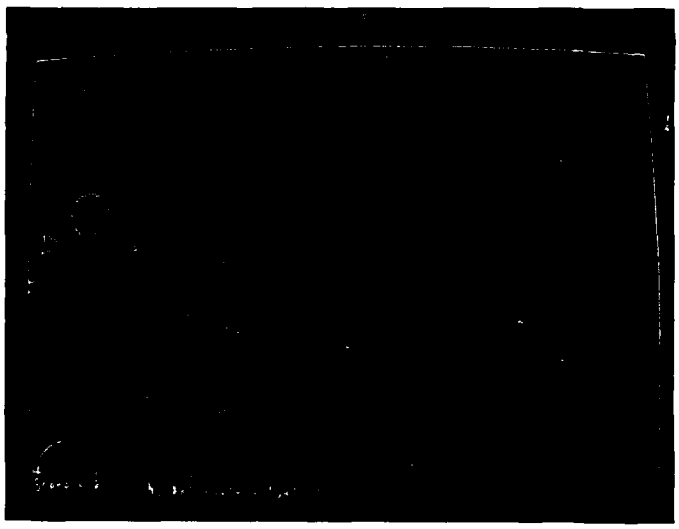

Figure 12

SPEED CONTROL OF A MISSILE WITH THROTTLEABLE
DUCTED ROCKET PROPULSION
by
Dieter Thomaier
Messerschmitt-Bölkow-Blohm GmbH
Unternehmensbereich Apparate
Postfach 80 11 49
8000 München 80

719

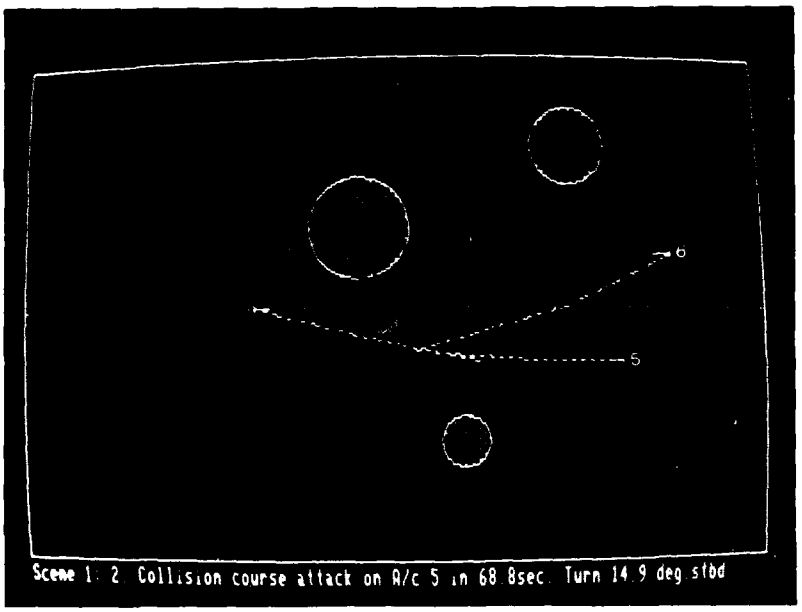

Figure 13

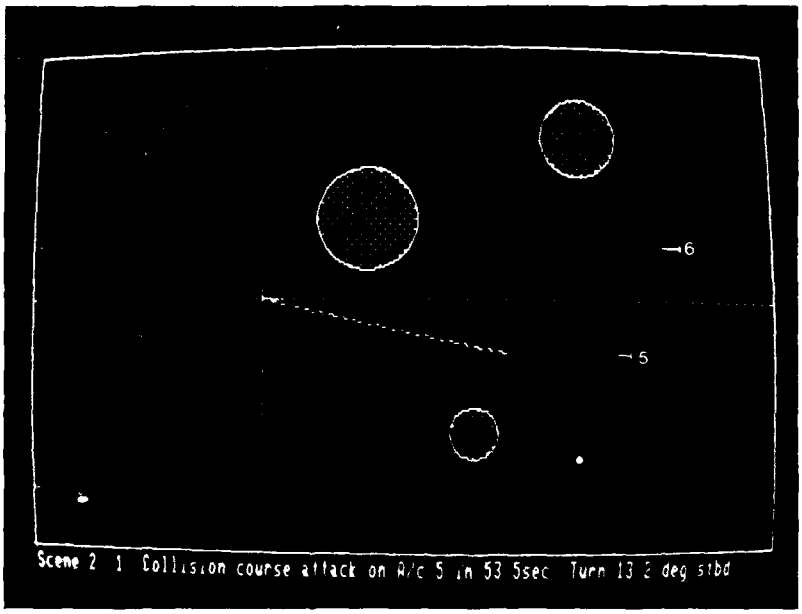

Figure 14

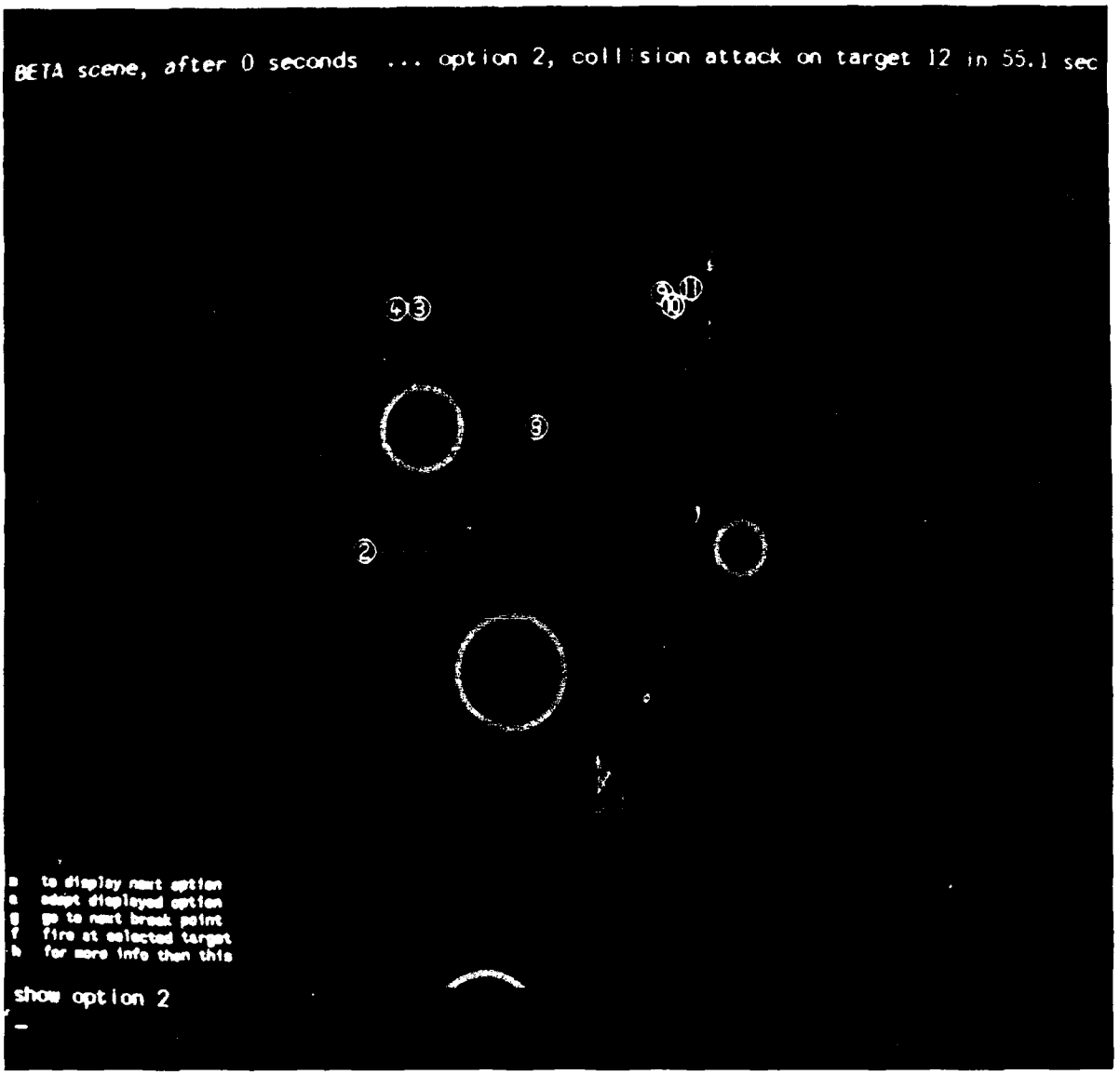
BETA scene, after 0 seconds ... option 2, collision attack on target 12 in 55.1 sec
to display next option
adopt displayed option
go to next break point
fire at selected target
for more info then this
show option 2

Figure 15

AD-P005 718

A FIBER OPTIC GYRO STRAPDOWN REFERENCE SYSTEM FOR GUIDED WEAPONS

by
D. RAHLFS, W. AUCH, O. GLASER, D. RUPPERT
SEL - STANDARD ELEKTRIK LORENZ AG
LORENZSTR. 10, D-7000 STUTTGART-70
FEDERAL REPUBLIC OF GERMANY

SUMMARY

The experiences with the gyro error behaviour made during the development of fiber optic gyros (FOG) at SEL are stimulating a number of new system implementations. Among them the use of FOGs within strapdown reference systems for guided weapons looks very favourable because of the high FOG bandwidth, its low noise operation and the absence of maneuver-dependent gyro-errors (as opposed to mechanical sensors).
System design considerations lead to an integrated strapdown reference system solution for guidance and line of sight stabilization. The principal error sources of such a system based on FOGs are investigated by means of simulations including original sensor signals. The investigations indicate that these systems can be realized on the basis of the SEL-FOG which is now under preparation for mass production.

1. INTRODUCTION

Within the past years flight control and seeker technologies for guided weapons became more and more sophisticated. A very important contribution to the solution of the cost and weight problems associated with more complex navigation, flight control and seeker attitude reference systems can be earned from the implementation of inertial strapdown reference systems which use low cost fiber optic gyros. The use of a single low cost fiber optic gyro strapdown attitude reference system for all guidance needs onboard an airlaunched weapon system will be investigated in the following.

The basis of this work is the development of fiber optic gyros started at SEL in 1980. Two different types of gyros mainly differing in their readout method - the phase modulated and the frequency modulated one - are in an advanced development phase. The first type with a drift specification of about 10 deg./hours is specially designed for use in low cost systems with no compensation of the earthrate which itself contributes a drift of up to ± 15 deg./h. The second type demonstrated a high scalefactor stability (see /3/) combined with an improved driftrate of about 1 deg/h which enables applications in medium accuracy inertial navigation systems.

The experiences from the development and the tests of the phase modulated gyro form the basis for the following system design and simulation considerations.

2. FIBER OPTIC GYRO DEVELOPMENT

At SEL FOGs based on both previously published modulation techniques (phase nulling frequency modulation and open-loop phase modulation) are under development (see /1/,/2/). The justification for this twofold effort are different applications requiring different sensitivities, rate capabilities and scale factor stabilities. The solution for the problem of split activities is to keep the difference between the two gyro types as small as possible. This is achieved by using a modular interferometer design which is characterized by its optronic hybrid technology. Integrated-optics modules, all-fiber components and even miniaturized bulk components are combined to form optimized setups. The common interfaces are single-mode fiber pigtails. A subunit, consisting of the source module (V-groove multimode laserdiode with thermoelectric cooler), first beam splitter (fiber coupler in fused-taper technique), PIN detector and fiber polarizer can be combined with the different fiber coils and modulator types.

2.1 The Phase Modulated FOG Concept

The phase modulated fiber gyro is basically designed as a rate gyro and employs open-loop phase modulation signal processing. It is built as all guided wave sensor with an integrated-optics $LiNbO_3$ phase shifter. The high bandwidth and good linearity of this phase modulator determined the key features of this gyro. It is characterized by its short fiber length and its scale factor stabilization technique. The fiber length of L=100m together with the coil radius of R=3.5cm compresses the dynamic range to Sagnac phase shifts below 90deg for rotation rates up to 400deg/s. The optimum modulation frequency is $f_m=c/(2nL)=1MHz$ which is only achieved satisfactorily with an integrated-optics modulator. Sinusoidal phase modulation with amplitude Φ_o leads to the well known detector output signal as a function of rotation rate or Sagnac phase shift. The amplitudes of the harmonics are given by Bessel functions:

$$i(t)\sim I_o(1+J_o(2\Phi_o)\cos\Delta\Phi_s) + 2I_oJ_1(2\Phi_o)\sin\Delta\Phi_s\cdot\cos(2\pi f_m(t-\tau/2)) - 2I_oJ_2(2\Phi_o)\cos\Delta\Phi_s\cdot\cos(2\pi 2f_m(t-\tau/2)) + \ldots$$

Phase sensitive detection of the first harmonic gives the rotation rate signal. Scale factor stabilization (compensation for varying attenuation, coupling efficiency or laserdiode output) is accomplished by detection of the dc component and a control loop which drives te gain for the f_m component as a function of the measured dc value. The resulting gyro output becomes

$$U_{Signal} = U_{ref} \cdot \frac{2J_1(2\Phi_o)\cdot\sin\Delta\Phi_s}{1 + J_o(2\Phi_o)\cdot\cos\Delta\Phi_s}$$

The modulation amplitude Φ_o is set to $\Phi_o = 1.2$ rad with $J_o(2\Phi_o) = 0$. Thus the rotation dependent part in the denominator of the scale factor vanishes and the output signal is proportional to the sine of the rotation rate.

The functional block diagram of the optical and electronic part of the 100m rate sensor is shown in Fig. 1. Its parameters and target specifications are summarized in the table below:

Target specification of phase modulated FOG

Dimensions and parameters

Diameter:	80 mm
Height:	25 mm
Weight:	200 g
Fiber length:	100 m
Coil radius:	35 mm

Performance

Signal format:	digital, 15 bit parallel + 1 sign bit update rate 1 kHz
Scale f ' :	0.012 deg/s/LSB
Scale factor error	0.5 %
Range	± 400 deg/s
Bandwidth	500 Hz
Noise	10 deg/h $\sqrt{Hz}$
Bias uncertainty (T=const)	10 deg/h

Environment

Temperature	-54...71 °C
Vibration	20...2000 Hz 10 g sin
Shock	60 g/3 ms sine halfwave 20 g/100 ms

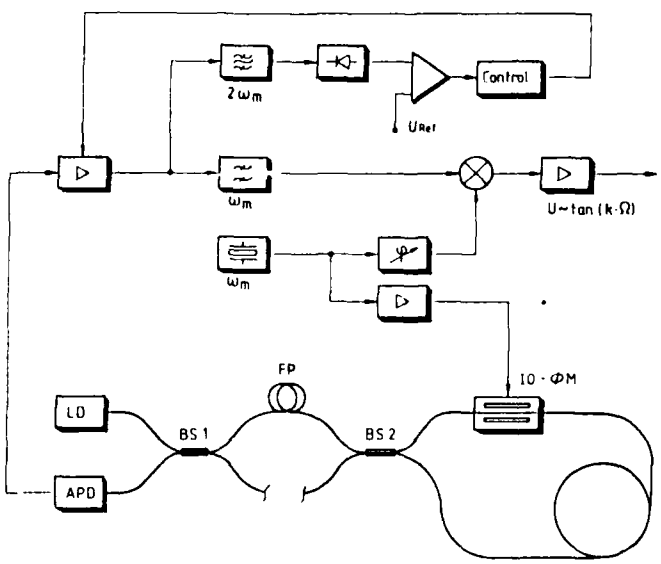

Figure 1. Phase Modulated Fiber Optic Gyro Configuration

3. FIBER OPTIC GYRO STRAPDOWN REFERENCE SYSTEM DESIGN

On the basis of the 80mm diameter phase modulated fiber optic gyro at SEL a new type of reduced dimensions with 40 mm diameter was designed for small volume applications such as in guided weapons. As shown in Fig. 2 the strapdown attitude reference system consists of a three fiber optic gyro (FOG) package and four electronic boards. The individual gyro has a maximum dimension of 40 mm. The reduced microbending effects of new polarization preserving fibers now available allow such small dimensions. The basic characteristics of this new FOG are:

maximum input rate:	± 800 deg/sec
maximum bias uncertainty:	40 deg/h
scale factor error:	0.5 %

The gyro electronics performs a direct digitizing of the gyro output signal with a resolution corresponding to 16 bits. Processing of the strapdown algorithm is carried out at a high speed of 500 Hz on a fourth card.

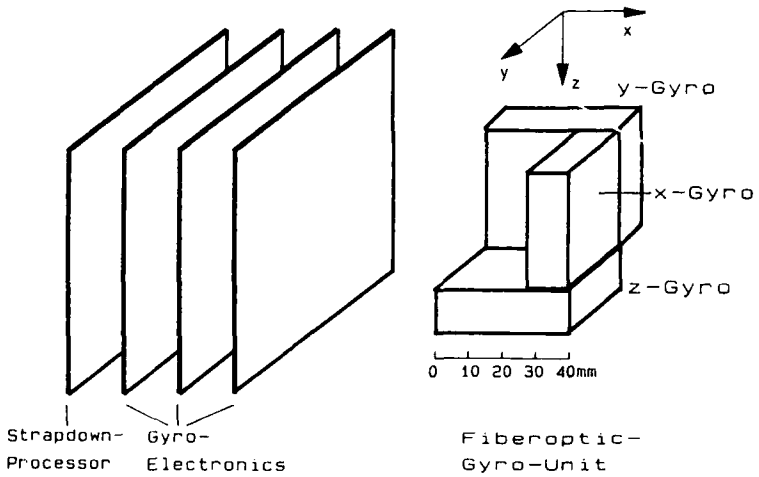

Figure 2. Strapdown Attitude Reference System with Miniaturized Fiber Optic Gyros

The classical design of a guidance system of a weapon system includes two different inertial sensor sections. Fig. 3 shows the seperate flight control using a reference gyro for yaw and pitch corrections and the additional seeker equipment (in this case a optical device including a tracker) employing a second reference gyro system for line of sight stabilization.

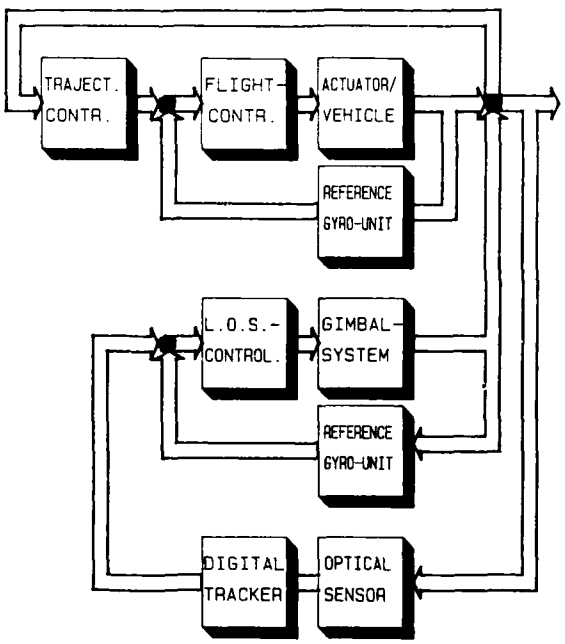

Figure 3. Functional Diagram of a Classical Guidance & Seeker System with Seperate Gyro References

The verification of compact and low cost strapdown attitude reference systems allows the designer to simplify the allover guidance system architecture. As shown in Fig. 4a one strapdown reference system consisting of the reference unit and the strapdown computer can serve simultaneously for referencing both the flight control and the seeker system. It is well known that the seeker itself has to be stabilized with a very small stablization error in order to allow high resolution and long distance detection. When this is not performed by a directly gimballed reference gyro a very high bandwidth is needed for the strapdown reference system. Exactly this point can be ideally achieved by fiber optic gyros. The SEL-FOG-type for instance operates at a 1000 cycles/s refresh rate of the digital output signal corresponding to a sensor bandwidth of 500 Hz. Together with the matched strapdown computer update rate of 500 cycles/s this means that with the proposed reference system a high quality gimbal servoing will be possible in the future, thus allowing new mechanical seeker solutions.

The search for cost effective solutions for the guidance and seeker tasks leads to an integration of all processing tasks of a weapon system into one processor of the next generation as shown in Fig. 4b. This system uses the advances in the field of digital processing speed for a minimum solution in terms of cost and weight which should be very suitable for guided weapon applications.

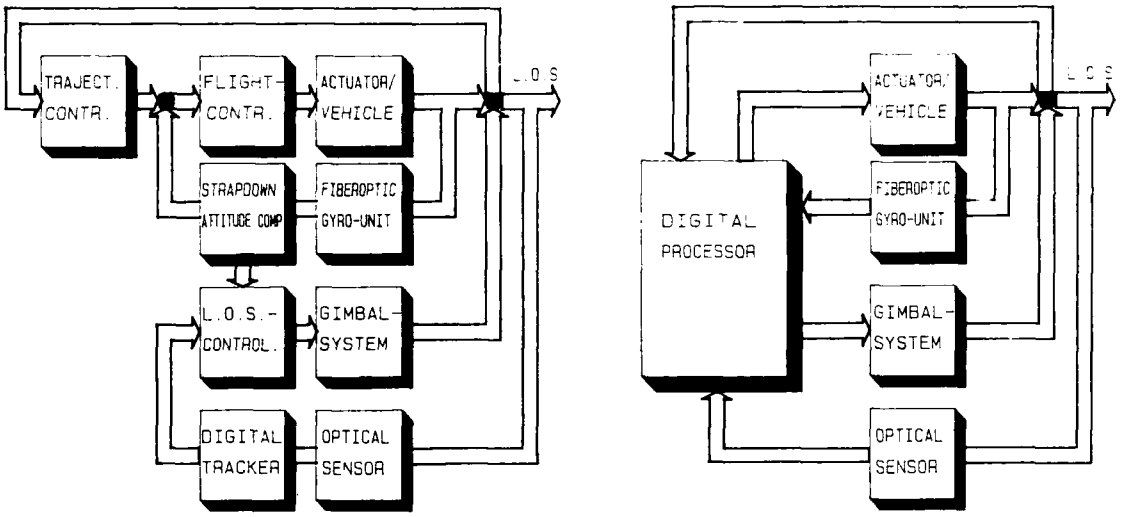

Figure 4. Functional Diagram of a Guidance & Seeker System with a Strapdown Reference
a - Distributed Electronics b - Low Cost Version with an Advanced Processor

4. THE NAVIGATION SOFTWARE DEVELOPEMENT SYSTEM

4.1 Concept

For the design, implementation and validation of realtime software modules for strapdown systems a special software tool is available at SEL : the Navigation Software Development System (NSD). This efficient tool was used for all the investigations described in this paper. A short review of the basic functions of this program system will be given below.

As shown in Fig. 5 the outmost simulation shell consists of a flight path and vehicle motion generator (APG Attitude and Position Generator) and the sensor error models (SEG Sensor Error Generator), which simulate the real world environment in terms of linear and rotational motion as well as the sensor characteristics.

The simulated sensor signals are transferred to the realtime-kernel modules which perform Sensor Error Correction (SEC) and Strap Down Calculation (SDC).

The results are compared with reference data by a special data evaluation program (SAP Signal Analysis and Plot Processing).

The complex input data are handled by a input processor which allows easy modification of single coefficients out of the total set and supports input data file control and documentation.

This allows to optimize the real time navigation software with respect to

- algorithm errors (numerical approximation)
- roundoff errors (word length)
- program loop timings (sampling)
- quantization errors (sensor digitizing)
- sensor characteristics, and
- flight dynamics

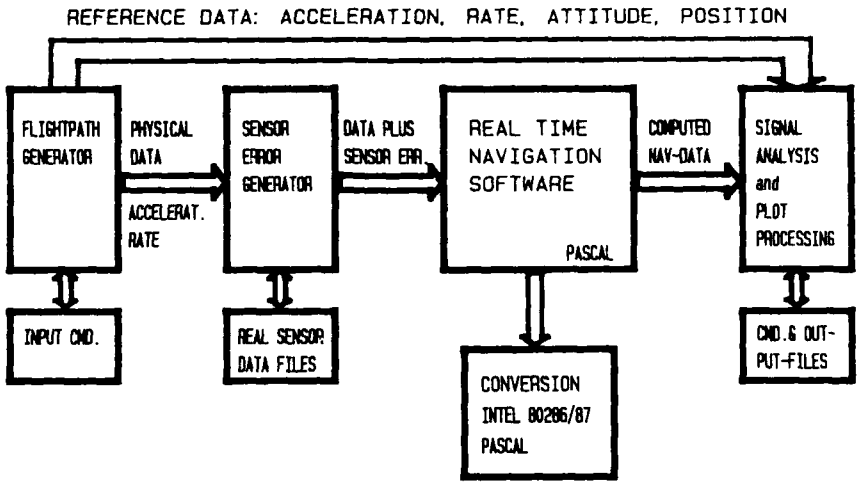

Figure 5. Structure of the Navigation Software Development System (NSD)

4.2 Flight Path Generator

The flight path generator (Attitude and Position Generator APG) computes all reference data of a special vehicle motion with respect to the navigational coordinate frame. The data are stored for error analysis and transformed to the body-frame thus yielding the required correct sensor input-signals, as for instance the rate values for the gyros and the acceleration values for accelerometers in body-fixed coordinates.

Different types of carrier movements including sinusoidal movements can be carried out. A geometrical displacement of the sensing unit with respect to the center of the carrier's movement, giving rise to additional acceleration signals, is also included.

4.3 Sensor Models

The body fixed sensor input signals are compounded with the sensor error contribution by the sensor error generator. Both classes of errors - compensatable and noncompensatable sensor errors - are taken into account. For fiber optic gyros the following errors are modelled:

- bias of angular rate
- scale factor error
- scale factor nonlineraity
- Crosscoupling between sensor axes

4.4 Realtime-Kernel Software Modules

The realtime software package for the inertial reference system consists of the following main components:

- the sensor error compensation module,
- the strap-down calculation module,
- the euler angle extraction module, and
- the application modules (i.e. stabilization module)

In the sensor error compensation module the deterministic errors which are included in the sensor models are corrected. In case of skewed sensors the signals are orthonormalized and transferred to the strap-down calculation module. For the strap-down calculation a quaternion mechanization of choosable order is used, which gives the possibility to find an optimal implementation with respect to timing and accuracy requirements. A standard euler angle extraction algorithm is used which may be adjusted to application requirements. The realtime-kernel software is developed in standard PASCAL on the simulation computer; this ensures correct transposion of these modules to the target processor.

4.5 Data Evaluation and Error Modelling

The resulting errors are analyzed by means of a special signal processing software which uses standardized file inputs/outputs for multiloop signal analysis. Graphic representation of all output files is supported.

5. SIMULATION RESULTS OF THE FIBER OPTIC GYRO STRAPDOWN REFERENCE UNIT

5.1 Choice of the Attitude Profile

To obtain meaningful results from simulations of a FOG strapdown attitude reference system one has to select an appropriate attitude profile. This selection is a tradeoff between two objectives:

- the profile should be as realistic as possible and encompass the whole vehicle dynamics
- the simulation results should be easily interpretable, i.e. the attitude errors which show up in the simulation results should be discernible and easily traceable to the sensor or algorithm level.

Fig. 6 shows the flight path and the associated attitude profile which was selected for the subsequent simulations of the FOG attitude reference system. It consists of a short climb flight from a lower to a higher altitude level, with a maximum pitch angle of 30 deg and a maximum pitch rate of 30 deg/s. Superimposed on this profile is an angular vibration about all three axes with an amplitude of 1 deg, a frequency between 1 and 10 Hz and a variable phase relationship between the three axes. These angular vibrations (which are not included in fig. 6) represent the influence of structural vibrations, which may be induced by aerodynamic effects or by a rocket motor.

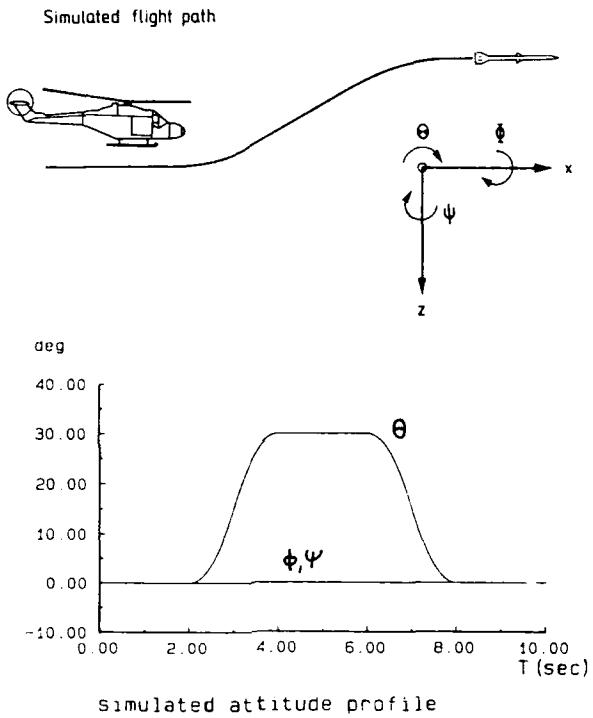

Figure 6. Simulation Input in Terms of Flight Path and Attitude Profile

Although this attitude profile may not seem very realistic, it is quite representative of the application and, because of the superimposed angle vibrations, all error sources of the system are excited in the simulation. The relative simplicity of this attitude profile allows an easy identification of the various error mechanisms.

5.2 Influences of Error Sources on System Performance

While investigating the influence of various error sources on overall system performance, we will have to deal with two major classes of error sources:

- strapdown algorithm errors
- sensor (i.e. gyro) errors

5.2.1 Strapdown Algorithm Errors

Errors which are generated in the strapdown calculation result from the discrete implementation of continuous differential equations (which always involves series expansions) and from the sampling of quantized sensor signals in discrete time

intervals. The magnitude of these algorithm errors depends on the specific algorithm, the update frequency and the motion profile.

Although the 3rd order quaternion algorithm, which we have chosen, is very good in this respect, there are certain unfavorable cases, where quite large algorithm errors may arise.

5.2.1.1 Coning Motion Error

One of these unfavorable cases is the coning motion, which consists of mutually out-of-phase angle vibrations about orthogonal axes. Fig. 7 shows the attitude error which results from such a coning motion at a coning frequency of 10Hz and calculation frequencies of 50Hz and 500Hz. The attitude error, which is quite large at a calculation frequency of 50Hz (almost one degree after 10sec) and dominates all the sensor errors (20deg/h drift and 0.1% SFE were assumed), reduces to a negligible value at a calculation frequency of 500Hz. Thus one has to conclude that in high dynamic environments, where such coning vibrations may exist, an increase of the calculation frequency to several hundred hertz has to be considered.

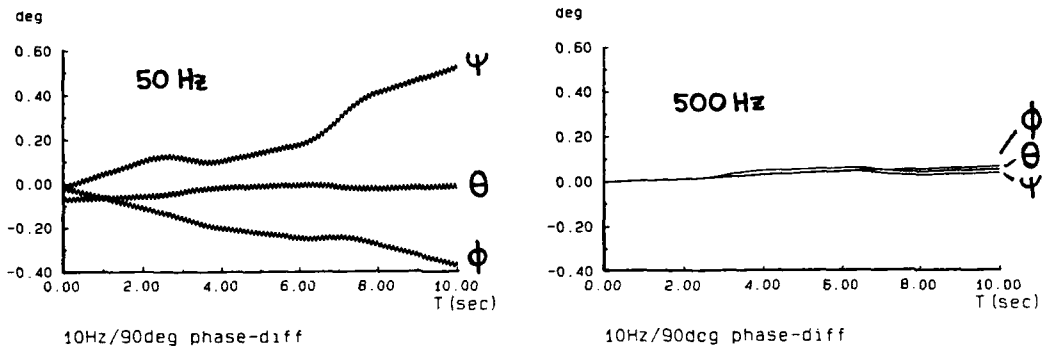

Figure 7. Coning Motion Error at Strapdown Calculation Frequencies of 50 Hz and 500 Hz

Such an increase in calculation frequency is reasonable only when it is accompanied by a corresponding increase in gyro bandwidth. This requirement is easily fulfilled by the inherently high bandwidth of the FOG, which makes it an ideal candidate for high dynamic strapdown environments where the existence of structural vibrations is suspected.

5.2.1.2 Continuous Rate Input

A second algorithm error becomes important when there is a continuous rate input about one axis, for example in the case of a missile spinning continuously about its roll axis. The resulting attitude error depends again on the calculation frequency. Fig. 8 shows the simulation results for an input roll rate of 4000 deg/s and calculation frequencies of 50Hz and 500Hz, assuming a skewed sensor configuration which accounts for the limited input range of the FOG. The roll axis error angle at a calculation frequency of 50Hz amounts to a huge 30 deg after only one second; and again the increase of the calculaton frequency to 500Hz reduces the roll angle error to a negligible value. This leads to the same conclusions concerning the gyro bandwidth as in the case of the coning motion; again the FOG is (from this point of view) a good candidate for strapdown attitude reference applications in spinning missiles.

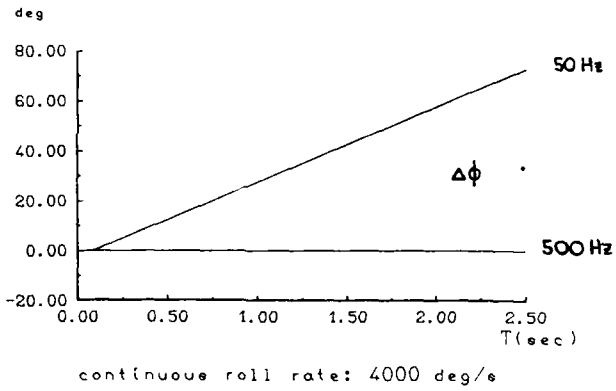

Figure 8. Roll Angle Error Due to Continous Roll Rate Input at Calculation Frequencies of 50 Hz and 500 Hz

5.2.2 Sensor Errors

The FOG has a remarkably simple error behaviour. Because of its massless principle of operation there are no contributions from linear acceleration dependent drifts or angle acceleration dependent drifts, which are common in mechanical gyros. Thus we will only have to consider

- gyro drift
- gyro scale factor error (SFE)

and, because we talk about high dynamics applications and want to point out the specific advantages of fiber optic gyros with respect to mechanical gyros, we will also deal with

- limited gyro bandwidth.

The error coefficients are taken essentially unmodelled as they are at present for the phase modulated SEL FOG.

5.2.2.1 Gyro Drift

Fig. 9 shows the influence of the gyro drift on the attitude error for the attitude profile introduced before, using drift values of 10, 20 and 100deg/h (top to bottom). The attitude angle errors are well within 0.5deg even for the 100deg/h case, and even below 0.1deg in the case of a 10deg/h drift. The maximum in the middle results from a scale factor error of 0.5%, which was included for comparison. Thus one can conclude that, assuming this kind of attitude profile, the gyro drift is definitely not the limiting factor for overall system accuracy. Even if one does assume a gyro drift of 100deg/h, which is an unrealistically high value for the SEL FOG, the angle errors are not excessively high and are of the same order of magnitude as the errors resulting from a scale factor error (SFE) of 0.5%. This indicates that the SFE may here be a more important error source.

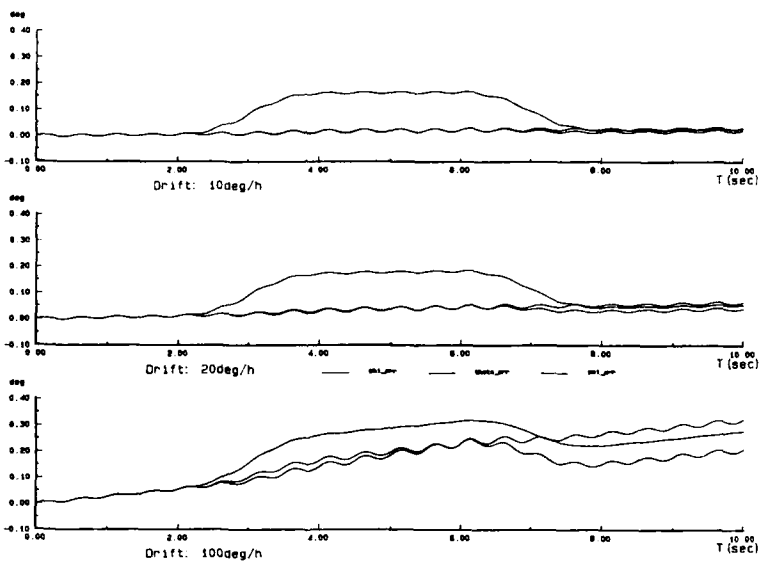

Figure 9. Attitude Error Due to Gyro Drifts (10 ,20 & 100deg/h) and Scale Factor Error (0.5%)

When applications in continuously spinning missiles are considered, gyro drifts become even less important, because the drift in pitch and yaw gyros is averaged out due to the continuously changing orientation of the missile body axes. The small roll angle error which is caused by the roll gyro drift is usually not critical.

5.2.2.2 Scale Factor Error

A scale factor error of 0.5%, which is the present uncompensated value for the SEL phase modulated FOG, yields with our attitude profile a pitch angle error of about 0.2deg, see Fig. 10. A reduction of the SFE to 0.1%, which one can hope to achieve by modelling, results in a corresponding reduction of the pitch angle error to a few hundredth of degrees.

An even more demanding application, as far as the scale factor is concerned, are attitude reference systems in continuously spinning missiles. When such a system is mechanized completely as a strapdown system, the gyro which measures roll rate is, due to the absence of a roll gimbal, subject to a high unipolar angular rate. Assuming a roll rate of 4000deg/s, a SFE of 0.1% leads to a roll angle error which increases linearly with time with a slope of 4deg/s. Although in spinning missiles the exact knowledge of the roll angle is usually not essential, a roll angle error which is

greater than a few degrees seriously affects pitch and yaw angle accuracy. However, the gyro which measures roll rate in these systems operates in a limited rate region, i.e. only at high rates. First measurements of the SFE characteristics of the SEL phase modulated FOG indicate that in such a limited rate region the scale factor may possibly be modelled to an accuracy substantially better than the value of 0.5% quoted from the current target specification.

One can thus conclude that among the "classic" gyro error sources the SFE is the most critical one for the attitude reference application considered here. The scale factor accuracy required for nonspinning systems are met by the SEL phase modulated FOG. For full strapdown applications in spinning missiles an optimization of the scale factor of the roll gyro at high rates will certainly be necessary.

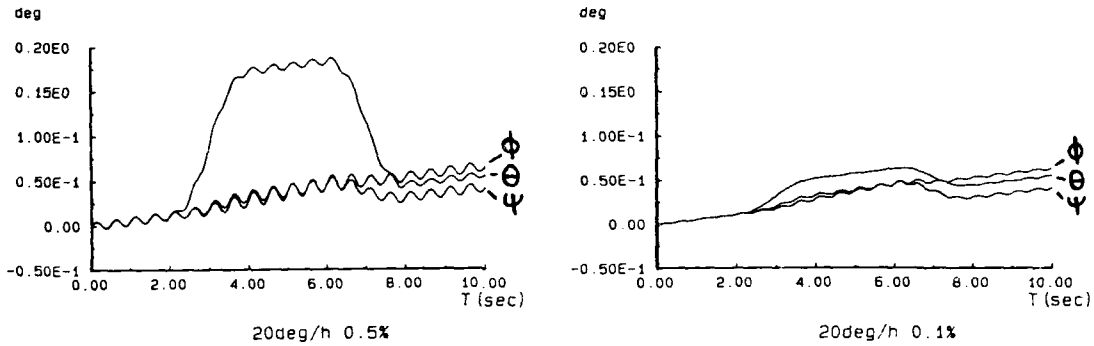

Figure 10. Attitude Error Due to Scale Factor Errors of 0.5% and 0.1%

5.2.2.3 Limited Gyro Bandwidth

As attitude control applications in high dynamic environments are considered, an additonal error source becomes important: the limited gyro bandwidth. This more or less obvious fact can easily be visualized in a simple simulation experiment which was carried out within the frame of our Navigation Software Development System which, for this purpose, was equipped with an additional low pass filter to get a coarse model for the gyro frequency response.

The simulated system input is shown in Fig. 11. It consists of a simple discontinuity on the rate acceleration level, which may stand for a "kick" caused, for example, by a rocket motor start. Fig. 11 shows the resulting attitude angle error for gyro bandwidths between 25Hz and 500Hz. With the gyro bandwidth limited to a few tenths of hertz, quite formidable attitude errors and, in a control application, correspondingly high control errors may result in a high dynamic environment.

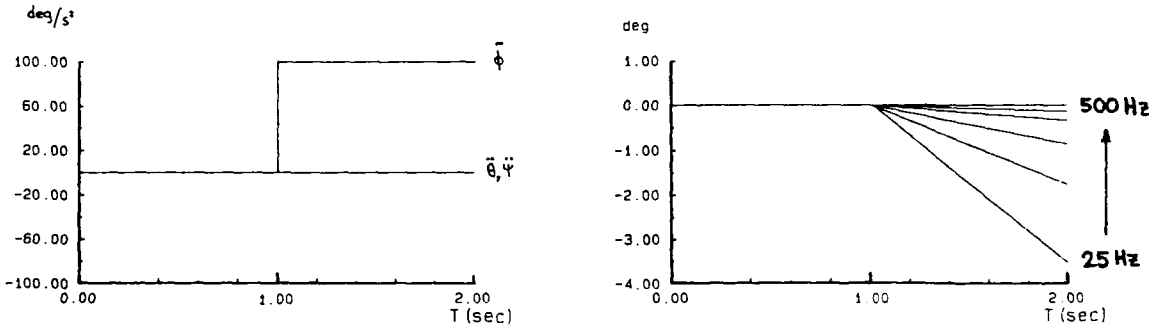

Figure 11. Simulation Input (left) and Resulting Attitude Error for Various Gyro Bandwidths

This simple simulation experiment merely serves to visualize the statement that high quality attitude control in high dynamic applications requires high gyro bandwidth in addition to a high strapdown algorithm update rate. The high bandwidth inherent to the FOG together with the compact, all solid state, low cost concept of the SEL phase modulated FOG make it a candidate for high dynamic control and stabilization applications.

6. SIMULATION OF A STRAPDOWN SYSTEM REFERENCED LINE-OF-SIGHT STABILIZATION SYSTEM

A block diagram for the line of sight (LOS) control is shown in Fig. 12. The inner loop contains the gimbal control including the controlled element (gimbal and torquer) and a high bandwidth angle transducer. The friction effects associated with all gimbal systems are represented by the nonlinear characteristics shown in Fig. 12.

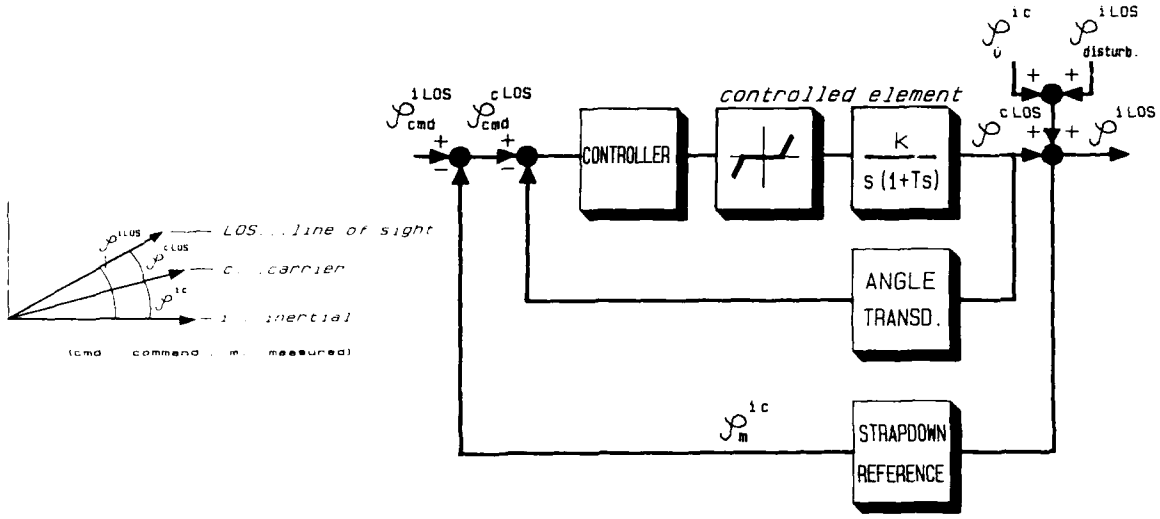

Figure 12: Block diagram of line of sight control

The need for a high bandwidth for the angle transducer can be seen from the simulation results in Fig. 13, which shows the stabilization errors for 200Hz and 400Hz angle sensor bandwidth, assuming a sinusoidal 1 degree command input.

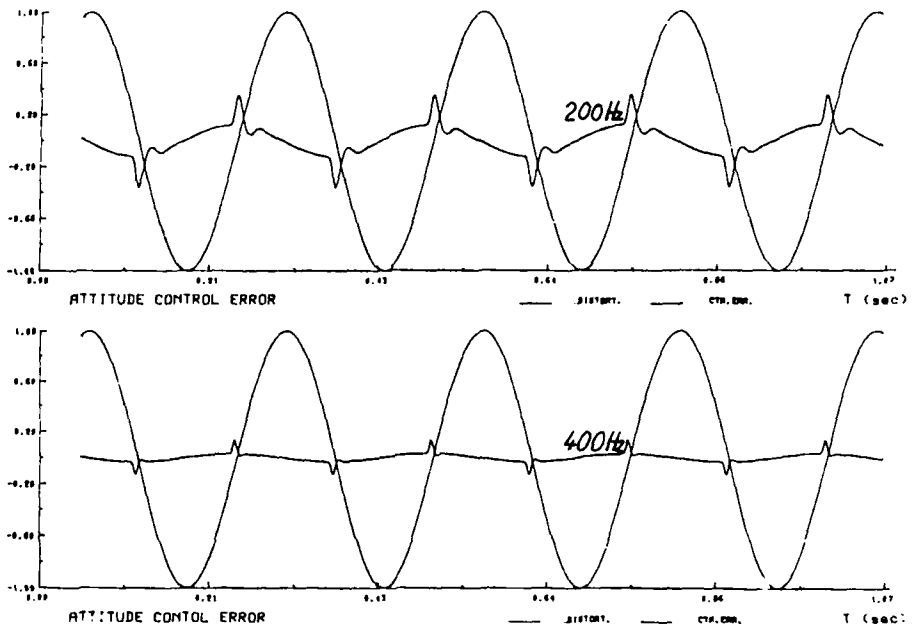

Figure 13: Attitude Error of a Gimbal System at 200Hz and 400Hz Angle Sensor Bandwidth

The limited angular freedom of a gimbal system used in the seeker section allows the implementation of simple linear transducers which have the required high bandwidth. The angular errors caused by the substitution of an angle measurement by a measurement of linear displacement can easily be compensated in the strapdown system computer.

It is obvious that especially in an offline strapdown steering mode of a LOS stabilization system a high bandwidth is essential for operation in a very dynamic environment. A constant 50 deg/sec movement yields a large velocity angle error of about 8.8 mrad at a gyro signal update rate of 100 Hz. The update rate of 1000 Hz which is typical for the SEL FOG yields only 0.88 mrad angle error.

Besides the deterministic LOS stabilization errors the contribution of random sensor noise has to be considered. From the block diagram in Fig. 12 it can be seen that the sensor noise can directly be added to the stabilization error. Strapdown Calculations using original input signals of the SEL FOG led to the typical strapdown reference output noise patterns shown in Fig. 14, indicating that only very small noise contributions are present.

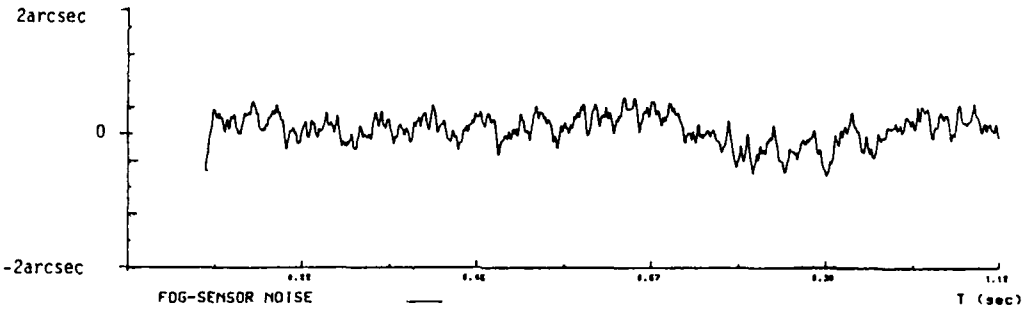

Figure 14: Typical FOG Angle Noise Pattern

7. CONCLUSION

Simulations based on the error behaviour of the phase modulated fiberoptic gyro, which was developed at SEL and is now going to reach production stage, have shown that this kind of rate sensor is becoming a serious competitor in the field of strapdown system sensors. Potential applications, taking advantage of the FOG's simple error behaviour, its inherent high bandwidth and its all-solid-state concept include missile attitude reference systems and high quality line-of-sight stabilization systems for high dynamic environments. These features encourage the development of integrated concepts, where attitude reference system and line-of-sight stabilization system are merged into one single strapdown sensing and controlling unit.

8. REFERENCES

/1/ Auch,W. Schlemper,E. — Drift behaviour of a fiber-optic gyro with polarization-preserving fibre. IEEE Conf. Publ. 221, London ,1983

/2/ Auch,W. — Optische Rotationssensoren Technisches Messen tm 52 pp.199-207, 1985

/3/ Fürstenau,N. Lübeck,E. Wetzig,V. Auch,W. Koch,M. — Drift and scale factor tests on the SEL fiber gyro in a controlled enviroment. Symposium Gyro Technology 1984, Stuttgart, 1984 DGON Conf. Proc. Stuttgart 1984.

/4/ Pio,R.,L. — Euler Angle Transformations. IEEE Trans. Automatic Control, no. 11, 1966.

/5/ Rahlfs,D. — Line of Sight Stabilization Symposium gyro technology 1981, Stuttgart.

/6/ AGARD — Advances in Strapdown Inertial Systems AGARD Lecture Series No. 133

AD-P005 719

SPEED CONTROL OF A MISSILE WITH THROTTLEABLE DUCTED ROCKET PROPULSION

by
Dieter Thomaier
Messerschmitt-Bölkow-Blohm GmbH
Unternehmensbereich Apparate
Postfach 80 11 49
8000 München 80

SUMMARY

The demand for higher flight velocities and ranges for tactical missiles favours increasingly the application of airbreathing engines. The wide range of altitudes, in which many missiles - particularly air launched - must be operational, makes the variation of thrust mandatory and leads ultimately to the control of propellant mass flow. Thus, with the choice of a solid propellant ducted rocket as propulsion-system, the gasgenerator must produce a variable mass flow rate. The widely applied method uses a propellant with a pressure sensitive burning rate. A valve with variable throat area controls the mass flow out of the gasgenerator.

Accordingly the mathematical model of the gasgenerator consists of the laws of propellant burning rate and chamber discharge and the fundamental equation of gas. This results in an opposing relation between mass flow and pressure for the first short control period after a valve throat variation. The controller design must consider this non-minimum-phase behaviour. For the presented example of a missile design a propellant mass flow measurement couldn't be realized. On the other hand the flight Mach number is the ultimate control value. This leads to the controller design described as follows:

The Mach number controller computes the suitable nominal value for the gasgenerator pressure while accounting for the pertinent gasgenerator dynamics. This procedure requires the knowledge of the pressure sensitive burning rate with adequate narrow tolerance limits. In case of high-g flight manoeuvres the system can optionally switch over to a simple command for the pressure nominal value.

An adaptive controller is nested within the Mach number loop to keep the gasgenerator pressure in closed loop control. Thus, an open loop control of the mass flow rate is provided. This loop is controlled by the flight Mach number loop, its value being derived from flight data.

The installation of prototype engines on test stands in a hardware-in-the-loop configuration and the required additional simulation procedure will be described. The presentation of test results concludes the paper.

LIST OF SYMBOLS

a	empirical parameter	Q	amount of heat
A	area	r	burn rate
c_p	specific heat at constant pressure	R	gas constant
c_v	specific heat at constant volume	S	reference area
c^*	characteristic velocity	t	time
C_F	thrust coefficient	T	temperature
C_W	drag coefficient	T_r, T_p	time constants
F	thrust	v	velocity
g	gravity acceleration	V	volume
H	altitude	α	angle of incidence
m	mass	γ	ratio of specific heats
$\dot{m}$	mass flow	ρ	density
M	mach number	Θ	inclination angle
n	pressure exponent	ω_0	control parameter
p	pressure		

SUBSCRIPTS

b	burning
d	discharged
g	gas
p	produced
r	references
s	set value
t	throat
o	free stream

AD-A194 648 ADVANCES IN AIR-LAUNCHED WEAPON GUIDANCE AND CONTROL PROCEEDINGS OF THE G..(U) ADVISORY GROUP FOR AEROSPACE RESEARCH AND DEVELOPMENT NEUILLY.. DEC 87 AGARD-CP-431 2/2

UNCLASSIFIED F/G 17/7.3 NL

END
DATE
FILMED
8 8

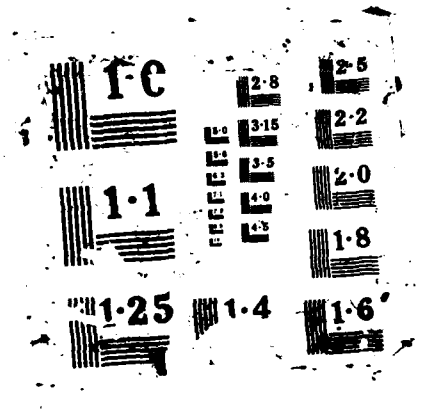
1·C
2·8
2·5
3·15
2·2
3·5
2·0
4·0
1·1
4·5
1·8
1·25
1·4
1·6

1. INTRODUCTION

The growing demand for higher flight velocities and ranges in the field of tactical missiles favours increasingly the application of airbreathing engines. The wide range of altitudes, in which many missiles - particularly air launched - must be operationel, together with requirements for improved manoeuvrability makes the variation of thrust mandatory. The most effective way to do this is the control of propellant mass flow.

With the choice of the propellant a strong preference of solid grains should be considered. A very attractive propulsion system which fits perfectly in this scenario is the solid propellant ramrocket or in the more usual american term the ducted rocket. The basic design of a missile with ducted rocket propulsion is shown in Fig. 1. The gasgenerator contains a grain of oxygen deficient propellant. After ignition it provides the ramcombustor with fuel rich combustion products. There they will mix and burn with the incoming air from the air inlets. The internal volume of the ramcombustor is suitable to accommodate an integral booster. For the most cases of air launched missiles the possible size of the booster is sufficient to accelerate to the required take over Mach number of the ducted rocket.

This paper describes the dynamic behaviour of the gasgenerator with the resulting design considerations for the control loop. A description of the complete engine control system shows the necessity to include some special features. The test philosophy with the according hardware-in-the-loop arrangement and the presentation of some test results will round off this paper.

2. GASGENERATORS WITH VARIABLE MASS FLOW

According to the requirements stated above the gasgenerator must produce a variable mass flow rate. This can be achieved in different ways based on the influence of the two main parameters

- burning rate
- burning surface.

A short survey of some proposed concepts shall be presented below (Fig. 2) without a discussion of the pros and cons.

o Pressure Sensitive Propellant
The widely applied method uses a propellant with a pressure sensitive burning rate. An end or cigarette burner is the common grain configuration. But also rod and tube grains are known. The control of the mass flow out of the gasgenerator and thus the gasgenerator pressure is managed by a valve with variable throat area.

o Matrix Propellant
This concept is a variation of the method before. The difference is given by the composition of the propellant. Preproduced granules of a propellant with low pressure sensitivity but high energy content could be embedded within a matrix of a low energy propellant with high pressure sensitivity. The result envisaged is a burning behaviour which resembles in some aspects a more or less erosive burning.

o Strand Augmented Propellant
The propellant composition of this method is somewhat reverse ot that above. One or more strands (small propellant "wicks") of high pressure sensitivity are embedded in a matrix propellant of high energy content but low pressure sensitivity. The now pressure dependent progress of the small burning front on top of the strands dictates how strong "coning" occurs in the matrix propellant. Coning means that a locally faster burn rate tends to deform at least the whole burning surface to a slope to this most progressive points. Therefore, the major effect is achieved by variation of the burning surface. The actuator nevertheless is still a throttling valve.

o Retractable Silver Wires
A burning surface modulation via controlled coning is the basis of this concept too. But differently from the method mentioned above the extend of coning is here influenced by the conductive heat flux through embedded silver wires. To maintain or stop the heat flux is the task of a somewhat complicated mechanism which retracts the silver wires at an adequate rate. This rate determines the relativ position of the silver wires to the burning surface and thus the corresponding heat flux.

o Longitudinal Tubes
A concept proposed by Thiokol as THERMATROL (R) (Thiokol Heat Exchange Rocket Motor Augmented Rate Control) uses the same effect of thermal induced coning but by other means. Instead of the retractable silver wires fixed small metal tubes would be installed. A flow rate control system connected to this tubes at the bottom of the grain allows a variable heat flux via the bleed rate of combustion gases.

As mentioned before a detailed discussion of the various concepts is not the aim of this survey. Nevertheless, one general aspect is very important to all control considerations. The variation of the burning surface is generally associated with relatively long time constants sometimes extending to a substantial part of the whole mission.

In the present case of an air-launched anti-ship missile the mission requirements postulated considerable versatility on the propulsion side. Thus, a gasgenerator with a pressure sensitive propellant became the heart of the speed control for the missile.

3. MATHEMATICAL MODELS

3.1 GASGENERATOR

A general arrangement of the selected type of gasgenerator is shown in Fig. 3. With the progress of the burning front to the left the free volume of the gasgenerator is filled with hot combustion products. This gas leaves the gasgenerator through the throttle-valve. The interaction of production and discharge of gas determines the pressure inside the free volume. A few words should be added referring to the nature of the combustion products. Beside their dominant gaseous portion these often contains liquid and solid phases. In particular with the application of propellants with high energy content the amount of these phases are not negligible. Nevertheless, with an assignment of suited material constants the mathematical treatment as an ideal gas leads to results of sufficient accuracy.

As mentioned before the conditions inside the free volume result from the difference between produced and discharged mass or energy respectively. Furthermore the volume of burned solid must be filled with gas. The burn rate of the propellant may be described by the known empirical formula

$$r = a \cdot p^n \tag{1}$$

The parameters a and n are propellant specific and not necessarily independent from pressure over the utilized pressure range as we will later see. The resulting mass production is given by

$$\dot{m}_p = \rho_p \cdot A_b \cdot a \cdot p^n \tag{2}$$

The mass flow discharged through the valve throat at a critical pressure ratio is, according to fundamental fluid dynamics, determined by

$$\dot{m}_d = \frac{p \cdot A_t}{c^*} \tag{3}$$

with

$$c^* = \frac{\sqrt{R \cdot T}}{\Gamma} \tag{4}$$

and

$$\Gamma = \sqrt{\gamma \left(\frac{2}{\gamma + 1}\right)^{\frac{\gamma + 1}{\gamma - 1}}} \tag{5}$$

The balance of mass is given by

$$\frac{dm}{dt} = \dot{m}_p - \dot{m}_d = \frac{d}{dt}\left(\rho_g \cdot V\right) \tag{6}$$

and corresponding the balance of energy

$$\frac{dQ}{dt} = \dot{m}_p \cdot c_p \cdot T_p - \dot{m}_d \cdot c_p \cdot T = \frac{d}{dt}\left(\rho_g \cdot V \cdot c_v \cdot T\right) \tag{7}$$

According to fundamental considerations /3/ temperature variations are small. Therefore, the assumption of constant temperature $T = T_p$ = const. is adequate.

With the basic assumption of an ideal gas the equation of state is valid

$$p = \rho_g \cdot R \cdot T \tag{8}$$

Thereby we obtain the differential equations of the gasgenerator

$$\frac{dp}{dt} = \frac{d\rho_g}{dt} R \cdot T = \frac{\dot{m}_p - \dot{m}_d - \rho_g \frac{dV}{dt}}{V} R \cdot T \tag{9}$$

$$= \frac{R \cdot T}{V}\left(\rho_p \cdot A_b \cdot a \cdot p^n - \frac{p}{R \cdot T} \cdot A_b \cdot a \cdot p^n - \frac{p \cdot A_t}{c^*}\right)$$

$$\frac{dV}{dt} = A_b \cdot r = A_b \cdot a \cdot p^n \tag{10}$$

With these equations the dynamic behaviour of the gasgenerator can be investigated. The parameter of interest is the discharged mass flow. Together with the air mass flow which is a function of the respective flight conditions this propellant mass flow determines the thrust of the missile.

An example illustrates this behaviour. As shown in Fig. 4 with a step function, the valve adjusting velocity assumed to be infinite, the throat area will be reduced. Now it is obvious that the mass flow shows a reverse-reaction behaviour. Due to the reduction of the throat area the mass flow is reduced proportionally for the first short period. This disturbance of the discharge causes the pressure to rise. But now, according to the rising pressure, the burning rate will also increase. Ultimately with a certain time constant presssure and mass flow will adjust to the new steady-state condition. The time constant is proportional to the free volume of the gasgenerator.

A very important aspect for the design of a controller is the question what kind of measurements are possible. With this the liquid and solid phases have to be considered. Of course, it is no problem to get a precise signal from a position indicator of the valve. But the corresponding throat area may depend on circumstances like burning time, pressure level etc. since the valve is exposed to deposits. With some precautions the measurement of pressures is feasible with sufficient accuracy. However, a reliable temperature recording of the hot gas is difficult and may depend on operating time.

Now, the possibility of a measurement of propellant mass flow is of dicisive significance. Extensive investigations [5] have shown that out of a multitude of physical principles only a few are really applicable. For practical use in the environment which a missile provides there remains at least one method. This method makes use of a smoothing or intermediate volume served by the discharge of the throttling valve and an outflow through a fixed nozzle. Assumed there are no temperature variations and a critical pressure ratio is provided the mass flow is proportional to the pressure in the volume (Fig. 4). The deposit problem at a sonic nozzle should not be considered as a severe one. Nevertheless, a disadvantage of this method is a rise of the operational pressure level.

Besides the measurement aspects another point of strong influence is the behaviour of the controlling element represented by the throttle-valve with its actuator. Approximately with a first order lag element the transfer function of the throttle-valve can be described.

$$\frac{dA}{dt} = \frac{1}{T_v} (A_s - A) \tag{11}$$

Furthermore must be observed

- the upper and lower limit of the valve throat area (according to design considerations it is impracticable to close the gasgenerator completely)
- the limit of the valve adjusting rate

3.2 MISSILE DYNAMICS

Related to the speed control the force balance along the flight trajectory is the significant portion of missile dynamics (Fig. 5). The resultant first order differential equation describes the acceleration along the flight trajectory:

$$\dot{v} = \frac{1}{m} \frac{\gamma}{2} p_0 \cdot M_0^2 \cdot S \cdot (C_F \cdot \cos \alpha - C_W) - g \cdot \sin \Theta \tag{12}$$

The thrust coefficient is a function of:

$$C_F = f\ (\dot{m}_p, M_0, H, \alpha) \tag{13}$$

and with a good approximation the drag coefficient is described by:

$$C_W = C_{W_0} + C_{W_\alpha} \cdot \alpha^2 \tag{14}$$

where the basic term is determined by

$$C_{W_0} = f\ (M_0, H) \tag{15}$$

Values of the drag coefficient are commonly provided by wind tunnel tests. Whereas with good accuracy the values of the thrust coefficient can be calculated by an engine cycle program.

The measurement of related flight data poses no problem. Practically each missile which such sophisticated requirements is equipped with an Inertial Navigation System (INS). Therefore, acceleration and velocity are available with great accuracy. Equally well it is possible to provide the Mach number by an aerodynamic probe.

4. DESIGN OF THE CONTROLLER

The considerations of the previous chapter points out that a design of direct or closed loop control of the propellant mass flow has to deal with the following aspects:

- reverse reaction or non-minimum-phase behaviour
- working pressure level of the gasgenerator is determined by two pressure losses (throttle-valve and sonic nozzle)
- intermediate volume has to be provided

On the other hand the parameter that ultimately must be controlled is the velocity or the Mach number. From this point of view it is obvious to reject the direct mass flow control and to attempt to design a control system which provides directly the required speed. With such a solution the propellant mass flow would be controlled in an open loop and the associated mass flow measurement can be rejected.

4.1 SPEED CONTROLLER

The requirements of the project mentioned in the beginning asked for

- Mach number control at different levels
- various flight profiles up to high altitude
- high-g manoeuvres at final approach to the target

To fulfill these requirements the following concept resulted from a somewhat difficult design process. The speed controller (Fig. 6) consists of a Mach number controller with a cascade controller for the pressure loop of the gasgenerator. Thus, an open loop control of the mass flow rate is provided.

At the high-g manoeuvres a control of the Mach number is no more opportune. In this case a set value adjuster will calculate the appropriate set value for the pressure controller from the required manoeuvre data. With that a sufficient thrust level will be provided to maintain a certain Mach number within specified tolerance limits during this flight period.

A short time before launch of the missile the required data must be transferred to the speed controller. Furthermore the interpretation of the signals given by a start sequencer and the timely start of the controller are properties of the initiation function block. Due to the transferred atmospherical and environmental data the applicable controller coefficients will be selected. The launch data decide the preadjustment of the throttle-valve. By this the appropriate mass flow rate for the transition phase will be provided.

In the next chapters both controllers will be described in more detail together with some design considerations. They are of the adaptive type. Thus, during the operation time a continuous parameter adaptation has to take place.

Furthermore the operation limits have to be taken into consideration. These limits consists of

- sufficient supercritical margin of the air inlets
  - minimum Mach number
  - maximum propellant mass flow
- heat resistance of radom
  - maximum Mach number
- strength of gasgenerator structure
  - maximum pressure inside the gasgenerator

A graph (Fig. 7) illustrates the remaining operational regime of the ducted rocket. During operation a supervisory function block determines the appropriate limitations.

Even without the discussion of the controllers in detail the above facts show that this task can only be done reasonably by direct digital control.

4.2 MACH NUMBER CONTROLLER

During the major part of the flight the speed control has to maintain a certain Mach number preset by the flight control system. A limiter controlled by the supervisory functions reduces the set value to $M_{smin} \leqslant M_s \leqslant M_{smax}$.

To improve the command behaviour this value will be treated with a filter. With the effected lag an overshoot of the Mach number progress will be virtually avoided.

A second limiter constrains the deviation to $DM_{min} \leqslant DM \leqslant DM_{max}$.

By this a violation of the specified Mach number limits due to the non-minimum-phase behaviour of the controlled system will be avoided.

At variations of altitude a fast adaptation of the set value of the gasgenerator pressure will be provided by a disturbance variable compensation.

The controller itself consists of a proportional-plus-integral controller for the processing of the Mach number deviation and a proportional controller. The latter stabilizes the loop with a feedback of d/dt(M) derived from the measured acceleration. The integral portion of the controller guarantees the static accuracy. Furthermore it provides a self learning capability. Therefore, the required gasgenerator pressure, which is a complex function of aerodynamic and environmental conditions, will be determined automatically.

The parameters of the Mach number controller will be adapted to the varying free volume and pressure inside the gasgenerator. The adaptation to the free volume, due to its slow variation, will be done continuously. However, the adaptation to the pressure has to consider that it is a state variable of the controlled system and will be done by parameter switching. At the switching points the continuity of the commanded value will be forced.

4.3 GASGENERATOR PRESSURE CONTROLLER

The considerations of chapter 3 demonstrated clearly that the pressure is the only variable of the gasgenerator which can be measured reasonably. It is described by the non-linear differential equation (9). From the viewpoint of the whole concept the purpose of the pressure control is primarily the stabilization of the gasgenerator. For it the behaviour of the pressure should correspond to the following reference model:

$$\frac{dp_r}{dt} = \frac{1}{T_p}(p_s - p_r) \qquad (16)$$

Thus, the transfer function of the gasgenerator will be linearized. Furthermore this function will be time-invariant. Consequently the design of the Mach number controller was simplified considerably. Due to the time-discrete realization of the controller and the limited valve adjusting rate the time constant T_p should be selected not too small.

The pressure set value can be provided by two modes:

- from the Mach number controller in the case of closed loop Mach number control

- from the set value adjuster in the case of open loop Mach number control at high-g manoeuvres.

The second mode is suitable for an open loop control of the mass flow (Fig. 9). At this the set value will be calculated with the known relation of mass flow and gasgenerator pressure (Equation (2) or tabulated data set). These conditions proved favorable at the design of the test concept.

The adaptive pressure controller (Fig. 10) consists of a proportional compensation controller with an additional proportional-plus-integral controller. According to Equation (16) the proportional compensation controller causes for the closed loop approximately the following transfer function:

$$\frac{dp}{dt} = \omega_0 \cdot (p_s - p) \qquad (17)$$

Without a violation of this behaviour the additional proportional-plus-integral controller provides the static accuracy. The portion of the correcting variable delivered by this additional controller can be limited. Thus, an excessive overflow of the integral value, e.g. caused by temporary jamming of the valve, with possibly resulting oscillations can be avoided. But with the increasing reliability of the valves this limiting functions lost its importance. Further will be limited:

- the set value of the pressure

- the set value of the valve throat area

both in accordance with the supervisory functions

- the valve throat area

due to design conditions.

Like these of the Mach number controller the parameters of the pressure controller will be adapted to the varying free volume and pressure inside the gasgenerator. The value of the free volume is known before ignition but there is no possibility to measure it during operation. Thus, it must be calculated continuously by the integration of the respectively produced increase of this volume. According to equation (10) the timely value is dependent on the gasgenerator pressure.

As indicated in chapter 3 the parameters a and n are not necessarily independent from the pressure. Typically the characteristic curve of the burn rate tends to minor gradients in the upper pressure regime. Therefore, the application of a tabulated form of this relationship and all parameters dependent of it proved favorable. The same is valid for the pressure dependence of the characteristic velocity c*.

During the development of the control system the test results suggested the inclusion of some special features. These accounts mainly for the behaviour of the particle-laden gas. Regardless of the measures taken at the valve the following provisions against the effect of deposits were made:

- identification of deviations from the valve characteristic curve
  At static operation phases continuous throat area deviations caused by deposits can be determined and compensated.

- wipe pulses
  At low pressure the preservation of the maximum throat area is particularly important. Wipe pulses at times can be helpful.

- switching of the loop gain
  At high pressure the control loop tends under some circumstances to oscillations. A reduction of the closed-loop gain in this regime solves the problem.

Furthermore a special initiation process provides for a smooth start and another feature opens the valve at burn-out for the largely utilization of the pressurized propellant gas.

5. SYSTEM TEST

Of course, an intense examination with simulations accompanied the design of the controller. At the same time the development of the engine takes place. For it the design of the throttle-valve was a very important matter. The various types with their pros and cons should not be discussed here.

Nevertheless, the applied and very approved design, a special kind of a rotary disk valve, shall be shortly presented. Fig. 11 shows a photograph of the valve seen from the gasgenerator side. The valve has four outlets in twos throttled by two rotary sliders with their axes perpendicular to the outlet plane. Shown is the full open position with the maximum throat area that can be provided. The control edges are shaped circular and rounded to form a nozzle. Thus, in the most critical position a geometry is provided which avoids largely deposition.

To obtain the above described state long series of tests were necessary. Of course, the early combination of the engine hardware with the control algorithms was very important. The resulting dynamic behaviour could be studied under real conditions.

5.1 HARDWARE-IN-THE-LOOP TEST TECHNIQUE

The test concept was strongly influenced by the following conditions:

- realization of the controller with direct digital control technique

- gasgenerator pressure control loop can be operated seperately

- necessity of propulsion system tests a long time before the availability of the controller hardware.

Under these circumstances a hardware-in-the-loop test technique offered a great advantage. Fig. 12 shows a comparison of the flight system with the conditions at the test plant. Due to the first point mentioned above the implementation of the controller software on a process computer instead of the engine control computer is possible without difficulty. At our test plant a VAX 750 computer was available for such purposes. Therefore, an operation of the (inner) gasgenerator loop at the test plant could be managed.

Although an electric drive is provided for the missile valve servo-system at the test plant a hydraulic actuator was used.

Much more complicated was the implementation of the Mach number controller. Therefore, a simulation of the missile behaviour due to inertia and aerodynamics must take place. Furthermore the test plant must be able to provide a varying air mass flow heated to the suitable temperature similar to the air inlets at supersonic flight.

Fig. 13 shows the situation in the form of a block diagram. The propulsion system is represented by

- the throttle-valve with the appropriate servo-system

- determining the mass flow out of the gasgenerator

- injected into the ramcombustor.

At flight conditions the achieved thrust acts against inertia and aerodynamics of the missile. The values of Mach number and acceleration measured by Mach meter and INS will be provided to the speed control system. The set value of the valve throat area closes the loop.

The algorithms of the speed control system can be performed either by the engine control computer or by a process computer.

As mentioned before the test plant must provide an appropriate air mass flow heated to the stagnation temperature. The available facility works according to the blow-down principle. The air mass flow out of an air reservoir will be controlled by a throttle-valve. A heater supplied with hydrogen provides the required temperature. Not shown on this diagram is the supply of the make up oxygen. This will be provided to an amount equal to that consumed by hydrogen.

However, the missing link for a successful test procedure is a substitude for the missile. This will be introduced by the simulation of the missile dynamics. Proceeding from the measured thrust all required parameters will be calculated. The corresponding simulation algorithms can also be performed by the mentioned process computer.

The block diagram of the simulation of the missile dynamics is shown in Fig. 14. Proceeding from the gas-generator pressure the produced mass flow will be calculated according to equation (2). With the integrated gas production the present missile mass can be calculated.

Simultaneously the coefficients of Thrust and Drag will be determined. The calculation of the fictive acceleration will be done according to equation (12). A first integration provides the velocity. Consequently the Mach number can be determined. Besides the preparation of the set values of the test plant controllers for air mass flow, heating hydrogen and make up oxygen the Mach number will be provided for the coefficient calculation of the next sample.

With an additional integration of the velocity times the cosine of the elevation angle the covered range over ground will be determined. The integrations will be performed with Runge-Kutta formulas.

Thus, the required values for the speed controller will also be provided.

5.2 TEST RESULTS

Fig. 15 shows a photograph of a ducted rocket propulsion system on the test facility. Lateral of the engine the hydraulic actuator of the throttle-valve is visible.

Results of two tests with the simulation of missile dynamics are presented in Fig. 16 and 17. Both show an acceleration process followed by a manoeuvre (open loop mode) in the second case. The diagrams on the left indicate the very good accordance of the gasgenerator pressure with its set value. The diagrams of the coefficients of drag and thrust show excess of thrust during the acceleration phase. The third set of curves illustrates the Mach number progress.

A photograph of a trial firing of a ducted rocket propulsion system (Fig. 18) closes this paper.

6. CONCLUSION

I think the now available combination of speed controlled airbreathing propulsion with a solid propellant offers very attractive possibilities not only for our current project but also for the whole spectrum of tactical missiles.

REFERENCES

[1] Kreuzer, W.; Schwellinger, U.
Speed Control of a Missile with an Airbreathing Ramjet Engine
MEDE 78, Wiesbaden 1978

[2] Besser, H.-L.
Solid Propellant Ramrockets
AGARD-LS-136, Ramjet and Ramrocket Propulsion Systems for Missiles
Monterey, London, Neubiberg 1984

[3] Jungclaus, G.
Das Regelverhalten von Gasgeneratoren
MBB-TN-RT31-6/75, August 1975

[4] Thomaier, D.
Untersuchung eines nichtlinearen Regelkonzeptes für den Gasgenerator des Feststauantriebs
MBB-TN-RT31-18/78, June 1978

[5] Weinreich, H.-L.
Untersuchung von Methoden zur Kontrolle der verbrauchten Energie bei FK-Antrieben
MBB-Abschlußbericht T/RF42/90034/91478, April 1981

REFERENCES (cont'd)

[6] Kreuzer, W.
Triebwerksregelung für einen FK mit Feststoff-Staustrahl-Triebwerk
A. Druckregelkreis des Gasgenerators
B. Machzahlregelung
MBB-TN-AE13-4 und 27/82, February & June 1982

[7] Kreuzer, W.
Triebwerksregelung für einen Flugkörper mit Feststauantrieb
MBB-TN-AE13-12/86, June 1986

[8] Thomaier, D.
Planung eines Prüfstand-Regelungsprogramms
MBB-TN-RT31-5/80, May 1980

[9] Thomaier, D.
Grundlagen zur Triebwerk-Regler-Simulation auf dem Prüfstand-Prozeßrechner
Teilabschnitte "Nichtlinearer Druckregler", "FK-Verhalten"
MBB-TN-RT31-24/80, August 1980

[10] Internal Reports, Test Procedures and Test Results
MBB 1984-1987

Missile with Ducted Rocket Propulsion System
Basic Design

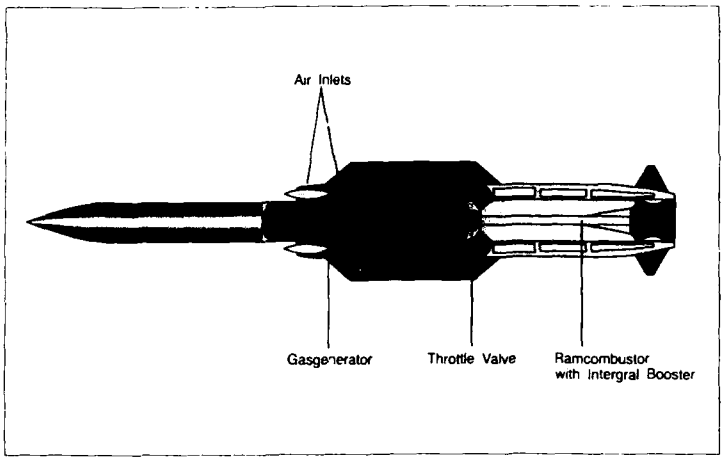

UA 005 052

Fig. 1

Gasgenerators
with Variable Mass-Flow

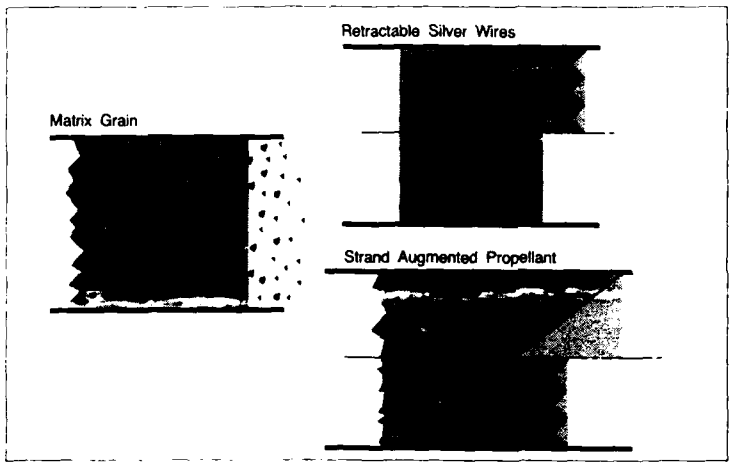

UA 005 050

Fig. 2

Gasgenerator
Pressure Determination

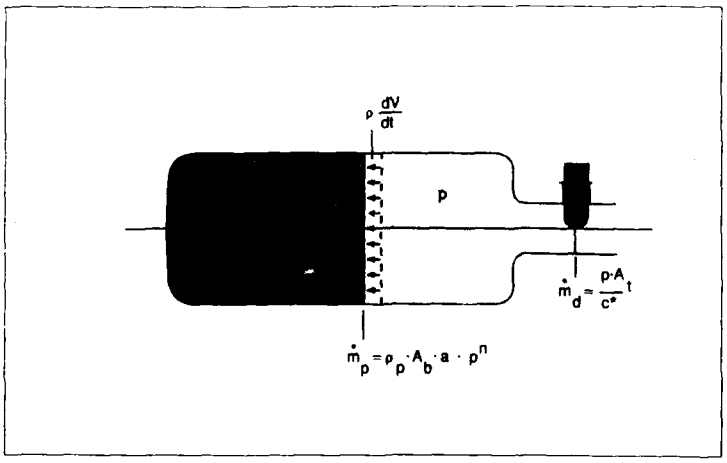

UA 005 049

Fig. 3

Gasgenerator
Non-Minimum-Phase Behaviour

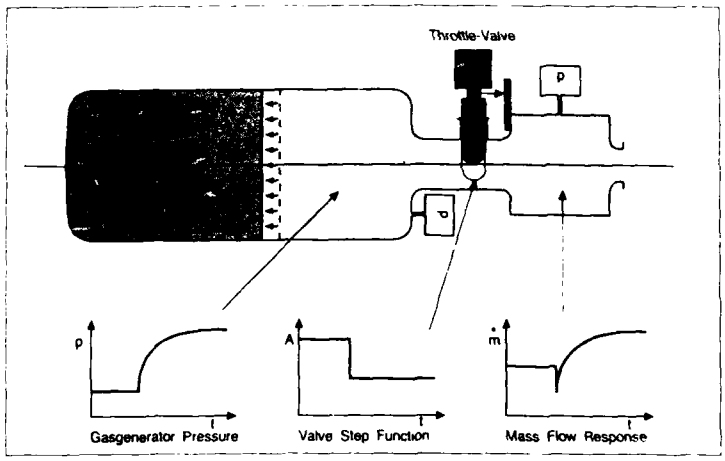

UA 005 051

Fig. 4

Missile Dynamics

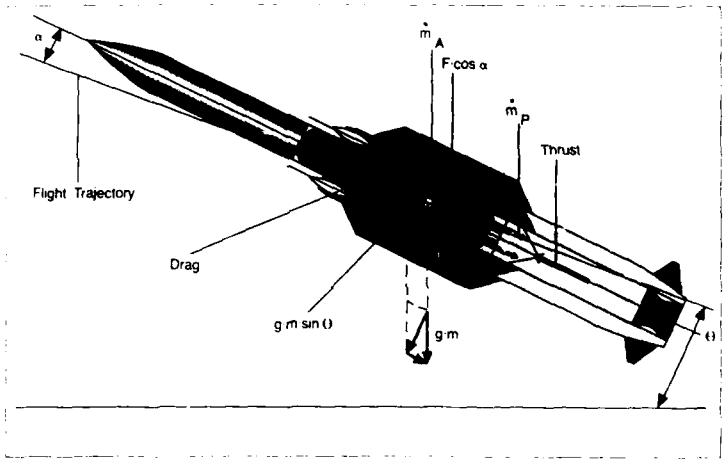

UA 005 053

Fig. 5

Speed Controller
Block Diagram

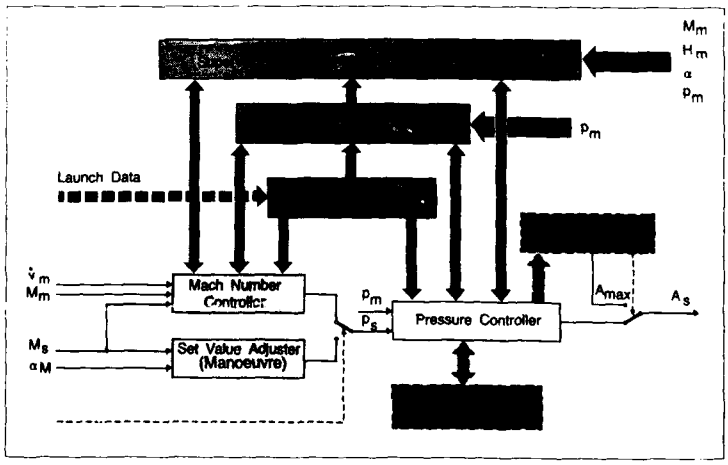

UA 005 047

Fig. 6

Speed Con[illegible]
Operation[illegible] Regime

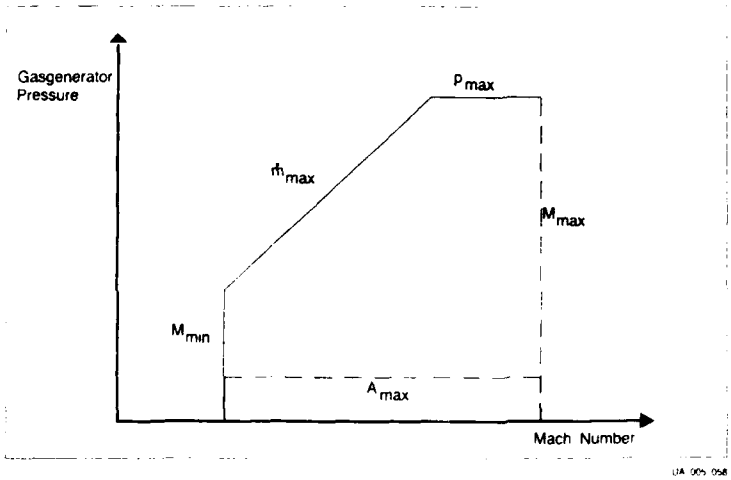

Fig. 7

Mach Number Controller
Block Diagram

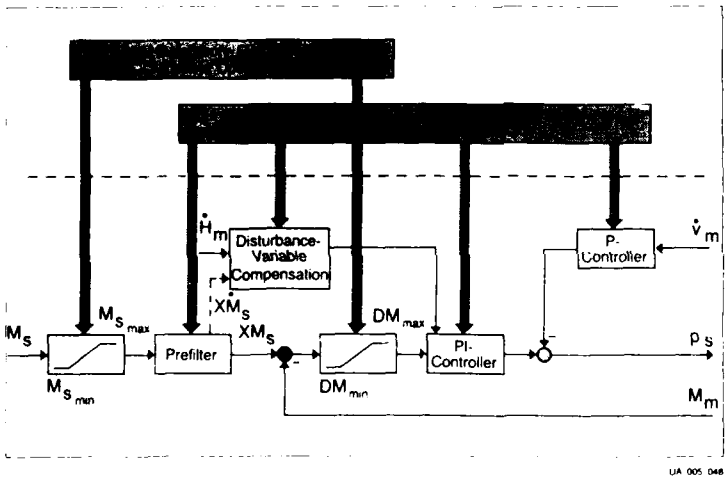

Fig. 8

Pressure Controller
Set Value Modes

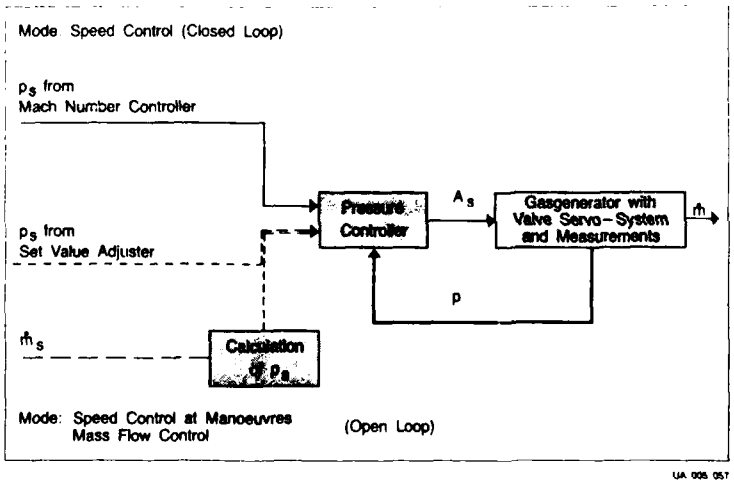

Fig. 9

Pressure Controller
Block Diagram

Defence Systems Group

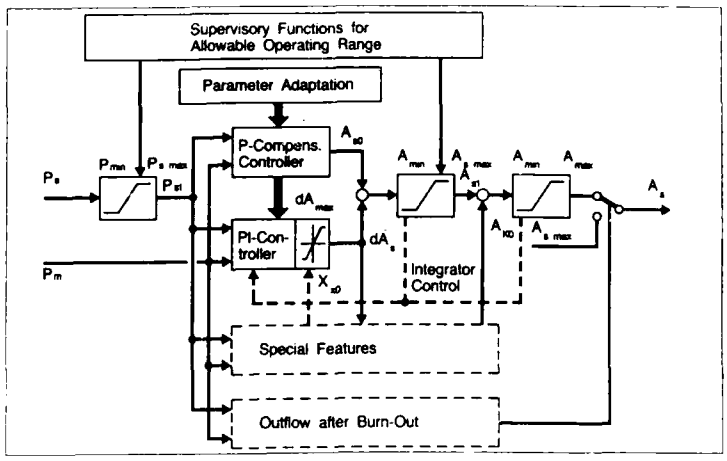

UA 005 054

Fig. 10

Throttle-Valve

Defence Systems Group

- 4 Outlets
- 2 Rotary Sliders
- Low Adjusting Torque
- Circular Control Edges
- Low Tendency to Deposition

Fig. 11

Test Philosophy
Comparison: Flight System/Test System

Defence Systems Group

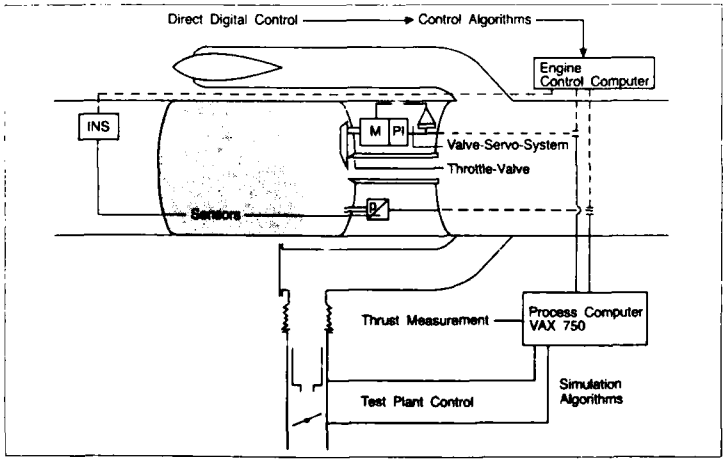

UA 005 055

Fig. 12

Hardware-in-the-Loop Test Technique

Defence Systems Group

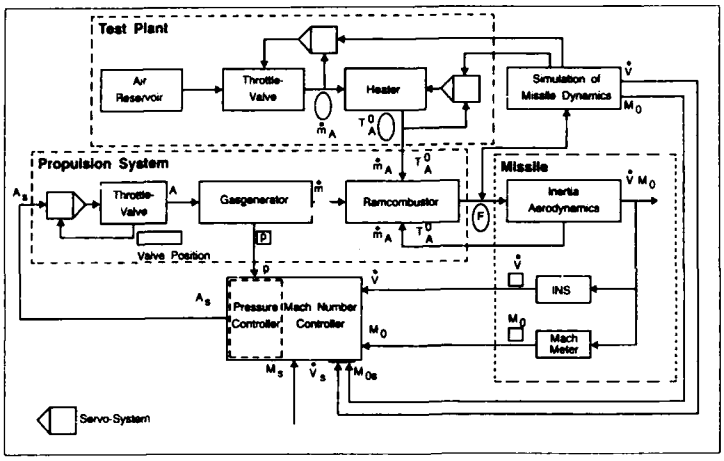

UA 005 056

Fig. 13

Simulation of Missile Dynamics
Block Diagram

Defence Systems Group

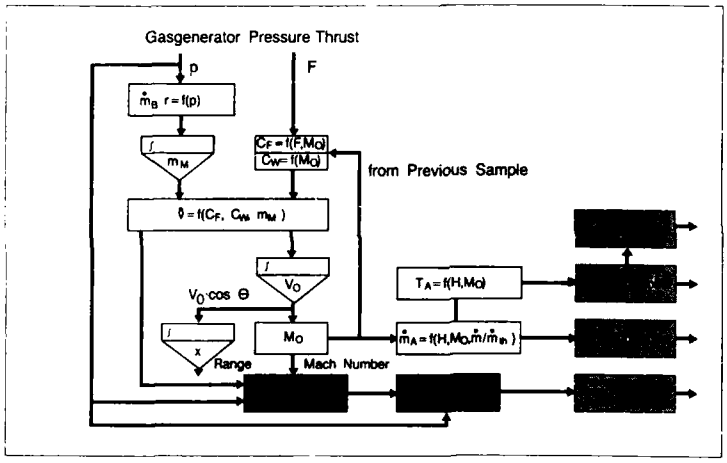

UA 005 048

Fig. 14

Test Plant with
Ducted Rocket Propulsion System

Defence Systems Group

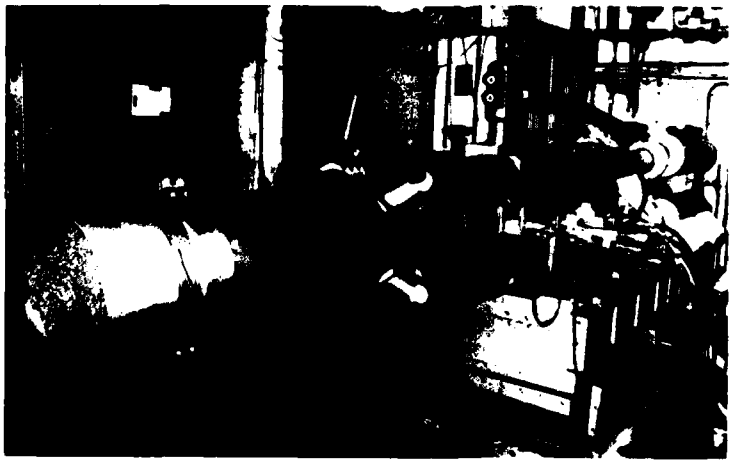

Fig. 15

Ducted Rocket Propulsion System
Test Results

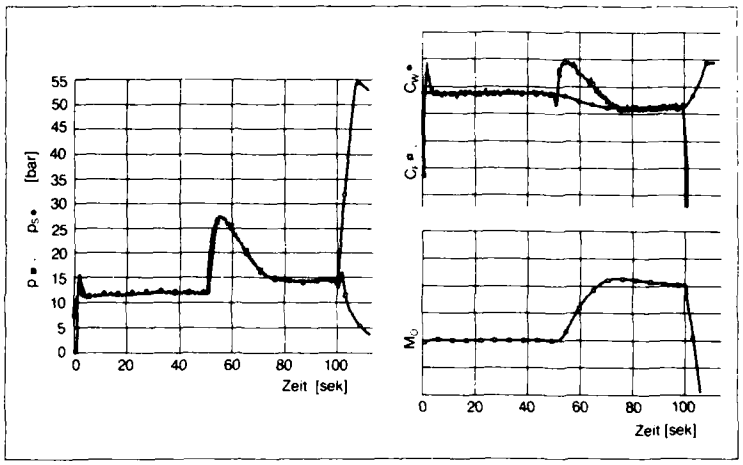

Fig. 16

Ducted Rocket Propulsion System
Test Results

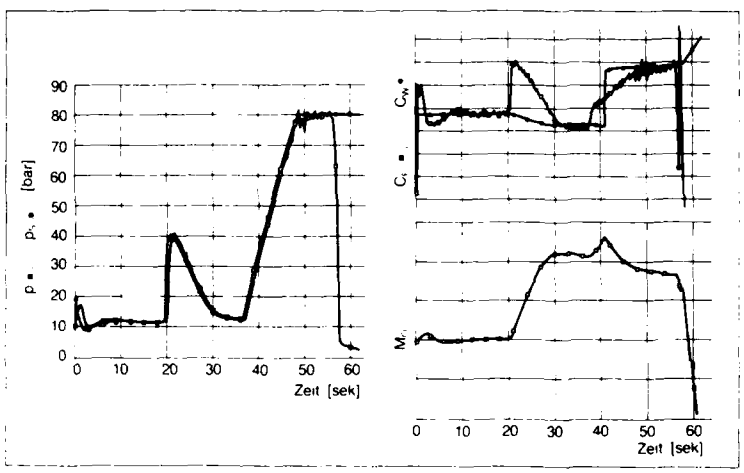

Fig. 17

Ducted Rocket Propulsion System
Trial Firing

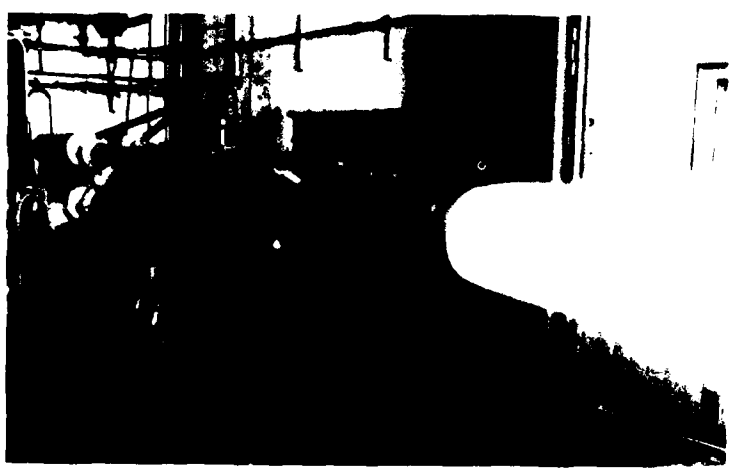

Fig. 18

AD-P005 720

The Use of Hardware-in-the-Loop-Techniques in the Development of a Modern Air-to-Surface Missile System

Dr. Thomas Küstner
MBB-GmbH, AE134
Postfach 80 11 49

D-8000 München 80

Summary:

Because of their increasing requirements, modern guided missiles today have a very high degree of complexity. In the development this results in need of time and high costs. To improve cost-effectiveness and to reduce risk and uncertainty at the same time, new test concepts are necessary. Realtime simulations like Software-in-the-Loop and Hardware-in-the-Loop simulations represent such new concepts. This means close loop simulation with actual present missile components in a laboratory environment where the physical environment is simulated and controlled by a special computer equipment. After a definition of SIL/HIL-simulation, ~~in this publication~~ the configuration of such a test equipment is presented. It gives an overview of the complexity of the thereby necessary hardware and software.

1. Definition of SIL/HIL-Simulation

The requirements on modern guided missile systems have increased because of their operational conditions. This results in a high degree of complexity of the whole system as well as of the single subsystems.

Such a missile (fig. 1) for example has a central missile computer where complex signal processing and control of all systems takes place. Additionally data-communication between the carrier and the missile must be possible during the captive flight for test- and synchronisation purposes.

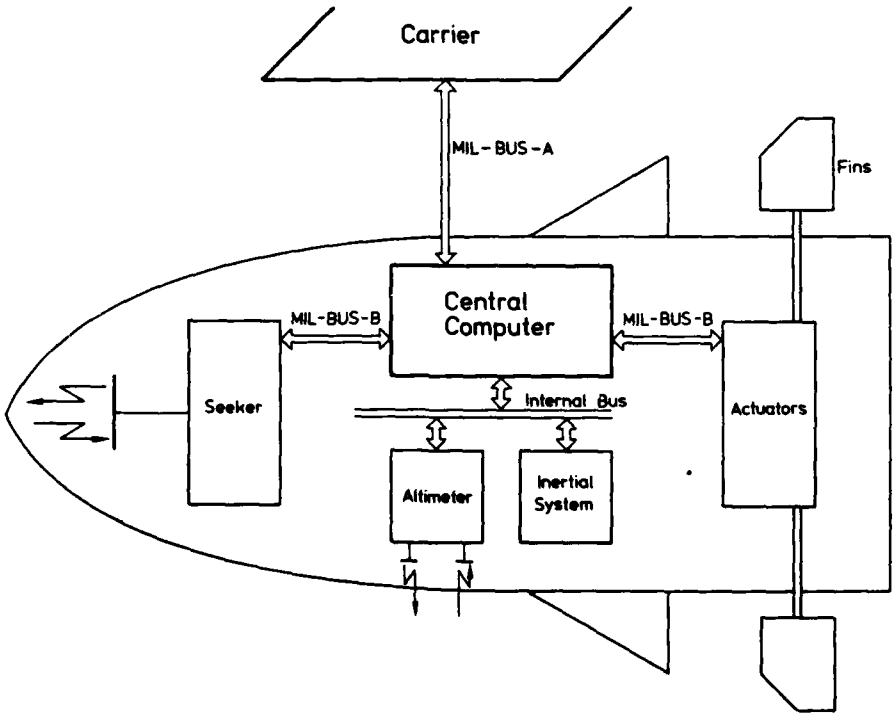

Fig. 1: Schematic Structure of a Guided Missile (Guidance and Control Components)

The influences of the operational environment are observed by several sensor systems such as

- an active seeker (radar, infrared etc.)
- altimeter (radar)
- inertial system (strap down)

These single subsystems, as a rule, have a local intelligence and realize a data preprocessing. The calculation of all data by complex guidance and control algorithms leads to commands for the fin actuator system so that the correct course is followed. The communication with the central computer takes place by suitable BUS-systems.

All described systems have digital components which enable the processing of the complex algorithms and, furthermore, the realization of changed requirements quickly and cost-effectively by software modification.

All these considerations lead to high development effort which takes time and results in high costs. A special problem is the testability of such systems. Tests of single systems on test rigs with deterministic signals provide at most knowledge only about the compliance of specifications, tolerances and correct logical flow.

Dynamic research into system behaviour, as well as of the hardware and also of the software, till now has only been possible by captive and free flight tests. Exactly these tests represent a very high cost factor in the development. Besides it has been clear that the performances of the missile cannot be registered sufficiently by flight tests alone. To assess the multivarious functions it is necessary to have a high number of tests in a controlled, reproducible environment with definite changes. Thereby it is possible to collect statistical data to enable an assessment of the performance.

New test concepts to fulfill all requirements are the software-in-the-loop (SIL) simulation and the hardware-in-the-loop (HIL) simulation. These are simulations which enable tests of single missile subsystems as well as of the whole system dynamically in a closed loop realized in a laboratory environment.

The basic difference between SIL and HIL is the simulation objective and therefore the subsystems which are involved in the simulation loop. For the SIL-simulation this is only the central missile computer. The implemented software is the actual object of test. The task of the SIL is the validation of the operational software. This means to check whether the transfer of the guidance and control algorithms from mathematical simulation models into the microcode of the microprocessor in use has been done correctly. Validation especially means the check of all dynamic functions. A successful SIL therefore is the first milestone to build up a HIL-simulation.

HIL-simulation in its complete form assembles all missile components which provide data necessary for guidance and control. The task of the HIL is the validation of the whole system, the analysis of its dynamic behaviour and also the check of the system effectiveness.

The commonality of both simulations is the simulation of complete operational missions. This requires for the missile and its sensors a realistic modelization of environment influences and of simulation in real time.

Which influences are necessary will be explained in the following for an actual example.

2. Configuration of an actual SIL/HIL-Simulation

There is no question that the configuration of a SIL/HIL-simulation is dependent on the configuration of the missile itself. Consequently the simulation equipment must be configured so as to serve the real hardware- and software-interfaces of the missile. This will be illustrated using the simulation equipment of an Anti-Ship-Missile as an example.

2.1 SIL-Configuration

The structure of the SIL-simulation is presented in figure 2. The real missile components are the complete missile computer with implemented mission software and a control unit for the fin actuators. The missile computer is supplemented by a special CYBER-interface. It serves to transfer data into the missile memory directly from those subsystems which are connected by an internal BUS in the original missile.

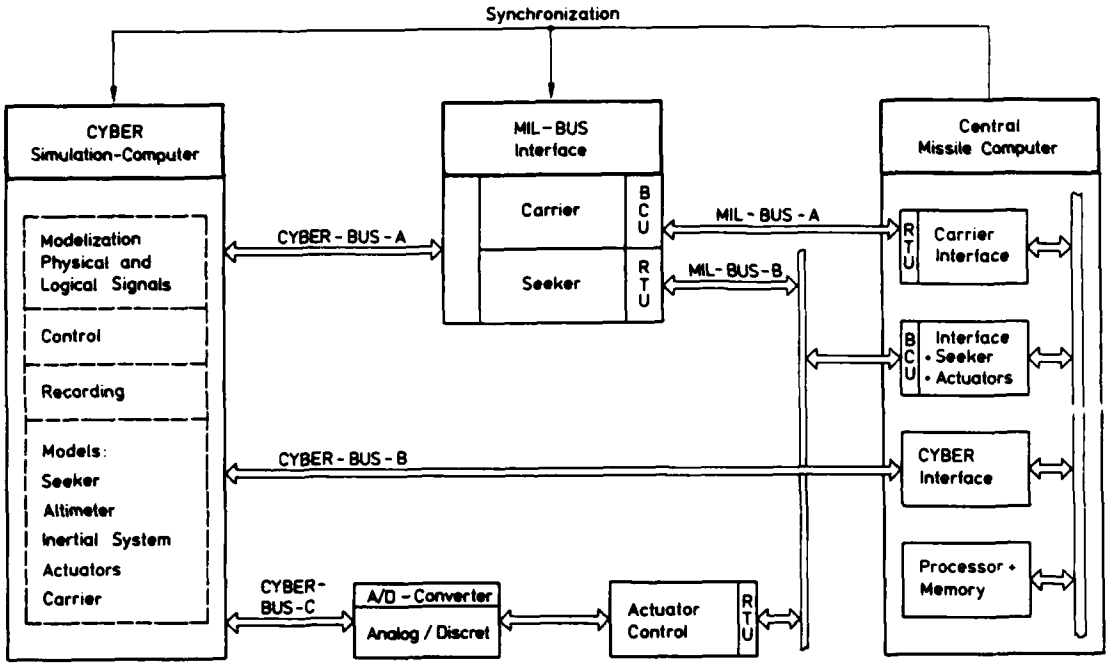

Fig. 2 : SIL - Configuration

Additionally this interface allows the recording of data which are necessary to validate a simulation run. The CYBER-simulation computer is the controlling unit. A main program is based upon the logical timing of the missile computer and controls the test scenario by adapted logical commands. Special simulation programs model all missile subsystems which are not actually present and also all necessary physical influences at the sensors and the missile itself. The data transfer between the missile computer and the CYBER simulation computer takes place over the original interfaces in the specified format. This requires an analog/digital-conversion of signals for the fin actuator system. Additionally there is a separate interface computer for MIL-BUS-formatting of seeker- and carrier-data and the control of the actuator system.

The whole simulation must run under real time conditions synchronously to the timing of the missile computer. A synchronisation pulse generated by the missile computer synchronizes the missile computer, the interface computer and the simulation computer. The actual system time is about 8 ms. This is the maximum integration time for the simultaneous solution of the systems of differential equations on the simulation computer. This available frame time will be shortened by the necessary system time and by the data transfer from and to the periphery. It is a special feature of this simulation computer and its operational system to recognize and process the synchronization interrupt fast enough so that the synchronization and real time conditions are fulfilled.

2.2 HIL-Configuration

Figure 3a shows the HIL-configuration. The substantial higher hardware effort can be noticed. It is necessary to generate the correct physical effects for the missile sensors which are actually present. The figure shows a complete configuration of the HIL which contains all missile systems as real hardware. It is clear of course that influences like aerodynamic or propulsion system behaviour etc. cannot be reproduced in a laboratory configuration.

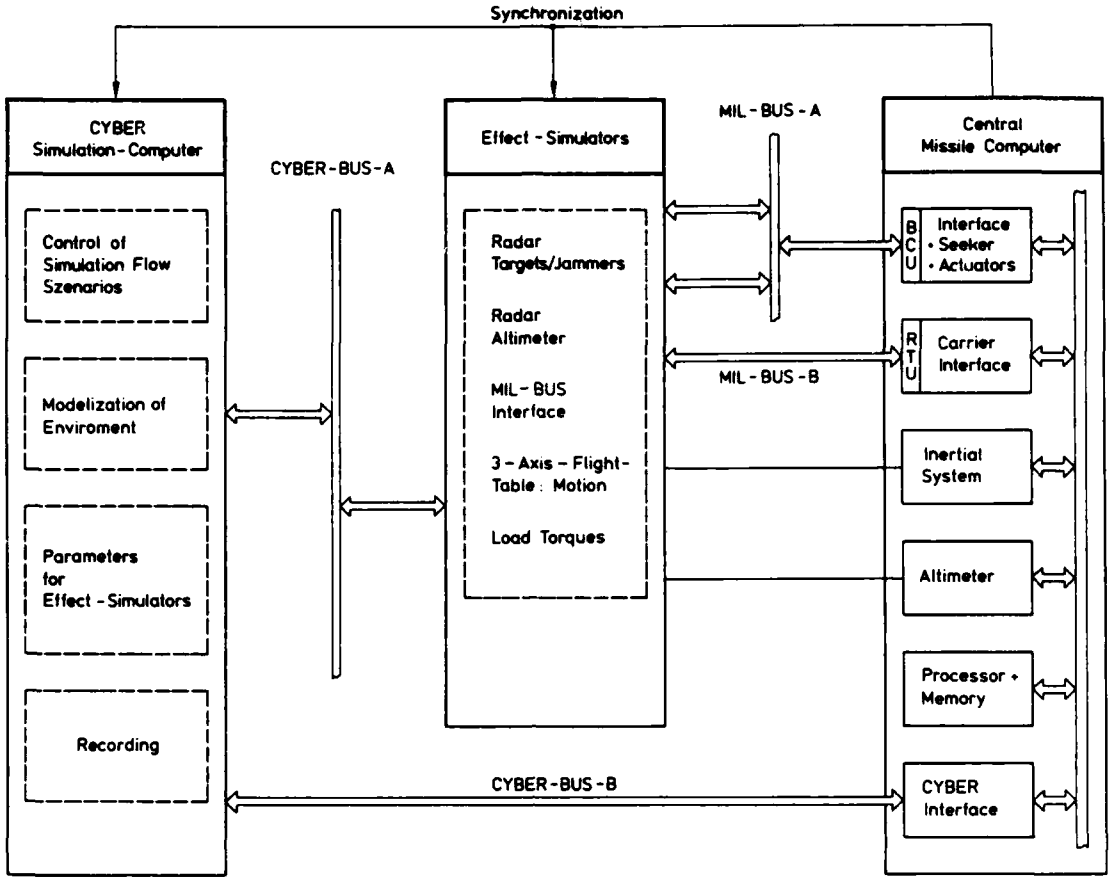

Fig. 3a: HIL - Configuration

The individual systems are (besides the missile computer):

- the radar seeker
- the fin actuator system
- the strap-down inertial system
- the radar altimeter

They all consist of a sensor system for physical data and a computer component.

The essential task of the HIL-simulation now is to provide each sensor with appropriate data. For this purpose special effect simulators have been built up which consist of a computer component and a component to reproduce the physical environment (fig. 3b):

- Radar simulator:

  Simulation of moving targets and jammers in an anechoic chamber.

- Load torque simulator:

  Generation of dynamic load torques at the fin shafts by an electro-hydraulic system.

- Motion simulator:

  Realization of rotational motion by an electro-hydraulic three-axis flight table for roll, pitch and yaw.

- Altimeter simulator:

  Dynamic simulation of altitudes by delaying the radar signal.

- MIL-BUS-interface:

  Imitation of the carrier interface. The seeker interface is not used here.

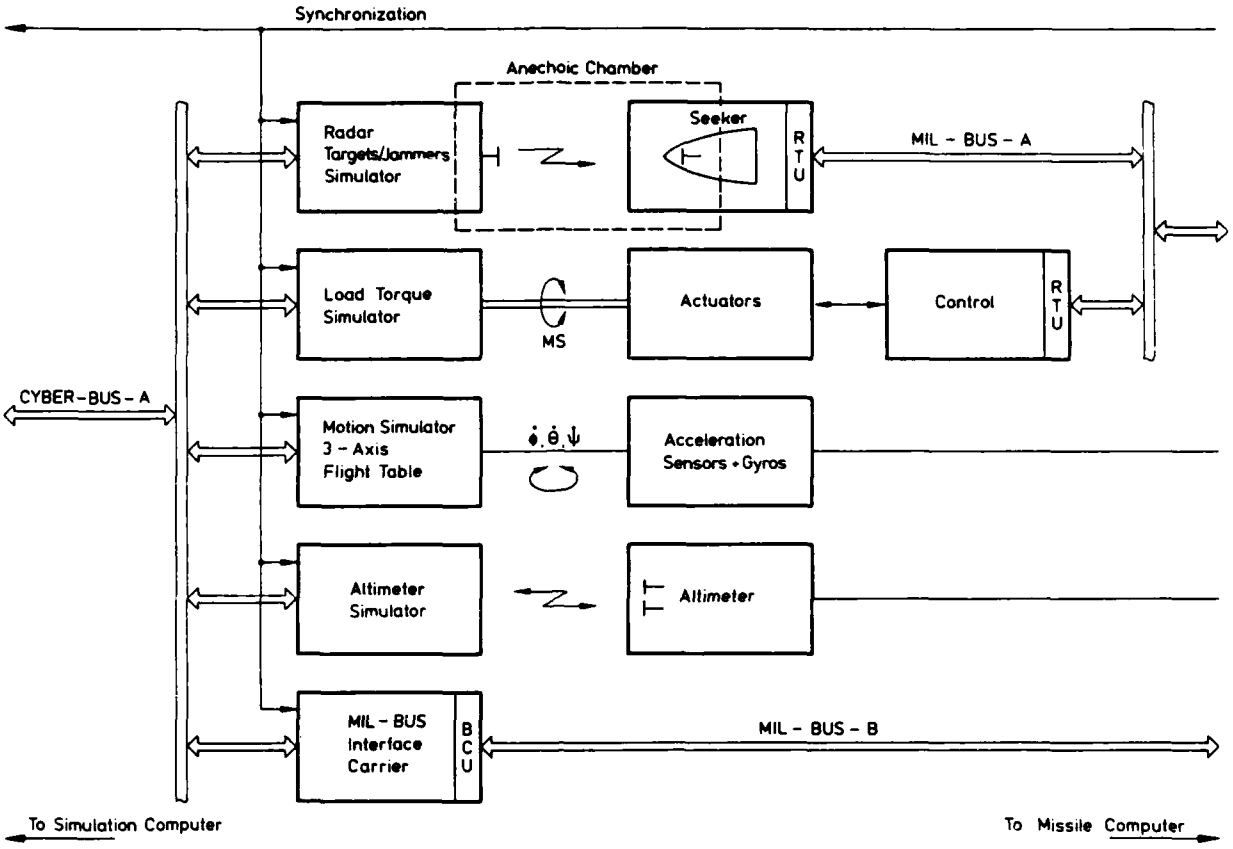

Fig. 3b: Effectsimulators

As for the SIL there is a direct coupling of data between the CYBER and the missile computer using an interface for data recording.

Simulation programs on the CYBER-simulation computer control the complete test and the data communication of the connected systems. They supply the effect simulators with parameters for the simulation of the physical effects. A great part of these special programs are implemented in these microcomputers itself for computation time reasons. To keep the realtime conditions all systems must also be synchronized to the timing of the missile computer.
With this configuration it is possible to evaluate the dynamic behaviour of the whole system. With the modular construction it is possible to replace a single actual component by a computer model. Dynamic tests of single components will therefore be possible.

Table 1 shows a summary of the computer models utilized in the HIL and SIL-simulation.

Model	Used in HIL	Used in SIL
Aerodynamic	x	x
Equations of motion	x	x
Propulsion system	x	x
Mass	x	x
Actuator control	real	x
Torques	real	-
SDP	real + translatoric	x
Altimeter	real + heights > 12 m	x
Seeker	real	x
Carrier-Interface	real	real
Carrier	x	x
Waves	real	x
Wind	x	-
Kinematic of targets/ jammers	real	x
Radar	real	x

x = mathematical model

real = real hardware present / stimulated by effect simulators

Table 1: Models used in HIL and SIL

3. Conclusion

The SIL- and HIL-simulation equipments presented here allow the dynamic testing of hardware and implemented software under realtime conditions. By variation of parameters various environment conditions and various operational missions can be realized. In this way a deeper knowledge of the system can be obtained and consequently a better preparation of necessary flight tests. The value of the thus reduced flight tests is thereby increased. In turn the results of these trials validate and improve the computer models.

Altogether one achieves

- a systematic development procedure
- a quick accomodation of new and changed requirements
- a reduction of development risks
- an improved cost effictiveness.

REPORT DOCUMENTATION PAGE

1. Recipient's Reference	2. Originator's Reference	3. Further Reference	4. Security Classification of Document
	AGARD-CP-431	ISBN 92-835-0439-9	UNCLASSIFIED

5. Originator Advisory Group for Aerospace Research and Development
North Atlantic Treaty Organization
7 rue Ancelle, 92200 Neuilly sur Seine, France

6. Title

ADVANCES IN AIR-LAUNCHED WEAPON GUIDANCE AND CONTROL

7. Presented at

the Guidance and Control Panel 44th Symposium held in Athens, Greece from 5 to 8 May 1987

8. Author(s)/Editor(s)	9. Date
Various	December 1987

10. Author's/Editor's Address	11. Pages
Various	120

12. Distribution Statement This document is distributed in accordance with AGARD policies and regulations, which are outlined on the Outside Back Covers of all AGARD publications.

13. Keywords/Descriptors

Fibre optics gyro
Low cost
Terrain following
Standardization

14. Abstract

This volume contains the Technical Evaluation Report and 9 unclassified papers of the papers presented at the Guidance and Control Panel 44th Symposium held in Athens, Greece from 5 to 8 May 1987. Except for the Keynote Address which was not available at the time of printing, the remainder of the papers and the Technical Evaluation Report are published in the classified volume CP 431(S).

The papers were presented under the following headings: Guidance data source advances; Flight path control advances; Operational requirements, systems considerations; Subsystem technology advances, guidance and control impacts; Test and evaluation techniques. The Symposium concluded with a Round Table Discussion under the chairmanship of the Programme Co-Chairman, Dr W.P.Albritton, USA.

AGARD Conference Proceedings No.431
Advisory Group for Aerospace Research and Development, NATO
ADVANCES IN AIR-LAUNCHED WEAPON GUIDANCE AND CONTROL
Published December 1987
120 pages

This volume contains the Technical Evaluation Report and 9 unclassified papers of the papers presented at the Guidance and Control Panel 44th Symposium held in Athens, Greece from 5 to 8 May 1987. Except for the Keynote Address which was not available at the time of printing, the remainder of the papers and the Technical Evaluation Report are published in the classified volume CP 431(S).

P.T.O

AGARD-CP-431

Fibre optics gyro
Low cost
Terrain following
Standardization

AGARD Conference Proceedings No.431
Advisory Group for Aerospace Research and Development, NATO
ADVANCES IN AIR-LAUNCHED WEAPON GUIDANCE AND CONTROL
Published December 1987
120 pages

This volume contains the Technical Evaluation Report and 9 unclassified papers of the papers presented at the Guidance and Control Panel 44th Symposium held in Athens, Greece from 5 to 8 May 1987. Except for the Keynote Address which was not available at the time of printing, the remainder of the papers and the Technical Evaluation Report are published in the classified volume CP 431(S).

P.T.O

AGARD-CP-431

Fibre optics gyro
Low cost
Terrain following
Standardization

AGARD Conference Proceedings No.431
Advisory Group for Aerospace Research and Development, NATO
ADVANCES IN AIR-LAUNCHED WEAPON GUIDANCE AND CONTROL
Published December 1987
120 pages

This volume contains the Technical Evaluation Report and 9 unclassified papers of the papers presented at the Guidance and Control Panel 44th Symposium held in Athens, Greece from 5 to 8 May 1987. Except for the Keynote Address which was not available at the time of printing, the remainder of the papers and the Technical Evaluation Report are published in the classified volume CP 431(S).

P.T.O

AGARD-CP-431

Fibre optics gyro
Low cost
Terrain following
Standardization

AGARD Conference Proceedings No.431
Advisory Group for Aerospace Research and Development, NATO
ADVANCES IN AIR-LAUNCHED WEAPON GUIDANCE AND CONTROL
Published December 1987
120 pages

This volume contains the Technical Evaluation Report and 9 unclassified papers of the papers presented at the Guidance and Control Panel 44th Symposium held in Athens, Greece from 5 to 8 May 1987. Except for the Keynote Address which was not available at the time of printing, the remainder of the papers and the Technical Evaluation Report are published in the classified volume CP 431(S).

P.T.O

AGARD-CP-431

Fibre optics gyro
Low cost
Terrain following
Standardization

The papers were presented under the following headings: Guidance data source advances; Flight path control advances; Operational requirements, systems considerations; Subsystem technology advances, guidance and control impacts; Test and evaluation techniques. The Symposium concluded with a Round Table Discussion under the chairmanship of the Programme Co-Chairman, Dr W.P.Albritton, USA.

ISBN 92-835-0439-9

The papers were presented under the following headings: Guidance data source advances; Flight path control advances; Operational requirements, systems considerations; Subsystem technology advances, guidance and control impacts; Test and evaluation techniques. The Symposium concluded with a Round Table Discussion under the chairmanship of the Programme Co-Chairman, Dr W.P.Albritton, USA.

ISBN 92-835-0439-9

The papers were presented under the following headings: Guidance data source advances; Flight path control advances; Operational requirements, systems considerations; Subsystem technology advances, guidance and control impacts; Test and evaluation techniques. The Symposium concluded with a Round Table Discussion under the chairmanship of the Programme Co-Chairman, Dr W.P.Albritton, USA.

ISBN 92-835-0439-9

The papers were presented under the following headings: Guidance data source advances; Flight path control advances; Operational requirements, systems considerations; Subsystem technology advances, guidance and control impacts; Test and evaluation techniques. The Symposium concluded with a Round Table Discussion under the chairmanship of the Programme Co-Chairman, Dr W.P.Albritton, USA.

ISBN 92-835-0439-9

AGARD

NATO OTAN

7 rue Ancelle · 92200 NEUILLY-SUR-SEINE

FRANCE

Telephone (1)47.38.57.00 · Telex 610 176

DISTRIBUTION OF UNCLASSIFIED AGARD PUBLICATIONS

AGARD does NOT hold stocks of AGARD publications at the above address for general distribution. Initial distribution of AGARD publications is made to AGARD Member Nations through the following National Distribution Centres. Further copies are sometimes available from these Centres, but if not may be purchased in Microfiche or Photocopy form from the Purchase Agencies listed below.

NATIONAL DISTRIBUTION CENTRES

BELGIUM
Coordonnateur AGARD — VSL
Etat-Major de la Force Aérienne
Quartier Reine Elisabeth
Rue d'Evere, 1140 Bruxelles

CANADA
Defence Scientific Information Services
Dept of National Defence
Ottawa, Ontario K1A 0K2

DENMARK
Danish Defence Research Board
Ved Idraetsparken 4
2100 Copenhagen Ø

FRANCE
O.N.E.R.A. (Direction)
29 Avenue de la Division Leclerc
92320 Châtillon

GERMANY
Fachinformationszentrum Energie,
Physik, Mathematik GmbH
Kernforschungszentrum
D-7514 Eggenstein-Leopoldshafen

GREECE
Hellenic Air Force General Staff
Research and Development Directorate
Holargos, Athens

ICELAND
Director of Aviation
c/o Flugrad
Reyjavik

ITALY
Aeronautica Militare
Ufficio del Delegato Nazionale all'AGARD
3 Piazzale Adenauer
00144 Roma/EUR

LUXEMBOURG
See Belgium

NETHERLANDS
Netherlands Delegation to AGARD
National Aerospace Laboratory, NLR
P.O. Box 126
2600 AC Delft

NORWAY
Norwegian Defence Research Establishment
Attn: Biblioteket
P.O. Box 25
N-2007 Kjeller

PORTUGAL
Portuguese National Coordinator to AGARD
Gabinete de Estudos e Programas
CLAFA
Base de Alfragide
Alfragide
2700 Amadora

TURKEY
Milli Savunma Bakanlığı
ARGE Daire Başkanlığı
Ankara

UNITED KINGDOM
Defence Research Information Centre
Kentigern House
65 Brown Street
Glasgow G2 8EX

UNITED STATES
National Aeronautics and Space Administration (NASA)
Langley Research Center
M/S 180
Hampton, Virginia 23665

THE UNITED STATES NATIONAL DISTRIBUTION CENTRE (NASA) DOES NOT HOLD STOCKS OF AGARD PUBLICATIONS, AND APPLICATIONS FOR COPIES SHOULD BE MADE DIRECT TO THE NATIONAL TECHNICAL INFORMATION SERVICE (NTIS) AT THE ADDRESS BELOW.

PURCHASE AGENCIES

National Technical
Information Service (NTIS)
5285 Port Royal Road
Springfield
Virginia 22161, USA

ESA/Information Retrieval Service
European Space Agency
10, rue Mario Nikis
75015 Paris, France

The British Library
Document Supply Division
Boston Spa, Wetherby
West Yorkshire LS23 7BQ
England

Requests for microfiche or photocopies of AGARD documents should include the AGARD serial number, title, author or editor, and publication date. Requests to NTIS should include the NASA accession report number. Full bibliographical references and abstracts of AGARD publications are given in the following journals:

Scientific and Technical Aerospace Reports (STAR)
published by NASA Scientific and Technical
Information Branch
NASA Headquarters (NIT-40)
Washington D.C. 20546, USA

Government Reports Announcements (GRA)
published by the National Technical
Information Services, Springfield
Virginia 22161, USA

Printed by Specialised Printing Services Limited
40 Chigwell Lane, Loughton, Essex IG10 3TZ

ISBN 92-835-0439-9

LMED

8